CHEMICAL TREATMENT OF CORRODING STEEL REINFORCEMENT AFTER REMOVAL OF CHLORIDE CONTAMINATED CONCRETE

by

William D. Collins

Thesis submitted to the Faculty of the
Virginia Polytechnic Institute and State University
in partial fulfillment of the requirements for the degree of
Master of Science
in
Materials Engineering

APPROVED:

Richard E. Weyers, Chairman

Ronald S. Gordon

Jesse J. Brown

June 12, 1991

Blacksburg, Virginia

CHEMICAL TREATMENT OF CORRODING STEEL REINFORCEMENT AFTER REMOVAL OF CHLORIDE CONTAMINATED CONCRETE

by

William David Collins

Committee Chairman: Richard E. Weyers

Materials Engineering

(ABSTRACT)

The increasing use of deicing salts has caused the accelerated deterioration of bridge decks due to cracking and spalling from chloride induced corrosion of steel reinforcement. One method being considered as a possible corrosion abatement measure is the removal of chloride contaminated concrete and the chemical treatment of the partially exposed rebar through ponding and/or placement of chemically treated mortar.

Reinforced concrete specimens were cast and subjected to repeated exposure to NaCl solution. Half-cell potential, corrosion rate, and chloride ion concentration measurements were conducted until the indication of active reinforcement corrosion. Chloride contaminated concrete was removed to the rebar level through a grooving process. The grooves were chemically treated through solution pondings and backfilling with treated mortar. Seventeen treatments and combination of treatments were evaluated including corrosion inhibitors, polymer sealers, and a possible chloride ion

scavenging mineral. The treatment effects were monitored using half-cell potential and corrosion rate measurements. In addition, mortar cubes were cast containing various treatment concentrations and were subsequently tested for compressive strength and change in resistivity over time.

Based on the electrochemical and mortar cube measurements, DCI (calcium nitrite) when applied as a ponding and mortar treatment, was determined most effective in abating corrosion after concrete removal. In addition, Alox 901, Cortec 1337, Cortec 1609, sodium tetraborate, and zinc borate were also found effective in mitigating rebar corrosion after concrete removal; however, both the borate compounds cause set retardation of portland cement. These chemicals were recommended as candidate treatments for further evaluation in both large-scale and field experimentation.

ACKNOWLEDGEMENTS

This research was sponsored by the Strategic Highway Research Program (SHRP) under the auspices of the National Research Council (NRC).

The author would like to express his sincere appreciation to the chairman of the graduate committee, Dr. Richard E. Weyers. Without his neverending support, guidance, and sincere concern for the author as both a student and friend, these studies would not have been possible. Sincere thanks are also extended to the members of the committee, Dr. Ronald S. Gordon and Dr. Jesse J. Brown for their time and energy devoted toward the author's studies and thesis.

Additional thanks are extended to Dr. Imad L. Al-Qadi, Dr. Tawei Sun, Steve Herald, and all of the author's fellow students in the Materials Section of the Civil Engineering Structures and Materials Research Laboratory, including Tapas Dutta, Mark Henry, Lalith Galagedera, Brian Prowell, Erin Larsen, Eric Peterson, and Mike Fitch.

This work is dedicated to the author's parents, Yong and James Collins. Thank you Chris for your patience, understanding, and love.

TABLE OF CONTENTS

Abstract.....ii

Acknowledgements.....iv

List of Tables.....ix

List of Figures.....xii

1.0 INTRODUCTION.....1

1.1 Description of Problem.....1

1.2 Current Repair Techniques.....2

1.3 Scope of Study.....5

2.0 BACKGROUND

2.1 Cement and Concrete.....8

2.2 Corrosion Overview.....10

2.3 Corrosion of Steel Reinforcement in Concrete....12

2.4 Factors Affecting Corrosion in Reinforced Concrete.....16

2.5 Measuring Corrosion in Concrete.....18

2.5.1 Potential and Potential Mapping Techniques.....19

2.5.2 Electrical Resistance/Resistivity Measurements.....21

2.5.3 Polarization and Impedance Techniques....22

2.6 Inhibitor Use in Reinforced Concrete - Overview.....26

2.7 Polymer Use in Reinforced Concrete - Overview...29

3.0 EXPERIMENTAL DESIGN

3.1 Introduction to Experimental Design.....32

3.2 Materials.....34

3.2.1 Coarse and Fine Aggregates.....34

3.2.2 Cement.....34

3.2.3 Chemical Admixtures.....34

3.2.4 Corrosion Abatement Treatments.....34

3.3 Specimen Design.....37

3.3.1 Specimen Configuration.....37

3.3.2 Specimen Casting.....39

3.3.3 Post-Casting Treatment.....40

3.4 Corrosion Initiation.....41

3.5 Chloride Concentration Measurements.....43

3.6 Treatment of Specimens.....44

3.6.1 Removal of Chloride Contaminated Concrete.....44

3.6.2 Application of Treatments.....47

3.7 Treatment Monitoring.....50

3.8 Evaluation of Mortar Cube Strength and Resistivity.....50

3.8.1 Strength Measurements.....51

3.8.2 Resistivity Measurements.....51

3.9 Evaluation of the Chloride-Ion Scavenging Ability of Hydroxylapatite.....53

3.9.1 pH Measurements.....53

3.9.2 Specific Ion Probe Measurements.....54
3.9.3 Differential Thermal Analysis.....55
4.0 RESULTS AND DISCUSSION.....56
4.1 Pre-Treatment Corrosion Measurements and Observations.....56
4.2 Evaluation of Corrosion Abatement Treatments....61
4.2.1 Control Specimen.....64
4.2.2 DCI Treatments and Polymer Sealants.....67
4.2.3 Borate Treatments.....79
4.2.4 TCI Treatment.....85
4.2.5 Alox 901 Treatment.....88
4.2.6 Cortec Inhibitor Treatments.....91
4.2.7 Hydroxylapatite Treatments.....97
4.3 Selection of Most Effective Treatments.....103
4.4 Mortar Strength and Resistivity Evaluation.....105
4.4.1 Treatment Effects on Mortar Compressive Strength.....106
4.4.2 Treatment Effects on Mortar Resistivity.....114
4.5 Chloride Ion Scavenging Ability of Hydroxylapatite.....119
4.5.1 pH Measurements.....120
4.5.2 Specific Ion Probe Measurements.....122
4.5.3 Differential Thermal Analysis.....123
5.0 Conclusions.....126

6.0 Recommendations for Further Research.....129
REFERENCES 131
APPENDIX A.....136
APPENDIX B.....145
APPENDIX C.....153
VITA.....167

LIST OF FIGURES

Figure 1. Pad design and ponding configuration.....38

Figure 2. Specimen groove dimensions.....45

Figure 3. Mean pre-treatment half-cell potentials.....57

Figure 4A. Control specimen (B-1) mean half-cell potentials and post-treatment percent change.....65

Figure 4B. Control specimen (B-1) mean half-cell potentials and post-treatment percent change.....66

Figure 5A. Mean half-cell potentials for DCI treated specimens.....68

Figure 5B. Post-treatment percent change in half-cell potentials for DCI treated specimens.....69

Figure 5C. Mean corrosion rates for DCI treated specimens.....70

Figure 5D. Post-treatment percent change in corrosion rate for DCI treated specimens.....71

Figure 5E. Mean half-cell potentials for DCI ponded specimens with polymer sealers.....73

Figure 5F. Post-treatment percent change in half-cell potential for DCI ponded specimens with polymer sealers.....74

Figure 5G. Mean corrosion rates for DCI ponded specimens with polymer sealers.....75

Figure 5H. Post-treatment percent change in corrosion rate for DCI ponded specimens with polymer sealers.....76

Figure 6A. Mean half-cell potentials for borate treated specimens.....80

Figure 6B. Post-treatment percent change in half-cell potential for borate treated specimens.....81

Figure 6C. Mean corrosion rates for borate treated specimens.....82

Figure 6D. Post-treatment percent change in corrosion time for borate treated specimens.....83

Figure 7A. TCI ponding specimen mean half-cell potentials and post-treatment percent change.....86

Figure 7B. TCI ponding specimen mean corrosion rates and post-treatment percent change.....87

Figure 8A. Alox 901 ponding specimen mean half-cell potentials and post-treatment percent change.....89

Figure 8B. Alox 901 ponding specimen mean corrosion rates and post-treatment percent change.....90

Figure 9A. Mean half-cell potentials for Cortec inhibitor treated specimens.....92

Figure 9B. Post-treatment percent change in half-cell potential for Cortec inhibitor treated specimens.....93

Figure 9C. Mean corrosion rates of Cortec inhibitor treated specimens.....94

Figure 9D. Post-treatment percent change in corrosion rate for Cortec inhibitor treated specimens.....95

Figure 10A. Mean half-cell potentials for hydroxylapatite treated specimens with added inhibitors.....98

Figure 10B. Post-treatment percent change in half-cell potentials for hydroxylapatite treated specimens with inhibitor additions.....99

Figure 10C. Mean corrosion rates for hydroxylapatite treated specimens with added inhibitors.....100

Figure 10D. Post-treatment percent change in corrosion rate for hydroxyapatite treated specimens with inhibitor additions.....101

Figure 11. Mortar cube strength vs time for highest concentration Cortec 1609 and hydroxylapatite cubes.....107

Figure 12. Mortar cube strength as a function of DCI concentration.....109

Figure 13. Mortar cube strength as a function of sodium tetraborate concentration.....111

Figure 14. Mortar cube strength as a function of zinc borate concentration.....112

Figure 15. Resistivity as a function of sodium tetraborate concentration.....116

Figure 16. Resistivity as a function of zinc borate concentration.....117

Figure 17. Resistivity as a function of DCI concentration.....118

Figure 18. Differential thermal analysis of hydroxylapatite.....124

LIST OF TABLES

Table 1. Reference half-cells and their corresponding corrosion probability ranges.....20

Table 2. Corrosion abatement treatments.....48

Table 3. Mortar cube treatment concentrations.....52

Table 4. Mean pre-treatment corrosion current and chloride ion concentrations at the rebar level for specimens used in the treatment study.....59

Table 5. One-way analysis of I_{corr} variance between bars A and B in each specimen at an alpha = 0.05 level.....63

Table 6. Treatment effectiveness comparison measures.....104

Table 7. Measurement of pH as a function of time for hydroxylapatite treated NaCl solution.....121

Table A-1. Gradations of coarse and fine aggregates.....137

Table A-2. Characteristic properties of coarse and fine aggregates.....138

Table A-3. Concrete mix design for specimen set A.....139

Table A-4. Concrete properties for specimen set A.....140

Table A-5. Concrete mix design for specimen set B.....141

Table A-6. Concrete properties for specimen set B.....142

Table A-7. Backfill mortar mix design with treatment variations.....143

Table A-8. Mortar cube mix design with treatment variations.....144

Table C-1. Pre-treatment half-cell potentials for specimen sets A and B.....154

Table C-2. Post-treatment half-cell potentials as a function of time in reference to a CSE.....157

Table C-3. Percent change in half-cell potential after treatment, CSE reference.....159

Table C-4. Post-treatment corrosion current as a function of time.....161

Table C-5. Percent change in corrosion current after treatment.....163

Table C-6. Average mortar cube strength for treated specimens.....165

Table C-7. Average mortar cube resistivity for treated specimens.....166

1.0 INTRODUCTION

1.1 Description of Problem

Concrete normally provides reinforcing steel an excellent means of protection against corrosion. Chemical protection is provided by concrete's high alkalinity which passivates the steel and physical protection is afforded by concrete's low-permeability which minimizes the ingress of corrosion inducing agents. However, small amounts of chloride ions can destroy the corrosion inhibiting property of concrete.

Although marine environments are one source of chlorides, the increased use of chloride containing deicing salts has resulted in the most severe deterioration of bridge decks and other steel reinforced structures [1] due to corrosion and subsequent spalling. Deicing salt use has increase from less than one million tons per year in the 1950's to more than 12 million tons in 1979 [2].

Chloride-induced corrosion on bridge decks has received increased attention in the past 20 years due to its impact on the maintenance and construction funds of state highway agencies. The allocation of funds to address corrosion related problems on the highway system will only continue to increase because a large number of bridges built during the interstate construction program have only recently started

showing signs of deterioration [3]. A recent cost estimate of the rehabilitation of deteriorated bridges due to corrosion damage was placed at $20 billion and annually increasing at a rate of $.5 billion [4].

1.2 Current Repair Techniques

The measures which are employed in reinforced concrete construction to protect steel against corrosion can be categorized into three basic types of protection schemes:

1. Modifications to the concrete to either decrease the diffusion of chlorides or increase the threshold level of chlorides needed to initiate corrosion.
2. Modifications to the reinforcing steel.
3. Cathodic protection.

Most of the protection techniques currently used are grouped into the first category in which the concrete environment is directly altered. This can be accomplished in the concrete design stage by utilizing the lowest water/cement ratio possible within specifications and ensuring proper consolidation which reduce the permeability of concrete, and maintaining adequate cover depths. However, in severely aggressive environments, additional measures may be necessary to increase the impermeability of the concrete, either during construction or after a period of service life.

One technique to increase concrete impermeability that is in widespread use is the placing of overlay systems on bridge decks, which includes the use of latex modified concrete, polymer concrete, and low slump dense concrete. A study of bridge decks overlaid with latex modified concrete indicated an increase in existing deck service life by approximately 10 years, and if placed on new bridge decks, an increase of 15 years in service life [5]. The utilization of waterproof polymeric membranes in combination with an asphaltic top layer can also be placed on bridge decks to perform as a barrier to chloride and moisture ingress.

Polymers are also extensively used as both concrete surface coatings and as impregnation mediums. Epoxy surface coatings are effective in inhibiting the penetration of chloride-containing moisture and excluding the access of oxygen necessary to fuel the corrosion process. Polymer impregnation involves the penetration of a liquid monomer into the voids of hardened concrete and subsequent in situ polymerization. Current impregnation measures have centered around the use of methyl methacrylate.

Common corrosion prevention practice also incorporates the use of corrosion inhibiting admixtures, both organic and inorganic. The mechanism of inhibition varies depending upon the chemical nature of the inhibitor and the factors

causing the corrosion, but fundamentally, they act to form a stable film on the reinforcing bar surface which in turn requires higher levels of Cl^- in order to penetrate to the bare metal surface. Inhibitors are currently being used as admixtures in new concrete structures as a preventative measure and injected into existing corroding structures. Although a wide range of inhibitors have been studied, interest has remained concentrated on the use of nitrites and benzoates [6].

A new protection technique involving electromitigation to remove chloride ions from concrete has recently been developed [7]. A large DC voltage is applied between a surface anode and the top reinforcing steel mat in a bridge deck which causes the chloride ions to migrate toward the surface anode. Post-treatment when using this technique would most likely call for the application of an inhibitor or placement of an overlay/surface coating.

Besides modification of the concrete environment, the reinforcing steel surface may also be treated prior to concrete placement. Some use has been made of stainless steel or stainless steel cladded reinforcement, but more prevalent is the use of galvanized rebars where the zinc coating serves as a sacrificial anode layer. Organic rebar coatings, predominantly epoxies, have proved effective for protection as well. The chief difficulty in using epoxy-

coated bars has been preventing damage to the coating during transportation and handling, and also the unknown long-term effect on the corrosion behavior of uncoated rebar connected to coated rebar [8].

Cathodic protection requires no physical alteration of the concrete or rebar, but only the elimination of the potential difference between the anode and cathode within a reinforced structure. Using an impressed current or galvanic system (sacrificial anode), this potential difference can be negated, resulting in the stoppage of the corrosion process due to the lack of a current flow. The electrical current needed to achieve and maintain cathodic protection is small, on the order of a milliampere per square foot of concrete surface [9].

1.3 Scope of the Study

The primary objective of this study is to evaluate the effectiveness and feasibility of removing chloride contaminated concrete in conjunction with the application of chemical treatments as a possible method for mitigating corrosion in deicing salt contaminated bridge components.

This objective was fulfilled through the completion of two phases of testing. The first phase consisted of the accelerated exposure of small scale reinforced concrete specimens to a simulated deicing salt environment until the

initiation of corrosion. The chloride-contaminated concrete above the rebars in each specimen was removed and the remaining groove was treated chemically through a ponding of treatment solution and/or backfilling with a chemically treated mortar. Several corrosion inhibitors, polymer sealers, and a chloride scavenger were tested individually and in combination to ascertain the most effective treatment. Seventeen different treatment combinations were applied to specimens and an untreated control specimen was included. The corrosion behavior of the specimens was monitored after treatment. From this phase of the study, the relative effectiveness of the treatments could be compared over a prolonged exposure period.

The second phase of the study addressed the effects of the treatment chemicals on the strength and resistivity of mortar when admixed. The treatments were evaluated through the testing of mortar cubes cast with varying concentrations of the chemicals. The testing involved the measurement of compressive strength and electrical resistivity during several points in the curing stage of the mortar cubes. These tests would allow for the determination of set acceleration or retardation properties and changes in resistivity that might contribute toward the corrosion process.

In addition to the main objective, the mineral apatite,

a possible chloride ion scavenger, was further tested to determine its effectiveness in tying up otherwise mobile chloride ions.

2.0 BACKGROUND

2.1 Cement and Concrete

Concrete can be defined as a composite material consisting of aggregate and a binding medium. The aggregate portion consists of both fine (> 4.75 mm) and coarse (< 4.75 mm) particles. In most concretes, the fine aggregate is sand and the coarse aggregate consists of gravel or a crushed stone. The aggregate phase is mostly responsible for the elastic modulus, dimensional stability, and unit weight of the concrete. Although there exist nonhydraulic cements, hydraulic cements, mainly portland cement and its various modifications, are the principal cements used for making structural concrete.

The chemical reaction of cement with water, referred to as the hydration of cement, yields products that possess setting and hardening properties. The reaction of portland cement with water is essentially the reaction of the four clinker materials:

tricalcium silicate ($3CaO \cdot SiO_2$)

dicalcium silicate ($2CaO \cdot SiO_2$)

tricalcium aluminate ($3CaO \cdot Al_2O_3$)

tetracalcium aluminate ferite ($4CaO \cdot Al_2O_3 \cdot Fe_2O_3$)

These minerals react with water, producing highly insoluble precipitates of calcium silicate hydrates and calcium

aluminate hydrates which collectively are called the cement gel [10]:

$$3CaO \cdot SiO_2 + 6\ H_2O \rightarrow 3CaO \cdot 2SiO_2 \cdot 3H_2O + 3\ Ca(OH)_2$$

$$3CaO \cdot Al_2O_3 + (n-1)H_2O + Ca(OH)_2 \rightarrow 4CaO \cdot Al_2O_3 \cdot nH_2O$$

In addition to the cement gel, the tricalcium silicate and dicalcium silicate produce free lime ($Ca(OH_2)$), which is sparingly soluble. This free lime in turn reacts with the sodium and potassium salts which are present in small amounts in the cement clinker, resulting in the formation of highly soluble potassium and sodium hydroxide.

During the initial stages of the hydration process, the relatively high pH of the concrete stems from the production of supersaturated calcium hydroxide, and from the sodium hydroxide and potassium hydroxide in the pore solution. At later stages, the pH will predominantly be determined by the sodium hydroxide and potassium hydroxide in solution. The capillary and gel pores in hydrated cement contain a very alkaline solution with a relative composition of 0.6 M potassium hydroxide, 0.2 M sodium hydroxide, and 0.001 M saturated calcium hydroxide [11]. The resulting pH was found to be between 12.6 and 13.8 [12].

In addition to the high pH, the hydration process also serves to decrease the permeability of concrete. As the reaction continues, additional hydration products fill the

voids and capillaries present in the concrete thus reducing the ability of moisture to diffuse into the concrete.

2.2 Corrosion Overview

Corrosion has been defined as the deterioration of a material due to its reaction with its environment. Although corrosion has become synonymous with the rusting of iron and its products, it also encompasses all metals and any nonmetallic material.

It has been established that the corrosion of metals in aqueous environments proceeds by an electrochemical mechanism. In terms of a single homogeneous piece of metal, the surface of the corroding metal functions as a dual electrode, upon which both the anodic and cathodic reactions take place.

Metal atoms undergo dissolution into positively charged, hydrated ions at the anodic sites while the excess free electrons flow through the metal to cathodic sites at which an electron acceptor (e.g. hydrogen ion, dissolved oxygen) consumes them. The process is completed by the migration of ions through the aqueous medium, resulting in the formation of a soluble or insoluble corrosion product.

The corrosion process is governed by Faraday's first and second laws. Faraday's first law states that the corrosion rate is directly proportional to the corrosion

current of the electrochemical cell:

$$R = kI_{corr} \quad (1)$$

where,

R = rate of corrosion [=] grams/second

k = electrochemical equivalent [=] grams/Coulomb

I_{corr} = corrosion current [=] amperes

Faraday's second law states that in an electrochemical cell, the anodic reaction rate is always equal to the cathodic reaction rate, therefore the rate of oxidation always equals the rate of reaction in terms of electron production and consumption.

The rate of an electrochemical reaction can be controlled by various physical and chemical factors. An electrochemical reaction is considered to be polarized if it is affected by these environmental factors. The polarization of an electrochemical cell can be of two types, activation polarization and concentration polarization.

An electrochemical process that is limited by the reaction sequence at the metal-electrolyte interface is considered to be undergoing activation polarization. Concentration polarization, however, involves the limiting of a reaction by diffusion through the electrolyte. Activation polarization is usually the controlling factor in electrolytes containing a high concentration of active

species, while concentration polarization usually dominates in electrolytes of low active species concentration [13]. Concentration polarization plays a major role in reinforced concrete corrosion due to the diffusion of oxygen necessary to drive the corrosion process.

2.3 Corrosion of Steel Reinforcement in Concrete

Corrosion of steel in concrete occurs by an electrochemical reaction in which the anodic and cathodic reactions are:

Anodic reaction: $Fe \rightarrow Fe^{2+} + 2e^-$

Cathodic reaction: $H_2O + \frac{1}{2}O_2 + 2e^- \rightarrow 2OH^-$

The electrons released at the anode flow through the steel to the cathodic sites where they are consumed by the cathodic half-cell reaction. The development of anodes and cathodes is due to the presence of heterogeneities in the corrosion cell. Heterogeneities can exist at the surface of a reinforcing bar due to metallurgical segregation, varying grain orientations, and due to local differences in the electrolyte such as concentration gradients [14].

The anodic steel corrosion reaction quickly stops in a highly alkaline medium such as portland cement concrete, unless sufficient levels of chloride or other aggressive agents are present. The steel is passivated by the high pH

pore solution electrolyte. This passivation is due to the formation of a thin layer of gamma iron oxide (Fe_2O_3) that serves as a stable barrier to further metal dissolution. In the absence of chloride ions in solution, the gamma iron oxide film on steel is reported to be stable at pH levels as low as 11.5 [15].

The two major causes of the destruction of the passive layer on steel rebar are the presence of chloride ions in combination with oxygen and the decrease in the pH value of the pore solution because of carbonation reactions which consume both calcium and sodium hydroxides within the pore solution. Carbonation, however, is not a major problem for bridges because the penetration depth of carbonation is, in most cases, less than the reinforcement cover depth on decks. According to studies on reinforced concrete, concrete of normal water/cement ratio is unlikely to show carbonation beyond a depth of approximately 1/2 in. even under prolonged weathering exposure [16]. The resulting consequences of reinforcement corrosion is the decrease in rebar diameter, cracking and spalling due to the expansive iron oxide products, and a decrease in the rebar/concrete mechanical bond.

While the structure of the passive film formed in high pH environments and the mechanism of its deterioration by chloride ions is not fully understood, it is generally

accepted that the chloride ions become incorporated in the passive film, displacing some of the oxygen present and increasing both the passive film's solubility and conductivity.

Since there exist imperfections in the passive film and an inhomogeneous distribution of chloride ions along the rebar surface, the breakdown in the passive film layer occurs on a local scale, creating microgalvanic cells. The local areas of high chloride concentration and film imperfections act as anodic sites where the iron dissolution takes place, while the remaining passive areas serve as cathodes at which oxygen reduction occurs. In addition to chloride and oxygen availability, the rate of corrosion will also depend on the cathode/anode ratio and the electrical resistivity of the concrete between the cells.

In the concrete surrounding the anode area, the concentration of positive iron ions increases while the pH decreases, consequently the formation of the negative hydroxyl ions occurs at the cathodic sites. This drop in pH at the local anodic sites allows for the formation of a soluble complex of iron chloride [14]. This complex forms by the reactions:

$$Fe + 2Cl^- \rightarrow Fe^{2+} + Cl^- + 2e^-$$

$$Fe^{2+}Cl_2 + 2H_2O \rightarrow Fe(OH)_2 + 2H^+ + 2Cl^-$$

The soluble $Fe^{2+}Cl_2$ complex can diffuse away from the anode, promoting further corrosion. When the complex diffuses to point away from the anode at which both the pH and concentration of dissolved oxygen are higher, the complex breaks down and iron hydroxide precipitates. This frees the bound chloride ions which again react with ferrous ions at the anodic sites. As long as there is sufficient oxygen and moisture, the corrosion process is autocatalytic in nature.

Chlorides may be present in concrete due to several different sources. They may be introduced through unbound chloride-containing aggregate or by the addition of calcium chloride which is used as a set accelerator. The predominant source of chlorides, however, is from the environment, including deicing salts and sea water.

The transport of chlorides through concrete has both a primary and secondary mode. The primary mode of transport is chloride diffusion through the pore system in concrete. The secondary mode of transport is chloride penetration through cracks. These cracks can develop as a result of drying, shrinkage, and subsidence cracking or due to the expansive stresses placed on the concrete from the volume of corrosion products formed on embedded rebar.

Through diffusion and transport through cracks, a critical chloride threshold level is reached at the concrete/steel interface at which corrosion initiates. For

reinforced concrete, a limit value of 0.4% Cl^-/cement wt. [17] and 1.2 lbs Cl^-/yd^3 of concrete [18] have been determined. The threshold value has also been studied in terms of a chloride ion to hydroxyl ion ratio in which a ratio greater than 0.6 Cl^-/OH^- would need to be exceeded to initiate corrosion [19].

2.4 Factors Affecting Corrosion in Reinforced Concrete

A number of factors play a role in the initiation and propagation of corrosion in reinforced concrete. In terms of concrete, cement composition, permeability dictated by the water/cement ratio and consolidation, rebar cover depth, and curing conditions can all be optimized to decrease the diffusion rate and increase the length of diffusion of chlorides into concrete. Cement composition can additionally aid in arresting corrosion by controlling the concrete alkalinity and chemically bonding with free chlorides.

The chloride ion can affect the corrosion reaction differently depending upon the cation associated with it. The rate of corrosion in concrete mixed with calcium chloride has been found to be greater than the rate in concrete mixed with sodium chloride. Although the mechanism for this effect is not well understood, the difference in corrosion rates is partially due to calcium chloride's

diffusivity which is three to four times that of sodium chloride [20].

An essential factor required for corrosion of steel in concrete is the presence of oxygen. The rate of oxygen diffusion through concrete is significantly affected by the extent to which the concrete is saturated with water. Investigations have shown that conditions will be conducive to corrosion in those parts of a concrete structure that are exposed to periods of intermittent wetting and drying, and the rate of steel corrosion will be slow if the concrete is continuously water-saturated [21].

In wet concrete, dissolved oxygen will primarily be diffusing through solution, while in dry concrete, the diffusion of gaseous oxygen is more rapid. However, in order to react at the cathode, the oxygen must be in a dissolved form, therefore, corrosion is more active in reinforced structures that are partially dry or undergo intermittent wetting and drying.

Another factor of importance is the effect of concrete resistivity on the corrosion reaction. Resistivity is mainly controlled by water content, with dry concrete having a resistivity of 1×10^9 Ω-cm and water saturated concrete's resistivity being 1×10^3 Ω-cm [20]. When concrete is dry, the corrosion cell no longer has the electrolyte provided by the ion containing pore solution; therefore, lower moisture

contents reduce the ionic conduction in the concrete which reduces the corrosion rate. Admixtures can also affect the resistivity of concrete by contributing or binding ions, or filling pores which reduces amount of electrolyte.

2.5 Measuring Corrosion in Concrete

The corrosion of reinforcing steel in concrete undergoes three stages: initiation period, corrosion period, and damage period. The embedded steel can corrode over time during the corrosion period without any external signs of deterioration. In order to monitor the corrosion behavior of reinforcement during this stage, a number of techniques were developed and can be applied without disturbing or deteriorating the system.

One nonelectrochemical technique for determining corrosion damage in reinforced concrete is chloride ion monitoring. Although not a definite indicator of corrosion, sampling of the chloride ion concentration at varying depths in concrete can determine if chloride content thresholds for corrosion initiation have been reached. Through either titration or specific ion electrode measurements, the chloride profile as a function of depth can be generated which can aid in both predicting corrosion activity and modelling of chloride diffusion.

The use of electrochemical methods for assessing the

state of rebar corrosion originates from the use of simple potential measurements to monitor the corrosion behavior of buried pipelines. The electrochemical techniques used can be divided into three categories: potential techniques, electrical resistance/resistivity techniques, and methods using polarization and impedance.

2.5.1 Potential and Potential Mapping Techniques

The measurement of the free corrosion potential of reinforcement in concrete consists of determining the voltage difference between the steel and a reference half-cell in contact with the concrete. Reference half-cells are reversible electrodes at which single charge transfer reactions are in equilibrium under defined conditions of concentration and temperature. The utilization of a particular electrode is equivalent to choosing an arbitrary zero-point on the potential scale. The ASTM C-876-87, "Half-Cell Potentials of Uncoated Reinforcing Steel in Concrete," standard for potential measurements on concrete specifies the use of a copper sulfate electrode and indicates the potential ranges in relation to the probability of corrosion. The potential ranges for three different half-cells along with their corresponding reversible reaction and corrosion probability are listed in Table 1.

Table 1. Reference half-cells and their corresponding corrosion probability ranges [22,23].

Reference Half-Cell	Reaction	E_{SHE} scale	E_{corr}	Corrosion Probability
Standard Hydrogen Electrode (SHE) (in 1.2M HCl)	$2H^+ + 2e^- \leftrightarrow H_2$	0.00 V	< -.03 V > +.12 V +.12 to -.03 V	> 90% < 10% uncertain
Copper Sulphate Electrode (CSE) (in aqueous saturated $CuSO_4$)	$Cu^{2+} + 2e^- \leftrightarrow Cu$	+0.32 V	< -.35 V > -.20 V -.20 to -.35 V	> 90% < 10% uncertain
Saturated Calomel Electrode (SCE) (in aqueous saturated KCl)	$Hg_2Cl_2 + 2e^- \leftrightarrow 2Hg + 2Cl^-$	+0.25 V	< -.28 V > -.13 V -.13 to -.28	> 90% < 10% uncertain

Since the potential of any metal in contact with concrete is a function of a number of variables, no quantitative conclusion can be drawn from it and no rate of corrosion can be assigned. However, the use of reference half-cells to create a potential map of a reinforced structure can be useful in locating areas of high corrosion probability and identifying anodic zones based on areas of potential sinks.

2.5.2 Electrical Resistance/Resistivity Techniques

Electrical resistivity measurements are another indicator of corrosion behavior. Using a soil resistance meter, the resistivity of concrete can be determined by the placement of electrodes on the concrete surface. The resulting measurements can be interpreted based on the following guidelines [24]:

1) Values greater than 12,000 Ω-cm indicate corrosion is unlikely.
2) Values between 5,000 and 12,000 Ω-cm indicate probable corrosion.
3) Values less than 5,000 Ω-cm indicate almost certain corrosion.

The changing resistance of thin metallic sections embedded in concrete has also been used as a tool in determining the rate of corrosion. As the resistance of a

metal sheet or wire is inversely proportional to its thickness or diameter, the metal becomes thinner as corrosion proceeds and the resistance shows a corresponding increase. The major advantage of electrical resistance measurements is that time-dependent changes in the rate of corrosion can be evaluated. The method, however, can only give you information on the corrosive nature of the environment and rate of corrosion expected at the particular location where the metallic resistance probe is placed. Since conditions may vary from one position to the next in a large reinforced structure, the probe behavior is not always indicative of the entire rebar network. The electrical resistance method is not as effective when used on existent reinforced structures because the probe will not be placed into the same concrete, but into fresh concrete that may not exhibit the same characteristics.

2.5.3 Polarization and Impedance Techniques

The change in potential due to the change in intensity of current passing through a working electrode is known as polarization. The graphic function of the potential variation versus the current variation is the polarization curve. In terms of concrete, the working electrode is the reinforcing steel and its potential response to an applied current from an auxiliary (counter) electrode is monitored

against a reference electrode. The partial anodic and cathodic curves present in the overall polarization curve can be extrapolated to a point of intersection from which the corrosion current, I_{corr}, can be determined. This technique is known as the Tafel extrapolation method, but it is often laborious and often inaccurate.

One polarization measurement that has proven effective in monitoring corrosion in concrete is polarization resistance. In 1957, Stern and Geary showed that for a simple corroding cell, there existed a relationship between a small step of potential applied at the corrosion potential (E_{corr}) and the resulting current response whose slope they defined as the polarization resistance [25]:

$$R_p = (\Delta E/\Delta I)_{\Delta E \to 0} \qquad (2)$$

where,

R_p = polarization resistance

ΔE = change in potential

ΔI = change in current

This slope is related to the instantaneous corrosion rate through the Stern-Geary equation [25]:

$$I_{corr} = \{(\beta_a \times \beta_c)/2.3(\beta_a + \beta_c)\} \times (\Delta I/\Delta E) = B/R_p \qquad (3)$$

where,

I_{corr} = corrosion current

β_a = tafel slope of the anodic polarization curve

β_c = tafel slope of the cathodic polarization curve

B = value between 13-52 mV in most metal/medium systems

Two main sources of error arise with the use of polarization methods. When a polarization potential of more than 5-10 mV is applied to the working electrode, the metal/electrolyte system is disturbed and is not at the same exact state prior to polarization. A concrete system may take hours and possibly days, depending upon the degree of polarization, to achieve a new equilibrium condition after a DC perturbation [24]; therefore, the method can be considered destructive in nature. The other source of error lies in the ohmic drop between the reference and working electrode which influences the polarization measurements. The ohmic drop caused by the high resistance of the concrete increases as the polarization does, therefore, measurement devices must have electronic compensation of the ohmic drop.

One solution to the problem of the destructive nature of DC techniques is the use of electrical impedance measurements which has recently been applied toward measuring corrosion rate in concrete. The impedance technique involves the application to the working electrode a small-amplitude (a few millivolts, ΔE, peak to peak) sinusoidal voltage over a wide range of frequencies via a

digital Frequency Response Analyzer. The current response ($\hat{\Delta}I$) at every frequency is another sinusoidal signal with a different amplitude and a phase shift relative to the input signal. The ratio:

$$\Delta E/\Delta I = Z \qquad (4)$$

is the impedance of the system which is frequency dependent. The impedance can be further decomposed into resistive and capacitive terms [26]:

$$Z = R_e + [R_T/(1 + jwCR_T)] \qquad (5)$$

where,

R_e = electrolyte ohmic resistance (solution resistance)

R_T = charge transfer resistance assumed equivalent to R_p

C = capacitance of the electrode (double layer capacitance)

j = square root of -1

w = angular frequency

Plotting the impedance data in the complex plane (Nyquist plot) describes a semicircle whose dimensions allow for the calculation of the resistive and capacitive terms.

Further analysis of the mechanisms of corrosion can be done using impedance by modelling the impedance in terms of an equivalent circuit whose elements are composed of resistive, capacitive, and diffusional terms. However, such analysis is reserved for the fundamental study of corrosion

processes and not as a means of measuring relative corrosion rates.

The greatest advantage of impedance measurements is that it is not an destructive technique. The polarization required is too small to cause damage to the electrochemical system. Disadvantages lie in that it is a slow measurement technique because of the wide range of frequencies that must be covered and in its inhomogeneous distribution of current along rebars [27]. An attempt has been made to confine the current distribution using a "guard ring" device which has been incorporated into current AC impedance measurement devices.

2.6 Inhibitor Use in Reinforced Concrete - Overview

There is no general theory of corrosion inhibition that applies to all situations because the mechanism of inhibition will vary depending upon the factors causing corrosion and the nature of the inhibitor. The fundamental concept of inhibition is the development of a stable compound with the metal surface and the formation of an adsorption complex with the metal oxide.

Inhibitors are of three basic types: anodic, cathodic, and mixed. Anodic inhibitors function in an effort to arrest the reaction at the anode. In ideal situations, they react with existent corrosion products to form a highly

insoluble film that adheres tightly to the metal surface [28]. This film can act as a barrier to metal dissolution by preventing the metal surface from coming in contact with the corrosive electrolyte. Cathodic inhibitors function to reduce the cathodic reaction. However, cathodic inhibitors are less effective than anodic inhibitors because their reactive products do not bond as well to the metal surface. A mixed inhibitor may be desired in many cases because microcell corrosion is common in reinforcing steel. The microscopic distances separating the anodic and cathodic areas that characterize microcell corrosion may warrant the use of a mixed inhibitor since the anodic and cathodic sites cannot by isolated. The mixed inhibitor would affect both the anodic and cathodic reactions simultaneously.

Numerous chemical admixtures, both organic and inorganic, have been recommended as specific inhibitors of steel corrosion. However, many of the admixtures have deleterious effects on concrete, such as set retardation. Some inorganic compounds which have been suggested as inhibitors are stannous chloride, zinc and lead chromates, potassium dichromate, calcium hypophosphite, sodium nitrite, and calcium nitrite [29]. Organic inhibitors that have been recommended are sodium benzoate, ethyl aniline, and mercaptobenzothiazole [29]. Calcium nitrite has been the most promising inhibitor used in the United States [30].

Sodium nitrite, which is still used extensively in Europe, was used prior to the development of calcium nitrite, but it caused a number of side effects. Some of the side of effects that are avoided using calcium nitrite are low strength, erratic setting times, efflorescence, and the increased probability of alkali-aggregate reaction [31].

One form of inhibitor that has received little attention for use in concrete is the scavenger. Scavengers are substances that remove corrosive reagents from solution through binding reactions. Most of all the scavengers used in corrosive environments act as scavengers of dissolved oxygen from aqueous solutions. Substances such as sodium sulfite and hydrazine react with dissolved oxygen to form reaction products that do not contribute to the corrosion process. Unfortunately, these scavengers show little promise in terms of concrete due to the normally unlimited supply of oxygen. If added to concrete, these substances would be depleted of their scavenging ability within a short time period. Although scavengers are not currently used in reinforced concrete, interest exists in finding or developing substances to bind chloride ions in reinforced concrete

The application of inhibitors originally centered around their use as admixtures in fresh concrete as a means of preventing future corrosion. However, with the increased

problem of corrosion in existent structures, inhibitors are being applied through impregnation and diffusion through the surface of reinforced concrete.

2.7 Polymer Use in Reinforced Concrete - Overview

The increasing concern with chloride diffusion into concrete has resulted in the use of polymers in a wide variety of protection methods. Current use of polymers in excluding external sources of chloride from reaching concrete reinforcement consist of overlays, waterproof membranes, impregnation, and rebar coatings.

Latex-modified concrete (LMC) and polymer concrete (PC) are two overlay systems in wide use as a barrier to chloride ingress. LMC contains the same materials as normal portland cement concrete with the addition of a colloidal suspension of polymer in water. Elastomeric polymers based on styrene-butadiene and polyacrylate copolymers are commonly used as the latex system [32]. Unlike the polymerization of monomers by additives and thermal activation, the hardening of a latex is a result of the loss of water upon drying. The most impressive properties of LMC is its ability to develop a strong bond with old concrete and its resistance to moisture penetration.

Polymer concrete, unlike LMC, is a mixture of aggregates with a polymer as the sole binding agent. The

aggregate is mixed with a monomer or resin which is subsequently polymerized in place. Using a polymer binder seems expensive, but this cost is reduced by achieving the maximum possible dry-packed density of the aggregate. The polymer used is predominantly an epoxy or methyl methacrylate. The advantages of PC are its rapid setting and durability properties. Water absorption of less than 1 percent and a high resistance to freeze-thaw damage [33] make it an excellent overlay material.

Waterproof polymer membranes have been used extensively to minimize chloride ion ingress in bridge decks. The membranes are manufactured as either preformed sheets or liquid-applied materials. Although the membranes serve as excellent barriers, they are difficult to install and their long term stability is questionable [34]. Blistering caused by the expansion of entrapped gases, solvents, and moisture in the concrete is the greatest problem encountered in membrane use.

The fundamental concept underlying the use of polymer impregnated concrete (PIC) is that voids are responsible for both the poor durability of concrete in severe environments and low concrete strength, therefore, by limiting the voids through polymer impregnation, these properties would be improved. Polymer impregnation involves the water evacuation of the voids in concrete through drying to a

finite depth and the subsequent penetration of a low viscosity, high boiling point monomer. After penetration, the monomer is polymerized in situ. The polymer impregnation serves to increase both the strength and durability of the concrete. Water absorption is reduced by more than 99 percent, the resistance to chemical attack and frees-thaw is improved, and both resistance to abrasion and cavitation are increased [33]. The monomers used for PIC are predominantly methyl methacrylate and styrene.

One of the more effective methods of reinforcing steel corrosion protection is epoxy coating of rebar. Both dry and powdered epoxies have been used a means of isolating the rebar surfaces from corrosive chlorides and electrolytes. Studies have demonstrated that epoxy-coated, deformed reinforcing bars embedded in concrete can have bond strengths and creep behavior equivalent to those of uncoated bars [35,36]. Epoxy coated rebar has become standard practice in many newly constructed reinforced concrete structures susceptible to corrosive environments.

3.0 EXPERIMENTAL DESIGN

3.1 Introduction to Experimental Design

The state of a bridge deck subjected to deicing salt applications was simulated in the laboratory using scaled down reinforced concrete specimens. Thirty two specimens were cast containing two lengths of reinforcing steel in each specimen. After an initial period of curing, the specimens were exposed to alternate wetting with sodium chloride solution and drying at an elevated temperature.

The corrosion activity of the specimens was monitored using both a saturated calomel half-cell (SCE) to measure corrosion potentials and a linear polarization device (3LP) to measure corrosion rates. When corrosion activity in the reinforced concrete was confirmed through both electrochemical measurements and measurements of the chloride ion concentration at the rebar level, seventeen specimens were deemed suitable for the application of anticorrosion treatments.

The treatment substances consisted of commercial and experimental inhibitors, two polymer sealants, and an experimental chloride scavenging mineral. The application of the treatments involved removal of chloride-contaminated concrete above the corroding rebars in each specimen and the subsequent treatment through ponding and/or backfilling with

a treated mortar. Comparison of the treated specimens to an untreated control specimen and evaluation of the pre- and post-treatment corrosion behavior allowed for the determination of each treatment's effectiveness in reducing corrosion activity. From this study, the most effective treatment could be selected for large-scale study and possible field application.

In addition to the electrochemical testing, tests were also conducted to determine the effect of using the treatment admixtures on mortar strength and resistivity. Mortar cubes were cast containing various concentrations of treatment substances. During the first twenty days of curing, cubes were periodically tested for both compressive strength and mortar resistivity. These measurements served as an indicator of any deleterious effects caused by admixing the treatment substances. The suitability of each treatment is not only dependent on its corrosion arresting ability but also its effect on the properties of concrete that may prove detrimental.

Apatite was incorporated into the scope of this study as a possible chloride ion scavenging mineral. Unlike the other treatments used, apatite has had no formal investigation of its ability to aid in the reduction of corrosion in reinforced concrete. As a result, tests were conducted to determine its effectiveness in consuming

chloride ions in both an aqueous medium and in concrete.

3.2 Materials

3.2.1 Coarse and Fine Aggregates

The coarse aggregate used in this study was crushed limestone quarried near Blacksburg, Virginia. The fine aggregate used was natural sand, primarily containing mica, quartz and sandstone, and is processed near Wytheville, Virginia. The gradations and other physical characteristics of both aggregates are given in Appendix A, Tables A-1 and A-2.

3.2.2 Cement

For all concrete and mortar mixes in this investigation, Type I Portland cement was used.

3.2.3 Chemical Admixtures

In order to attain the desired concrete and mortar characteristics, an air-entraining admixture, water reducing agent, and initial set retarder were used.

3.2.4 Corrosion Abatement Treatments

The substances selected for treatment study include inhibitors, polymer sealants, and a suspected chloride ion scavenging mineral.

Based on a previous study [37] involving aqueous

corrosion tests in simulated pore solution, the following inhibitors and sealants were recommended as treatments after removal of chloride contaminated concrete:

1. DCI (calcium nitrite, $Ca(NO_2)_2$): An anodic inhibitor developed by the WR Grace Company that currently has widespread use as an admixture in new reinforced concrete structures. DCI reacts with Fe^{2+} according to the following reaction:

$$2Fe^{2+} + 2OH^- + 2NO_2 \rightarrow 2NO\uparrow + Fe_2O_3 + H_2O$$

Calcium nitrite competes with the chloride ions for the ferrous ions produced in concrete and changes them into a passive layer which closes off the iron surface, thus stopping further corrosion [38].

2. TCI (sodium monofluorophosphate, Na_2PO_3F): An inhibitor developed by the Domtar Corporation that interacts via adsorption of fluoride and/or phosphate on rebar that leads to oxide layer enhancement. The exact mechanism for this enhancement is still unclear. TCI is added to deicing salt applications and allowed to diffuse to the rebar surface. There is still some question as to its effectiveness as a corrosion inhibitor.

3. Sodium tetraborate ($Na_2B_4O_7$): Experimental inhibitor that interacts to form a coating on a rebar surface which serves as a barrier to metal dissolution [38]. Borate is the reactive agent. This study evaluated the

hydrated form of sodium tetraborate ($Na_2B_4O_7 \cdot 10H_2O$).

4. Zinc borate ($2ZnO \cdot 3B_2O_3$): Experimental inhibitor evaluated in conjunction with sodium tetraborate to determine the effectiveness of varying borate forms. This study evaluated the hydrated form of zinc borate ($2ZnO \cdot 3B_2O_3 \cdot 3.5H_2O$).

5. ALOX 901 (proprietary): An organic inhibitor manufactured by the Alox Chemical Company.

6. CORTEC VCI-1337 (proprietary blend of surfactants and amine salts in a water carrier): This is an organic corrosion inhibitor designed to migrate through concrete and is attracted to the surfaces of steel reinforcing bars. The inhibitive substance migrates via vapor phase transport and forms a protective molecular monolayer on the rebar surface. This inhibitor is applied through surface injection.

7. CORTEC VCI-1609 (Proprietary alkanolamine): This inhibitor works under the same principle as VCI-1337 but has a different formulation and is applied as an admixture to concrete.

8. Silicone: A Dow Corning sealer dissolved (10% w/w) in hexane. Serves as polymeric barrier on concrete, reducing any ingress of chlorides, oxygen, and water.

9. Styrene-acrylic: A National Starch copolymer sealer dissolved in (10% w/w) in distilled water and treated with a coalescence agent (ethyl acetate). Serves as a

polymeric barrier on concrete, reducing any ingress of chlorides, oxygen, and water.

In addition to the above substance, a synthetic hydroxylapatite ($Ca_{10}(PO_4)_6(OH)_2$) was evaluated as a possible chloride ion scavenging mineral. The hydroxyl form of apatite was chosen because it is the most widespread apatite mineral and it could be attained in the necessary quantities for experimentation. Hydroxylapatite has the general formula $M_{10}(XO_4)_6Z_2$ where M can be various metals or H_3O^+, X= As, Ge, P, Si, or Cr, and Z= OH, F, Cl, Br, CO_3, etc.. Apatite is being studied as a possible chloride ion scavenger because substitutional solid solution is extensive among the apatite series members [39]. Therefore, it has been hypothesized that the possible substitution of Cl^- for OH^- in the hydroxylapatite molecule may serve as a corrosion limiting reaction.

3.3 Specimen Design

3.3.1 Specimen Configuration

Molding forms for sixteen specimens were constructed in order to cast specimens of dimensions 16" L x 8.5" W x 3.25" H as shown in Figure 1. The forms were made of 3/4" A-C exterior plywood and fastened by drywall screws. The narrow ends of each form contained a wooden spacer in which two 5/8" diameter holes were drilled to support two pieces of

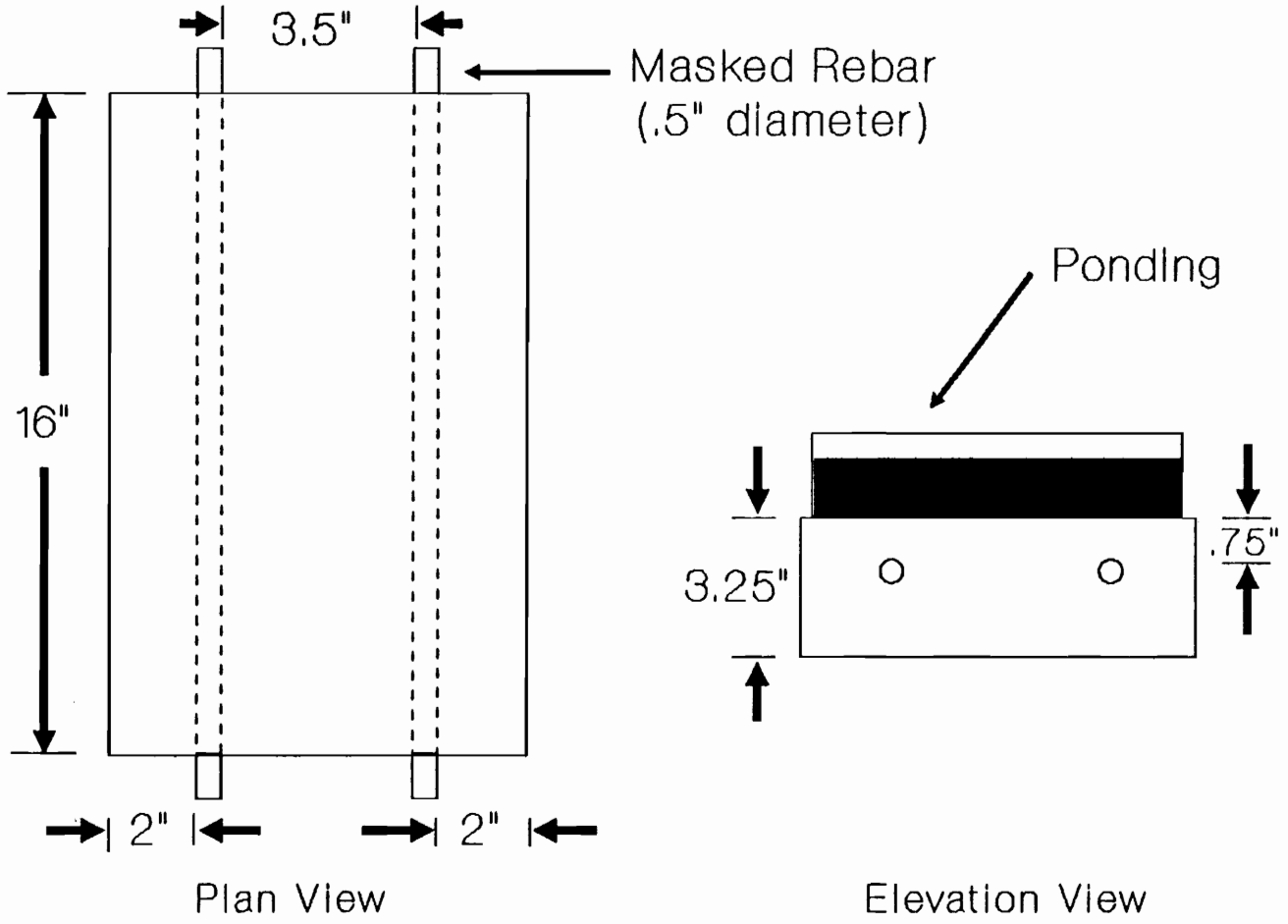

Figure 1. Specimen Design and Ponding Configuration

reinforcing steel at a height 3/4" above the bottom of the form and at a separation distance of 3.5".

The reinforcing steel used in the specimens was ASTM specification #4 rebar with a diameter of .5". For each specimen, two pieces of rebar were cut to a length of 17.5" and one end of each rebar was drilled and tapped to accommodate 1/8" diameter screws. The rebars were cleaned with hexane to remove any residual rust and oil, and 2.5" of each rebar end was masked with electroplating tape leaving a bare steel length of 12.5". Masking the ends of the rebars eliminated the possibility of the exposed ends corroding after concrete placement and provided a known corroding length of steel. Prior to the specimen casting, the forms were twice coated with form oil and the rebars situated in place.

3.3.2 Specimen Casting

In order to achieve a 3/4" cover depth over the rebars, the concrete specimens were cast inverted so that the top surface of the final specimen was formed at the bottom surface of the mold. This was done in order to minimize the possibility of subsidence cracking with such a small cover depth.

Several trial concrete batches were mixed to determine the mix composition that yielded the desired concrete

properties. The final mix composition and physical properties are detailed in Appendix A, Tables A-3 and A-4. Four batches of this concrete composition were mixed, with each batch providing concrete for four specimens. The forms were set on a Syntron vibratory table during placement of concrete to insure proper consolidation.

A second set (Set B) of sixteen specimens were cast approximately 45 days after the first set (Set A) using the same molds and procedure mentioned previously. The concrete mix composition and physical properties are listed in Appendix A, Tables A-5 and A-6.

3.3.3 Post-casting Treatment

In order to aid in accelerating the diffusion of chlorides and the eventual initiation of corrosion in the specimens, the cast specimens were only allowed to cure for a short period of time before application of sodium chloride solution. The short cure time allowed for only limited hydration of the concrete, thus leaving the concrete more permeable. Set A specimens cured in air at room temperature for 24 hours at which time they were removed from the formwork and their top surfaces (surface in contact with form bottom) were etched with muriatic acid to remove any residual form oil. Examination of the specimens indicated that cement could be removed from the surface with only a

slight abrasive force which indicated that the hydration process had not proceeded as far as desired. As a result, Set B specimens were allowed to cure for 72 hours in air before being removed from the formwork and etched.

After the etching process, the specimens from both sets were placed in a drying oven at 150 °F for 24 hours. Subjecting the specimens to an elevated temperature served to drive out a portion of the unbound water near the surface of the concrete. Removing water from the pore system would aid in accelerating the diffusion of chlorides through the concrete.

As a means of simulating the single surface diffusion on a bridge deck surface, the sides of each specimen were coated with a layer of EP-5 epoxy and later coated again with a Shell epoxy comprised of Epon 828 resin and DETA curing agent. The bottom surface of the specimens were left uncoated to allow for oxygen diffusion during the ponding stage.

A plexiglass ponding dike 15 1/2" L x 8" W x 3" H was attached to the top of each specimen using a silicon rubber sealant.

3.4 Corrosion Initiation

The specimens were subjected to alternating 3 day pondings with 750 ml of 6% by weight NaCl solution and 4 day

dryings in a conditioning chamber. The drying cycle consisted of 24 hours at room temperature and 72 hours at 150 °F. Plexiglass covers were placed over each ponding dike to minimize moisture loss and solutions were removed after each ponding cycle using a wet/dry shop-vac.

Prior to the first wetting cycle, half-cell potential measurements using a reference half-cell and hand held multimeter were taken at three positions spanning the area directly above each rebar. A saturated calomel electrode was used as the reference half-cell and measurements were correlated with the potential readings from a copper sulfate half-cell (ASTM C-876) based on the known potential difference cited in Table 1 (see section 2.5.1). Subsequent potential measurements were taken after the first day of drying following each ponding cycle. The procedure for half-cell potential measurements is detailed in Appendix C, Part 1.

Both sets of specimens were cycled until there was a sustained drop in the half-cell potentials to indicate a high probability of corrosion based on the corrosion probability ranges in Table 1 (see section 2.5.1). In order to support the indication of corrosion, a three electrode linear polarization device (3LP) developed by Kenneth C. Clear, Inc., was used to measure the corrosion current of each rebar. Details of the testing procedure is included in

Appendix B, Part 2. The 3LP test procedure is based on the Stern-Geary equation (3), with B = 40.76, and simply measures the amount of current change needed to polarize the working electrode (rebar) to a fixed change in potential. Since corrosion current (I_{corr}) is directly proportional to corrosion rate, the I_{corr} values could be used to determine the extent of corrosion activity in the specimens.

The resulting corrosion current values were interpreted based on the following guidelines [40]:

* $I_{corr} < 0.20$ mA/ft^2 -----> no corrosion damage expected
* 0.20 mA/ft^2 < I_{corr} < 1.0 mA/ft^2 -----> corrosion damage possible in the range of 10 to 15 years
* 1.0 mA/ft^2 < I_{corr} < 10 mA/ft^2 -----> corrosion damage expected in 2 to 10 years
* $I_{corr} > 10$ mA/ft^2 -----> corrosion damage expected in 2 years or less

Corrosion current values greater than 1.0 mA/ft^2 were considered indicative of adequate corrosion activity to start treatments.

3.5 Chloride Concentration Measurements

A third means used in characterizing the corrosion activity in the specimens prior to treatment was the measurement of the chloride ion concentration at the rebar

level. Using an impact hammer/drill and vacuum assisted collection device, concrete powder samples were taken from a total depth of 1/2" to 1" at a location between the rebars in each pad. The measurement of the chloride content of such a sample would approximate the chloride ion concentration at the rebar surface level (3/4").

The chloride ion concentration of each sample was measured twice using a specific ion electrode test procedure developed by Mark Henry under the Strategic Highway Research Program (SHRP) [41]. The basic procedure involved the extraction of Cl^- from the powder samples via an acidic digestive solution and the use of a Cl^- specific ion probe to measure the concentration in terms of a voltage. This voltage reading is used in a determined calibration equation that yields the ion concentration in terms of lbs/yd^3.

Chloride levels exceeding 1.2 lbs/yd^3 [18] were considered sufficient to initiate corrosion of the reinforcing steel in the specimens.

3.6 Treatment of Specimens

3.6.1 Removal of Chloride Contaminated Concrete

Before application of the treatment, the chloride-contaminated concrete above the rebar in each pad was removed. The ponding dikes were removed and a groove area 2" wide and 3/4" deep was marked off for removal along the

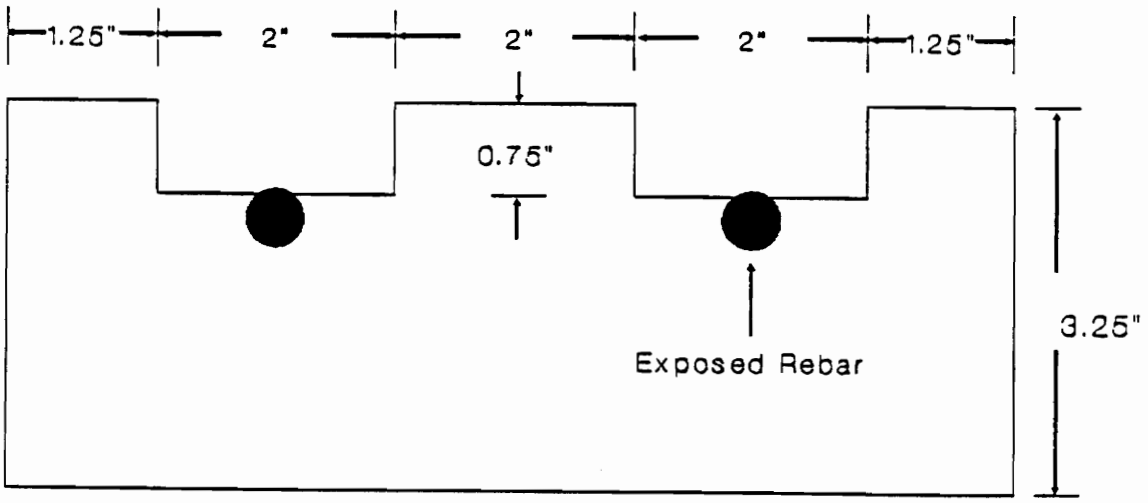

Figure 2. Specimen groove dimensions

length of each pad above each rebar as shown in Figure 2. The removal of this material would equal a contaminated concrete volume of 24 in^3. A masonry saw was used to make four 1/8" wide, 3/4" deep cuts within the 2" groove width above each rebar, being careful not to contact the rebar. The remaining concrete in the groove area was then removed using a masonry chisel so as to expose the top portion of each rebar.

Most of the specimens of Set A had developed cracks above the rebars due to the expansion of corrosion products prior to grooving. During grooving, the first specimen of Set A split into two as the crack above the rebar propagated under the stress of the masonry saw. The exposed bar was uniformly corroded and had lost about 1/8" of its diameter, thus, for the most part, specimens from Set A were determined to be too highly corroded for assessing the efficiency of the proposed abatement treatments. However, two of the specimens that exhibited lower corrosion currents and higher potentials were selected to be treated and will be referred to as specimen A-13 and specimen A-15. Specimen A-13 was left ungrooved while A-15 was grooved. No problems were experienced with the grooving of Set B,therefore, eighteen specimens were suitable for treatment.

The ends of each groove were closed off using a pliable epoxy putty.

3.6.2 Application of Treatments

The treatments and combinations of treatments applied to the eighteen specimens are listed in Table 2. The treatment concentrations are expressed in Molar concentrations for ponding application and in terms of % s/s cement for mortar applications. All ponding solution concentrations were based on recommendations from SHRP Subtask 2A work involving aqueous corrosion tests using the same inhibitors. Mortar concentrations were determined as follows:

1. DCI: The same concentration used in the mortar of the VA Route 460 grooving study was applied in this study as well.

2. Sodium and Zinc Borates: A concentration equivalent to using .1M solution as mortar mix water was applied based on SHRP Subtask 2A recommendation.

3. CORTEC 1609: Manufacturer's dosage recommendation.

4. Hydroxylapatite: The apatite concentration was based on the theoretical removal of Cl^- by the two hydroxyl groups in each molecule of hydroxylapatite. An apatite concentration was calculated that would theoretically remove 10 lbs Cl^-/yd^3 of concrete.

For both sodium and zinc borate, all concentrations were based on the unhydrated, reactive portions of their molecules, $Na_2B_4O_7$ and $2ZnO \cdot 3B_2O_3$ respectively.

Table 2. Corrosion abatement treatments

SPECIMEN	PONDING TREATMENT	MORTAR TREATMENT
B-1 (Control)	None	Untreated
B-2	None	DCI (@ 30% solids) added at 5% s/s cement
B-3	.1M DCI solution	DCI added at 5% s/s cement
B-4	.1M TCI solution	Untreated
B-5	None	Hydroxylapatite added at 24% s/s cement
B-6	None	Sodium tetraborate added at 1% s/s cement
B-7	.1M sodium tetraborate	Sodium tetraborate added at 1% s/s cement
B-8	.1M zinc borate solution	Zinc borate added at 1.7% s/s cement
B-9	.1M ALOX 901 (ethyl alcohol solvent)	Untreated
B-10	.1M TCI solution	Hydroxylapatite added at 24% s/s cement
B-11	None	DCI added at 5% s/s cement and hydroxyl-apatite added at 24% s/s cement
B-12	.1M zinc borate solution	Zinc borate added at 1.7% s/s cement and hydroxylapatite added at 24% s/s cement
B-13	.1M DCI solution and silicone sealant	Untreated
B-14	.1M DCI solution and styrene-acrylic sealant	Untreated
B-15	.1M DCI solution with silicone spray on Bar A, styrene-acrylic spray on Bar B	Untreated
B-16	Direct application of CORTEC 1609	CORTEC 1609 added at .017% s/s cement
A-13	Direct application of CORTEC 1337 to ungrooved surface	No grooves
A-15	Direct application of CORTEC 1337 to grooves	CORTEC 1609 added at .017% s/s cement

For the ponding treatments, the grooves were filled with the treatment solution, covered with plastic to limit evaporation, and allowed to sit for ten days. For specimens B-13 and B-14, the polymer sealants were poured into the bottom 1/4" of the grooves and allowed to remain for two hours upon which the remaining solvent solution was poured off. Each bar in specimen B-15 was treated with 10 g of sprayed polymer sealant solution. Specimen A-13 was left ungrooved in order to evaluate the effectiveness of CORTEC 1337 migratory inhibitor through concrete without exposed reinforcing steel.

Upon completion of the ten day treatment exposure period, the grooves were backfilled with doped or undoped mortar, depending upon the treatment combination (Table 2). The basic mortar mix for the backfill is detailed in Appendix A, Table A-7. The mix design is the same used in an inhibitor treatment study on VA route 460 in which concrete is removed and an inhibitor applied before backfilling [42]. In order to insure adequate bonding between the groove surfaces and the new mortar, the grooves were surface moistened with water mist and a thick cement slurry was applied to the grooves prior to placement of the mortar. The specimens were placed on a vibratory table during mortar placement to insure proper consolidation.

All the backfilled specimens were placed under moist

burlap and a plastic sheet cover and allowed to cure for seven days. During the curing period, the burlap covers would be moistened periodically.

3.7 Treatment Monitoring

At the completion of the seven day cure, half-cell potential and corrosion current measurements were taken for each bar in the specimens. The ponding dikes were replaced on the specimens and the ponding/drying cycle was resumed but with 3% by weight NaCl solution instead of 6%. The 6% solution was only used to accelerate the initial corrosion process. In evaluating the treatments, it was more feasible to use a lower concentration so as to get a longer period of evaluation before chloride threshold levels are regained at the rebar's top surface.

During the post-treatment corrosion monitoring, careful attention was paid to the formation of any cracks on the specimens, especially around the mortar/groove interface.

3.8 Evaluation of Mortar Cube Strength and Resistivity

A corrosion treatment's effect on mortar properties must be considered in addition to its corrosion abatement effectiveness if it is proposed for use in the field. In order to evaluate the proposed treatments' effects on mortar, 2" mortar cubes were cast, in accordance to ASTM C-109-80 " Compressive Strength of Hydraulic Cement Mortars,"

with varying treatment concentrations as shown in Table 3. The mortar cube mix design is listed in Appendix A, Table A-8. Nine cubes were made for each treatment concentration. During the first twenty days of curing, strength and resistivity measurements were taken periodically.

3.8.1 Strength Measurements

Mortar cube strength measurements were conducted after 1, 3, and 20 days of curing using a Forney compressive strength testing machine in accordance with ASTM C-109-80. Mortar cubes that had not cured sufficiently to be placed in the testing apparatus were considered to have zero strength.

3.8.2 Resistivity Measurements

Mortar cube resistivity measurements were taken after 1, 3, 10, and 20 days of curing. The cubes being used for the 20-day strength tests were utilized for the resistivity measurements. The resistivity of the cubes was obtained through the use of a modified Nilsson Soil Resistance Meter. The procedure for the resistivity measurements is detailed in Appendix B, Part 3. A resistivity measurement was taken across each of the three opposite faces on three cubes for each treatment concentration. After the completion of each set of measurements, the cubes were returned to baths of saturated lime water for further curing.

Table 3. Mortar Cube Treatment Concentrations

TREATMENT	CONCENTRATION
Control	Untreated mortar
DCI (calcium nitrite @ 30% solids)	2.50%, 5.00%, 10.00% s/s cement
Sodium tetraborate ($Na_2B_4O_7 \cdot 10H_2O$)	0.50%, 1.00%, 2.00% s/s cement based on $Na_2B_4O_7$
Zinc borate ($2ZnO \cdot 3B_2O_3 \cdot 3.5H_2O$)	0.22%, 0.43%, 0.85%, 1.70%, 3.40% s/s cement base on $2ZnO \cdot 3B_2O_3$
Hydroxyl apatite	6.25%, 12.50%, 25.00% s/s cement
CORTEC 1609	0.15%, 0.30%, 0.45% l/s cement

3.9 Evaluation of the Chloride-Ion Scavenging Ability of Hydroxylapatite

In order to evaluate hydroxylapatite's ability to scavenge chloride ions, three different tests were conducted to determine the possibility and extent of any substitution of Cl^- for OH^- in the hydroxylapatite molecule.

3.9.1 pH Measurements

The substitution of Cl^- for OH^- in an aqueous medium would result in the release of the hydroxyl ion into solution. A means for detecting the increased concentration of hydroxyl ions is a simple pH measurement. The pH of the solution that would theoretically result from a 100% Cl^-/OH^- substitution could be determined from the equation:

$$pH = 14.00 - pOH \qquad (6)$$

where,

pOH = -log [moles of OH^-/volume of solution in litres]

A 25 g sample of hydroxylapatite was placed in a beaker of 200 ml of 5% by weight NaCl solution. The solution was agitated using a magnetic stirrer and the pH was measured as a function of time over a span of 24 hours with an electronic pH meter. The pH of the salt solution and of a solution containing 25 g of hydroxylapatite with 200 ml of distilled water was taken for comparison. Another test was

run with the apatite/salt solution being heated to a temperature of 150 °F and pH measurements were taken over a span of 24 hours.

3.9.2 Specific Ion Electrode Measurements

The same technique used in determining the chloride ion concentration in the concrete specimens (see section 3.5) was employed to measure the ability of hydroxylapatite to pick up chloride ions. 25 g samples of hydroxylapatite were placed into containers containing 5%, 10%, and 15% by weight NaCl solution. One set of containers was agitated at room temperature for 24 hours while a second set was heated to 150 °F and agitated for 24 hours using a magnetic stirrer. The hydroxylapatite samples were then filtered from the solutions, rinsed and stirred with distilled water, filtered again, and allowed to dry. Each sample was subjected to 5 cycles of rinsing and drying.

3 g of each sample, including a control sample, were analyzed using the specific ion electrode technique to determine the presence of any chloride ions that may have been scavenged. Since hydroxylapatite is soluble in acidic solutions, any scavenged Cl^- would be released from the crystal structure when subjected to the acidic digestive solution prior to chloride measurement by the specific ion electrode.

3.9.3 Differential Thermal Analysis

Differential thermal analysis (DTA) was conducted on both untreated hydroxylapatite and hydroxylapatite exposed NaCl solution. Two 25 g samples of hydroxylapatite were exposed to 200 ml of 5% by weight NaCl solution at room temperature and at 150 °F for 24 hours. The samples were then subjected to the same rinsing/drying process as in the specific ion probe tests. DTA scans were performed on an untreated sample and on both the treated samples to determine the degree of the Cl^-/OH^- substitution. The procedure used for the DTA process is detailed in Appendix B, Part 4.

4.0 Results and Discussion

Throughout the course of this study, the following topics were subjects of the investigation:

1. Corrosion abatement effectiveness of chemical treatments applied to corroding reinforced concrete after removal of chloride-contaminated concrete.

2. The effects of treatment admixes on the physical properties of cement mortar.

In addition to the above, the chloride-ion scavenging ability of hydroxylapatite was evaluated.

4.1 Pre-Treatment Corrosion Measurements and Observations

Based on half-cell potential measurements taken after the first ponding with NaCl solution, the two sets of specimens exhibited remarkably different corrosion potentials during the first 70 days of exposure. The evolution of the mean corrosion potentials for Set A and Set B is shown in Figure 3 with the initial value indicating E_{corr} after the first ponding. The mean corrosion potentials for the individual bars in each pad are listed in Appendix C, Table C-1. Half-cell potential measurements were attempted prior to the initial ponding but stable values were unable to be obtained due to the highly dried concrete.

For ease of understanding and uniformity, the half-cell potential measurements will be referred to in terms of

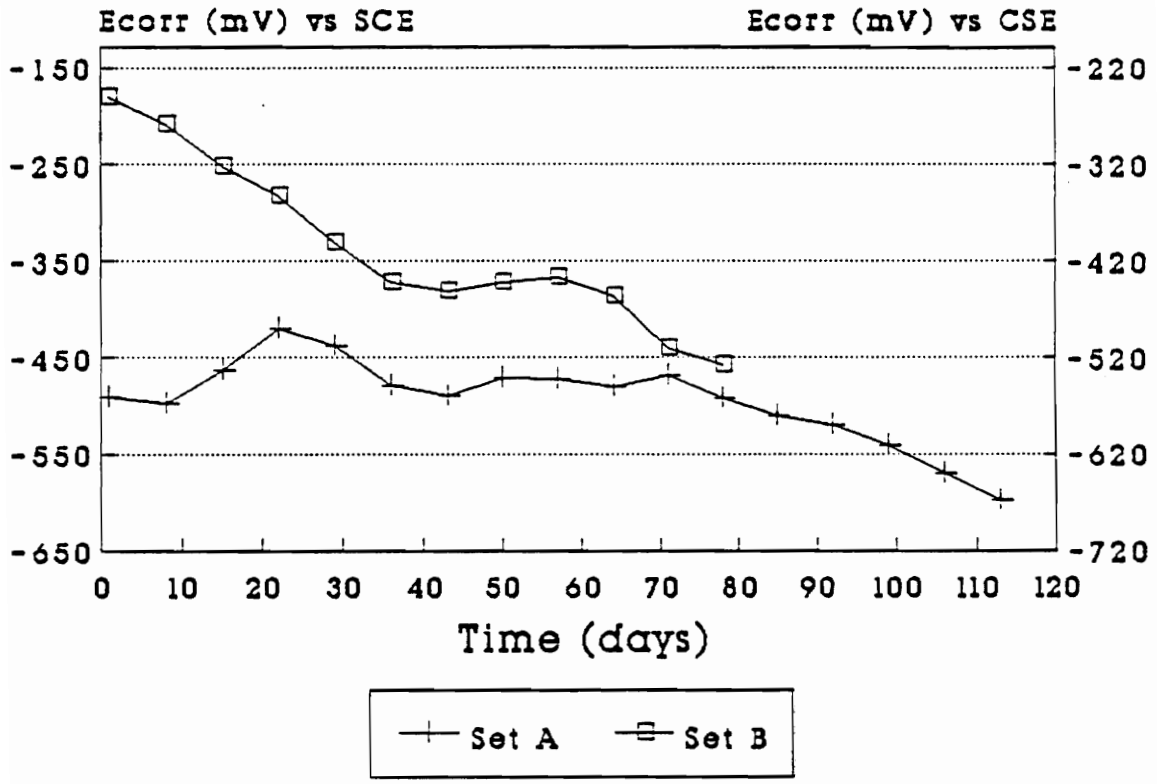

Figure 3. Mean pre-treatment half-cell potentials

copper sulfate reference electrode (CSE) values.

Since the concrete mix designs for both Set A and B were similar, the difference in curing time seemed to have played a major role in corrosion activity initiation. Set A, cured for one day, exhibited initial E_{corr} values less than -350 mV, indicating more than a 90% probability of corrosion (see Table 1). Set B , cured for three days, required exposure for more than 20 days before falling below -350 mV. The one day cure for Set A before ponding left the concrete's pore system extremely open due to the diminished time for cement hydration. This was exhibited during the first ponding in which the Set A specimens absorbed the entire 750 ml of 6% by weight NaCl solution in less than 24 hours.

After 100 days of exposure, 14 of the 16 specimens of Set A developed surface cracks caused by expanding corrosion products. These 14 specimens were deemed unsuitable for further evaluation because of the high degree of corrosion.

Verification of corrosion activity in the remaining 18 specimens can be seen in both the average corrosion current of bars A and B, and in the chloride ion concentration measurements taken prior to grooving, as listed in Table 4. I_{corr} values greater than 1.0 mA/ft^2 and chloride concentrations values greater than 1.2 lbs/yd^3 were taken as indicators of corrosion initiation.

Table 4. Average pre-treatment corrosion current of bars A and B combined, and chloride ion concentrations at rebar level for specimens used in treatment study.

Specimen	I_{corr} (mA/ft^2)	Cl^- Concentration at 3/4" depth (lbs/yd^3)		
		Trial 1	Trial 2	Mean
B-1	8.5	11.54	11.13	11.34
B-2	9.2	11.02	11.31	11.17
B-3	11.5	12.84	12.65	12.75
B-4	7.5	11.16	10.84	12.00
B-5	6.7	12.33	12.39	12.36
B-6	6.2	10.66	10.40	10.53
B-7	6.4	11.93	12.22	12.08
B-8	6.0	10.52	10.42	10.47
B-9	3.9	9.85	10.05	9.95
B-10	3.7	11.85	11.69	11.77
B-11	3.9	9.77	9.98	9.88
B-12	3.4	11.24	11.57	11.41
B-13	2.4	9.34	9.01	9.18
B-14	1.5	8.75	8.86	8.81
B-15	1.8	8.14	8.36	8.25
B-16	1.5	7.24	6.80	7.02
A-13	23.5	15.58	16.77	16.18
A-15	22.5	16.33	15.21	15.77

The values in Table 4 indicate a similarity in corrosion current and chloride ion concentration for each group of specimens made from the same concrete batch (B-1 to B-4, B-5 to B-8, B-9 to B-12, and B-13 to B-16). The decrease in I_{corr} and chloride concentration with succeeding concrete batches indicates improvement in the concrete quality. A possible explanation may lie in the human factors of increased efficiency and improved casting practices with succeeding batches.

A simple linear regression (SLR) analysis, using MINITAB statistical software, was conducted on both the average pre-treatment corrosion potentials and chloride ion concentrations to determine their degree of correlation with the corrosion current values. A SLR analysis yields the coefficient of determination (r^2) which represents the proportion of the total variability of I_{corr} values that are explained or accounted for by the E_{corr} or chloride concentration values. A high value of r^2 indicates a strong correlation. The r^2 value for the E_{corr} correlation with I_{corr} was 66.0% and the value for the chloride concentration correlation was 81.0%. The chloride concentration showed a greater degree of correlation than E_{corr}, as the chloride sample set was able to account for 15.0% more of the I_{corr} sample set.

I_{corr} is linearly proportional to corrosion rate, but

neither E_{corr} nor chloride ion concentration were found to have a high enough correlation (90-95%) to exhibit a linear relationship with I_{corr} and, therefore, they cannot be used as an accurate measurement of corrosion rate. As a result, in the analysis of the corrosion abatement treatments, I_{corr} measurements will predominantly be presented as an indication of treatment effectiveness.

4.2 Evaluation of Corrosion Abatement Treatments

To aid in the treatment effectiveness analysis, the following guidelines are used in data presentation:

1. Since corrosion potentials are only an indicator of the probability of corrosion and not the degree or rate of corrosion, E_{corr} data is presented but not focused upon unless pertinent to treatment evaluation in relation to I_{corr}. When displayed, all E_{corr} values are the mean of six measurements taken on Bars A and B in each specimen. All E_{corr} data is tabulated in Appendix C, Table C-2.

2. I_{corr} data is presented as the mean of the corrosion current in Bars A and B in each specimen. Since corrosion current is linearly proportional to corrosion rate, corrosion current and corrosion rate will be used synonymously through the analysis of results.

The statistical comparison of Bars A and B using a one-way analysis of I_{corr} variance was performed and their

evaluation based on F-ratios and p-values is listed in Table 5. Although some specimens showed significantly different behavior between the bars, it was predominantly due to differences in magnitude while the bars still exhibited similar trends. All raw corrosion current data is tabulated in Appendix C, Table C-4.

3. Due to the high variance in the final half-cell potential and corrosion current measurements prior to treatment, the absolute post-treatment values measured are not an accurate indication and good comparison measure of treatment effectiveness when used alone. Therefore, in addition to absolute values, the data is also expressed in terms of % change in reference to the last measured E_{corr} or I_{corr} prior to treatment. The % change is computed as follows:

$$\% \text{ change} = [(V_p - V_c)/V_p] \times 100 \qquad (7)$$

where,

V_p = final pre-treatment

V_c = current value

A positive % change indicates a increase in corrosion potential (more noble) or a decrease in corrosion rate (in terms of corrosion current) in reference to the final pre-treatment value. A negative % change indicates a drop in corrosion potential (more active) and an increase in

Table 5. One-way analysis of I_{corr} variance between Bars A and B in each specimen at an α=0.05 level.

Specimen	F-Ratio[1]	p-Value[2]	Significantly Different (Yes/No)
B-1	0.09	0.763	No
B-2	3.62	0.067	Yes
B-3	0.12	0.728	No
B-4	10.40	0.003	Yes
B-5	2.14	0.153	No
B-6	0.60	0.445	No
B-7	3.48	0.072	Yes
B-8	6.47	0.016	Yes
B-9	1.12	0.298	No
B-10	2.35	0.136	No
B-11	3.25	0.081	Yes
B-12	2.09	0.158	No
B-13	1.21	0.281	No
B-14	6.08	0.020	Yes
B-15	0.31	0.583	No
B-16	0.00	0.967	No
A-13	0.01	0.932	No
A-15	0.91	0.352	No

[1]Tabulated F-ratio for 16 observation sample sets (B-1 thru B-16) = 2.76. For 12 observation sample sets (A-13) F-ratio = 2.82, and for 11 observation sample sets (A-15) F-ratio = 2.95.

[2]P-values less than 0.10 indicate significant difference [43].

corrosion rate. All % change values for post-treatment E_{corr} and I_{corr} measurements are tabulated in Appendix C, Tables C-3 and C-5, respectively.

For convenience in data display and analysis, the treatments were divided into six treatment groups in addition to the control specimen:

1. DCI (calcium nitrite) and sealers
2. Borates
3. TCI (sodium monofluorphosphate)
4. Alox 901
5. Cortec Inhibitors
6. Hydroxylapatite and hydroxylapatite/inhibitor combinations

4.2.1 Control Specimen

Corrosion potential and corrosion rate evolution for the control specimen (B-1) after removal of contaminated concrete is displayed in Figures 4A and 4B. The control specimen's pre-grooving measurements indicated an extremely low E_{corr} in the > 90% probability of corrosion range and a high corrosion rate. After grooving, the specimen showed minimal improvement between days 1 and 10, most likely due to both the removal of chlorides and the placement of fresh mortar which aids in the pH restoration at the rebar surface. After day 10, the specimen exhibited increasing

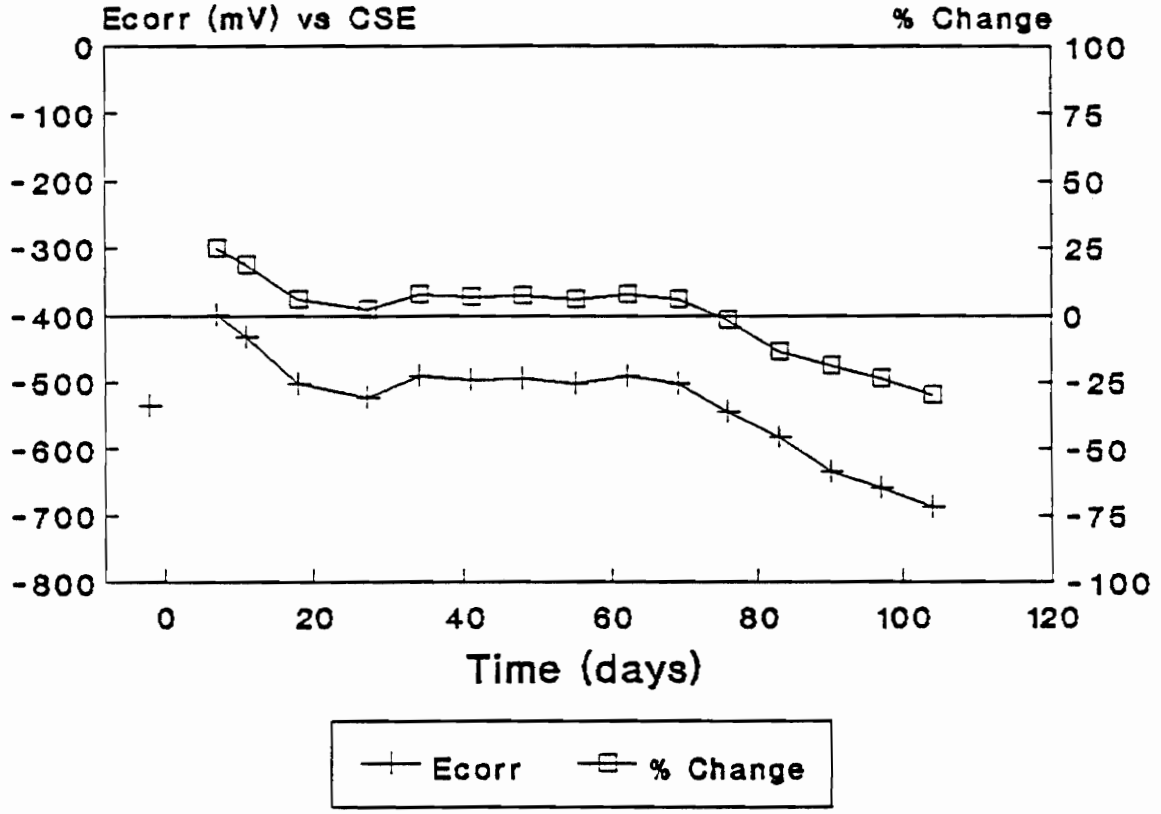

Figure 4A. Control Specimen (B-1) Mean Half-Cell Potentials Post-Treatment Percent Change

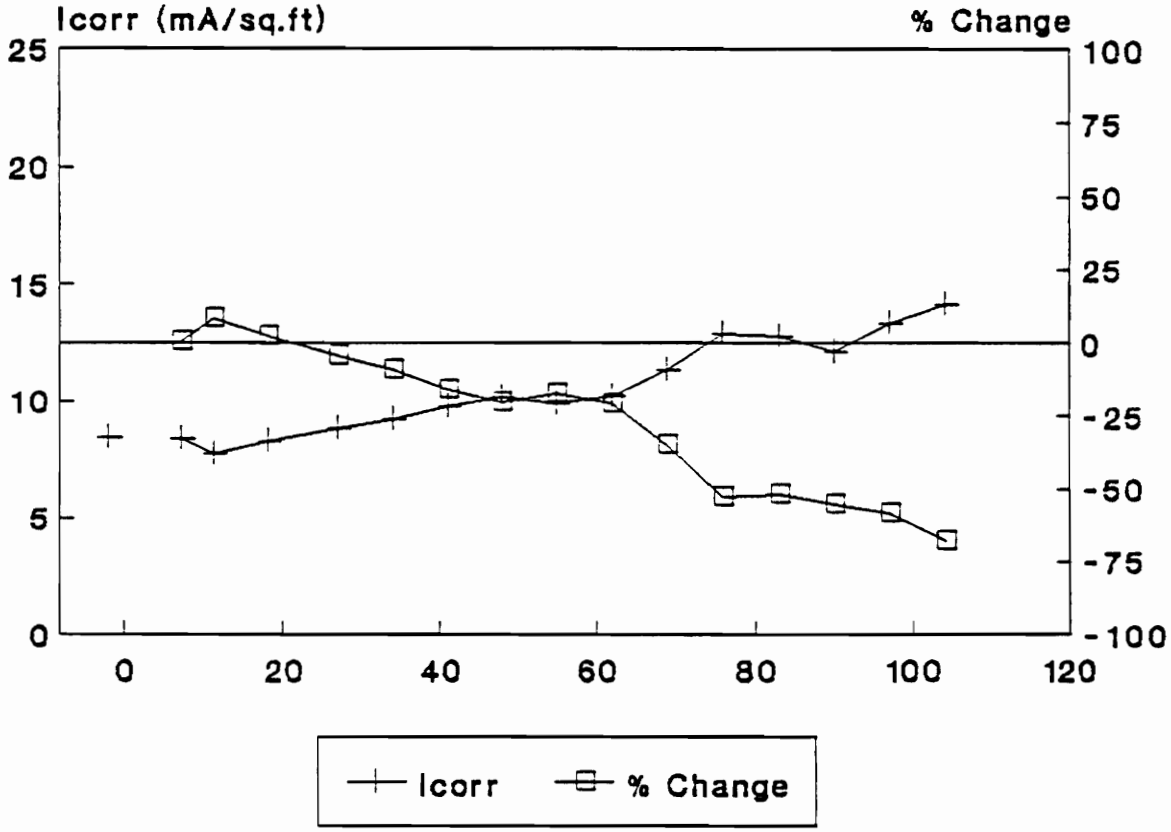

Figure 4B. Control Specimen (B-1) Corrosion Rates and Post-Treatment Percent Change

corrosion activity resulting in an approximate 70% increase in corrosion rate, indicating little benefit from the removal of the chloride-contaminated concrete.

4.2.2 DCI Treatments and Polymer Sealants

A comparison of the two DCI treated specimens in which one had DCI in the mortar and the other was ponded as well as backfilled with DCI mortar showed that the specimen which was ponded exhibited a far better corrosion abatement performance as reflected in Figures 5A thru 5D. I_{corr} values reflect an average 25% reduction in corrosion rate in the mortar treatment specimen (B-2) during the first 40 days and then a 65% increase to more than 15 mA/ft^2 at day 100. It appears as though the DCI present in the mortar in contact with the rebar and groove was sufficient to further stabilize the Fe_2O_3 passive layer which resulted in the slight reduction in the corrosion rate for a short period. However, diffusion of DCI was not great enough to sustain a high enough nitrite concentration at the rebar to compete sufficiently against diffusing chlorides; therefore, the Fe^{2+} ions in solution began complexing with the chlorides to further the corrosion process instead of reacting with the nitrite to eventually enhance the stability of the passive film. The specimen's initial performance was better than the control specimen, but

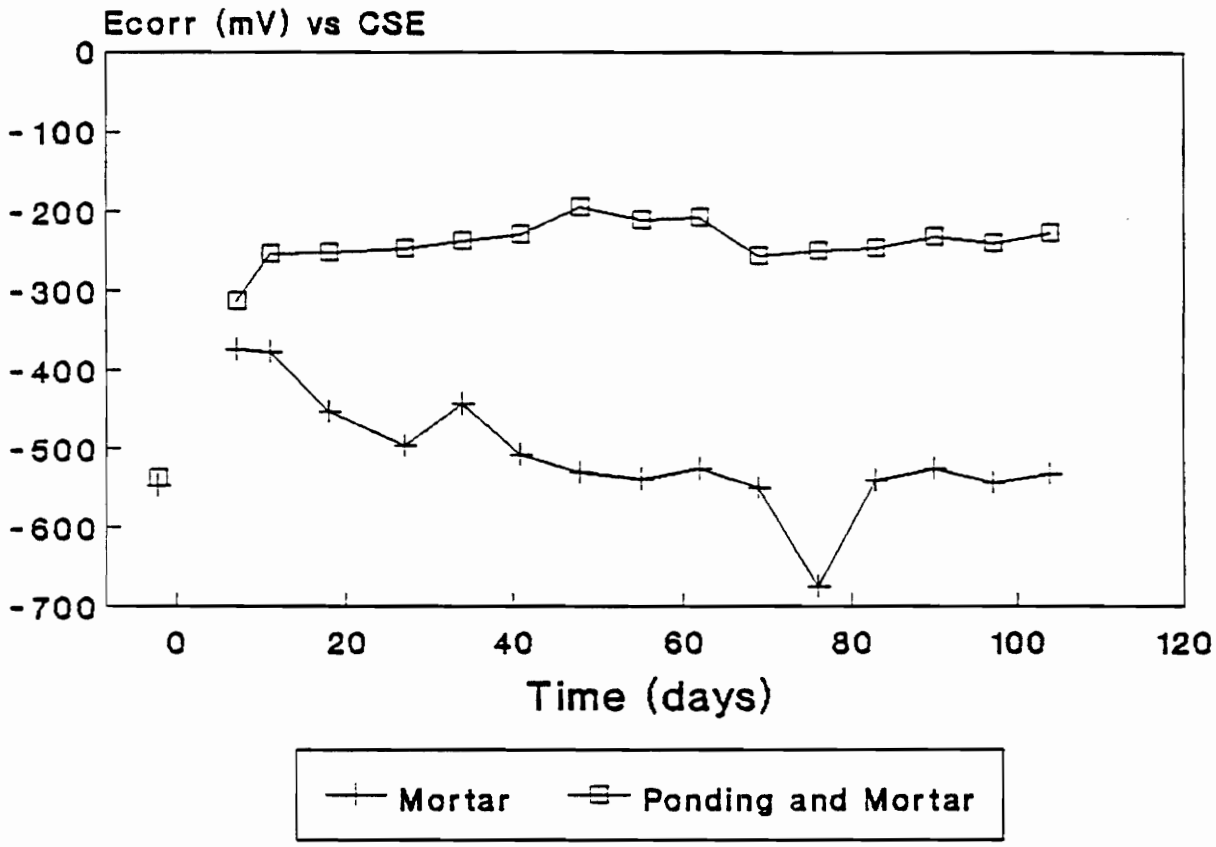

Figure 5A. Mean half-cell potentials for DCI treated specimens (B-2, B-3)

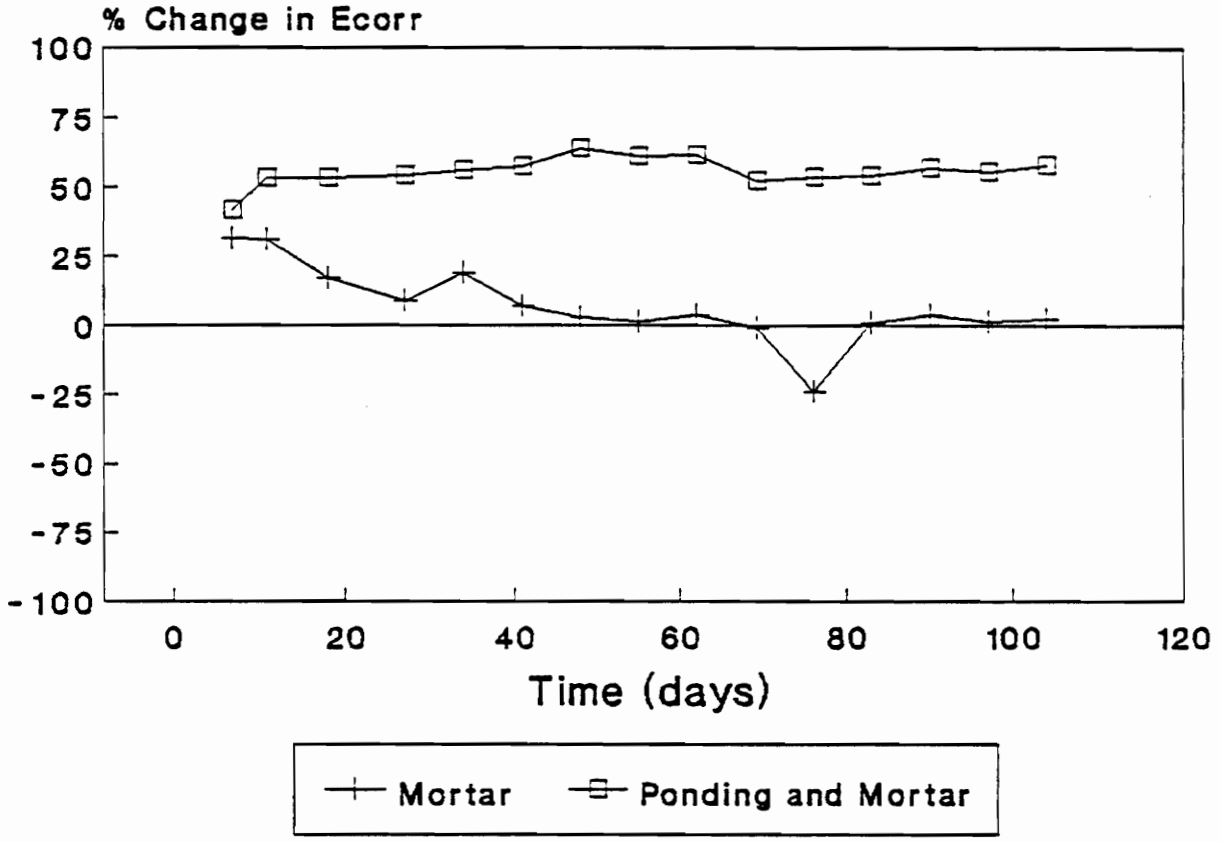

Figure 5B. Post-treatment percent change in half-cell potential for DCI treated specimens (B-2, B-3)

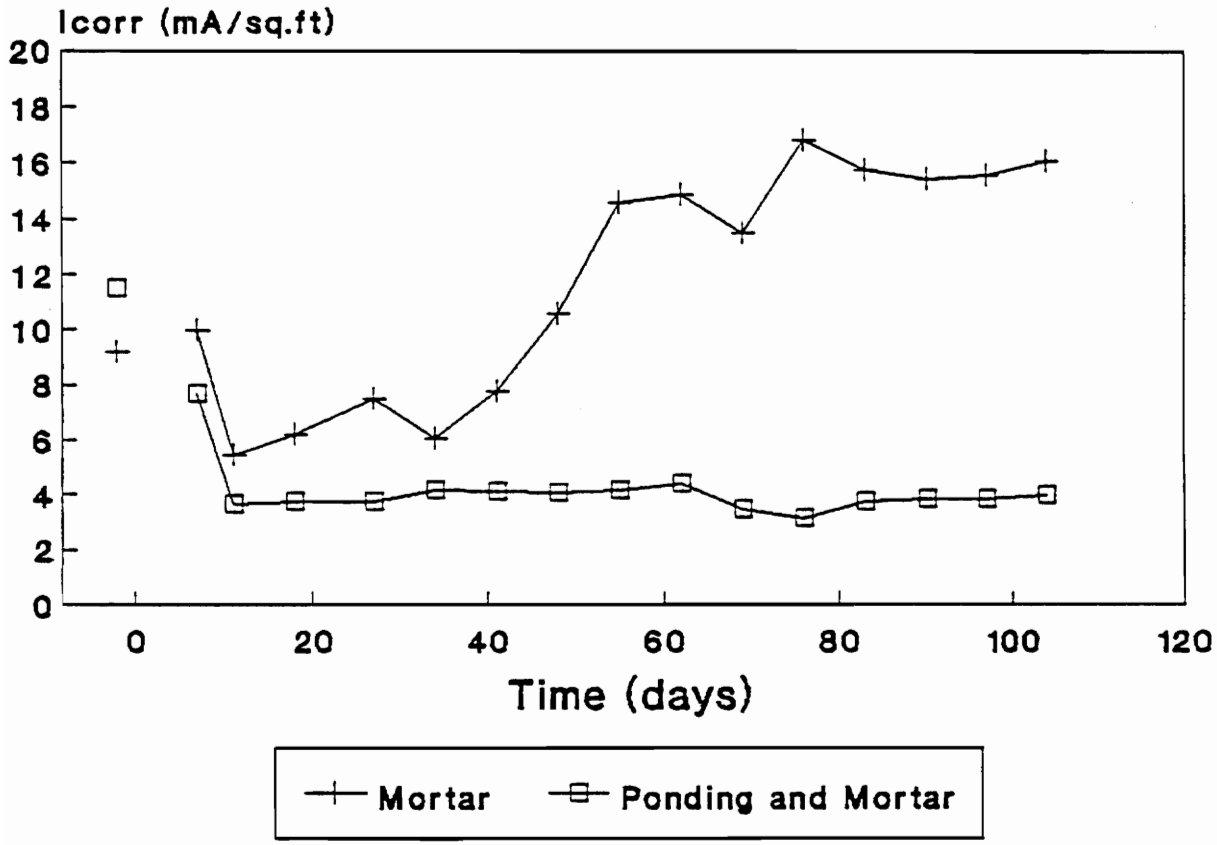

Figure 5C. Mean corrosion rates for DCI treated specimens (B-2, B-3)

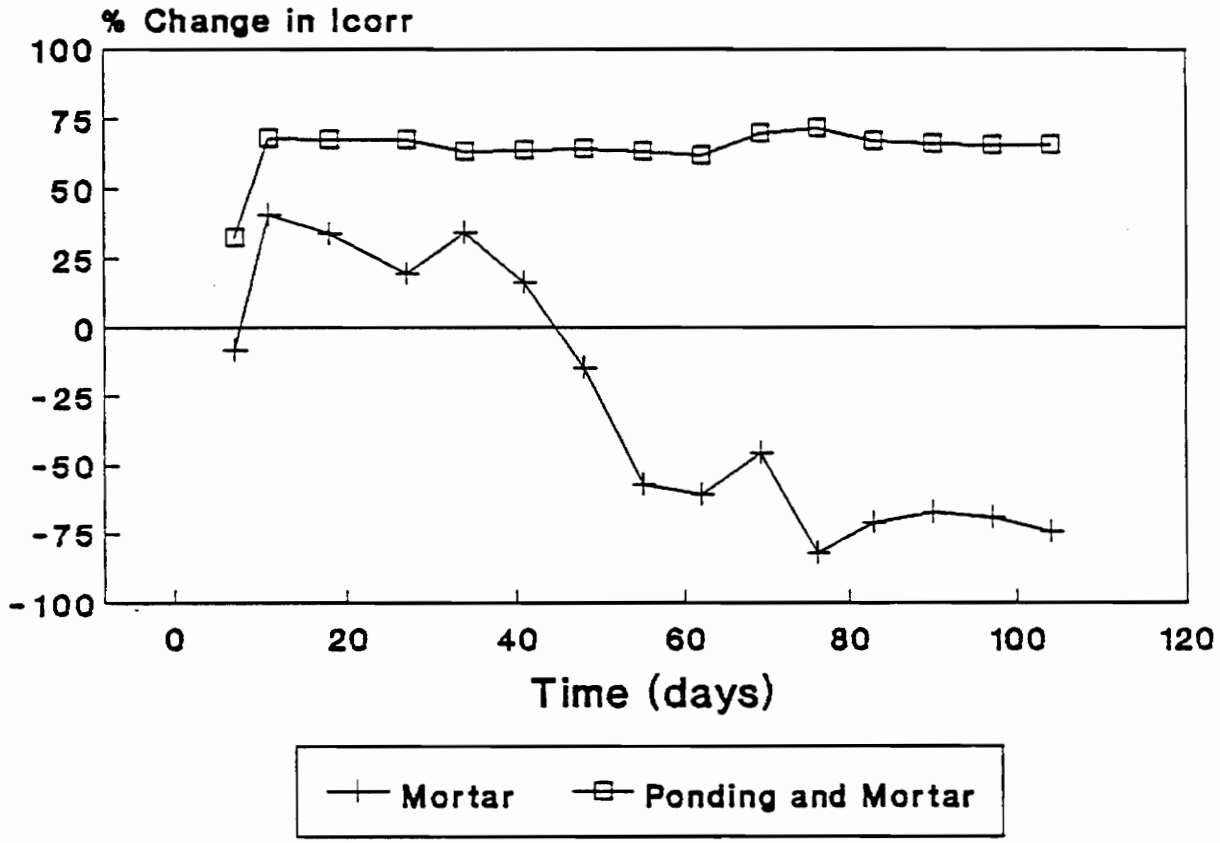

Figure 5D. Post-treatment percent change in corrosion rate for DCI treated specimens (B-2, B-3)

deteriorated rapidly after 40 days.

The DCI specimen treated both through ponding and mortar (B-3) exhibited highly effective corrosion abatement. After day 7, the specimen showed greater than a 50% increase in corrosion potential (more noble) and 60% decrease in corrosion rate for the entire exposure duration through day 104. The ponding appeared to allow the development of a sound passive layer on the rebars to inhibit the anodic reaction and promoted the diffusion of DCI into the concrete surrounding the rebars. This passive layer in combination with the high nitrite concentration provided by the ponding and subsequent mortar backfill was effective enough to provide a higher and longer corrosion abatement than just the mortar treated specimen.

The effectiveness of DCI ponding can also be seen in the three specimens (B-13, B-14, B-15) whose grooves were ponded with DCI and a polymer sealer was applied before backfilling with untreated mortar. The post-treatment E_{corr} and I_{corr} values for each polymer sealer applied (see Table 2) are shown in Figures 5E thru 5H. The corrosion measurements for the styrene-acrylic specimen (B-14) are expressed in terms of Bar A only, due to the development of a crack at the groove interface above Bar B which allowed the rapid diffusion of chlorides and the acceleration of corrosion.

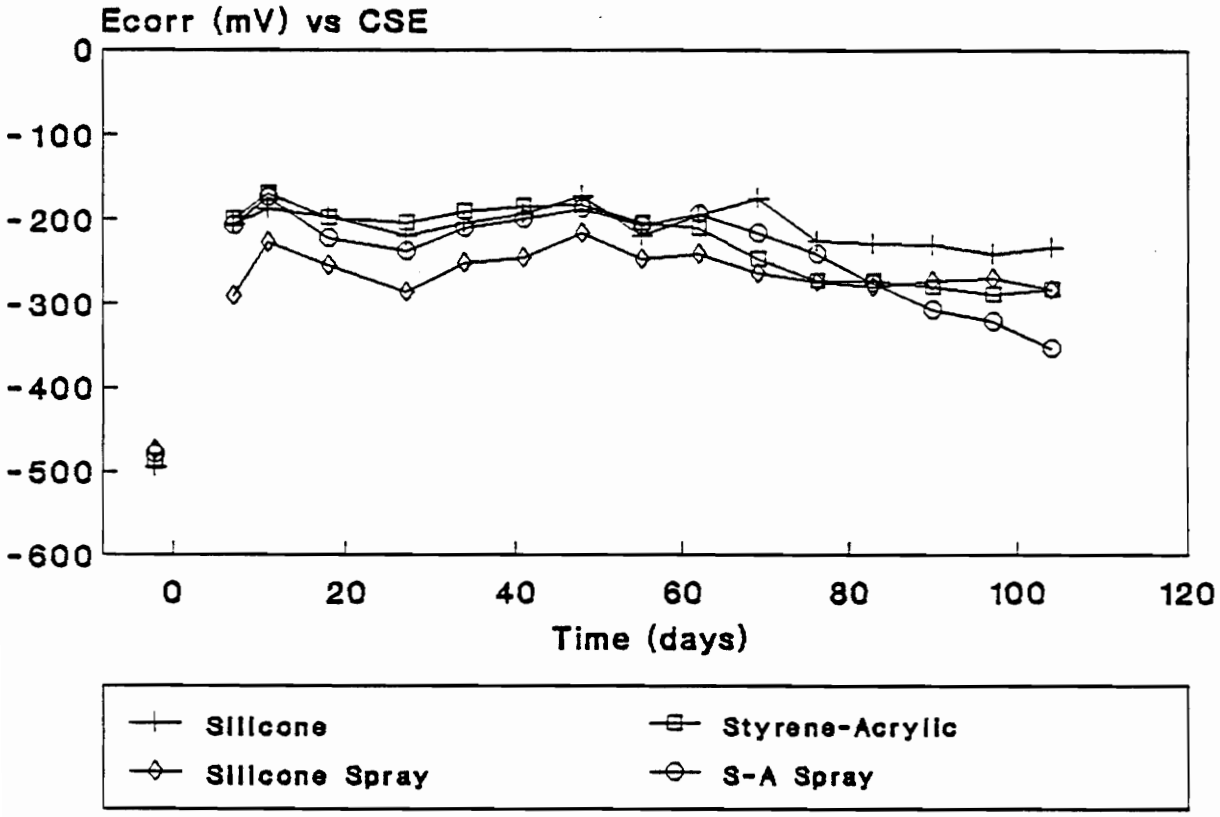

Figure 5E. Mean half-cell potentials for DCI ponded specimens with polymer sealers (B-13, B-14, B-15)

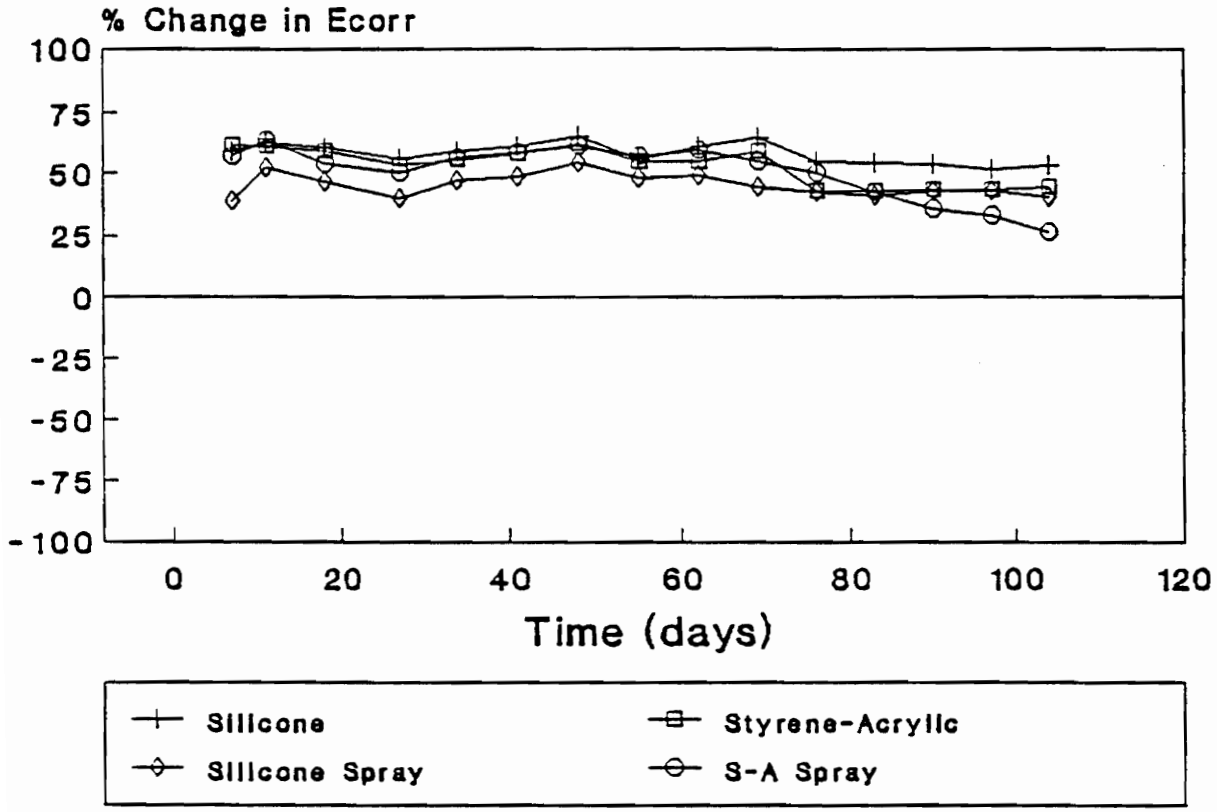

Figure 5F. Post-treatment percent change in half-cell potential for DCI ponded specimens with polymer sealers (B-13, B-14, B-15)

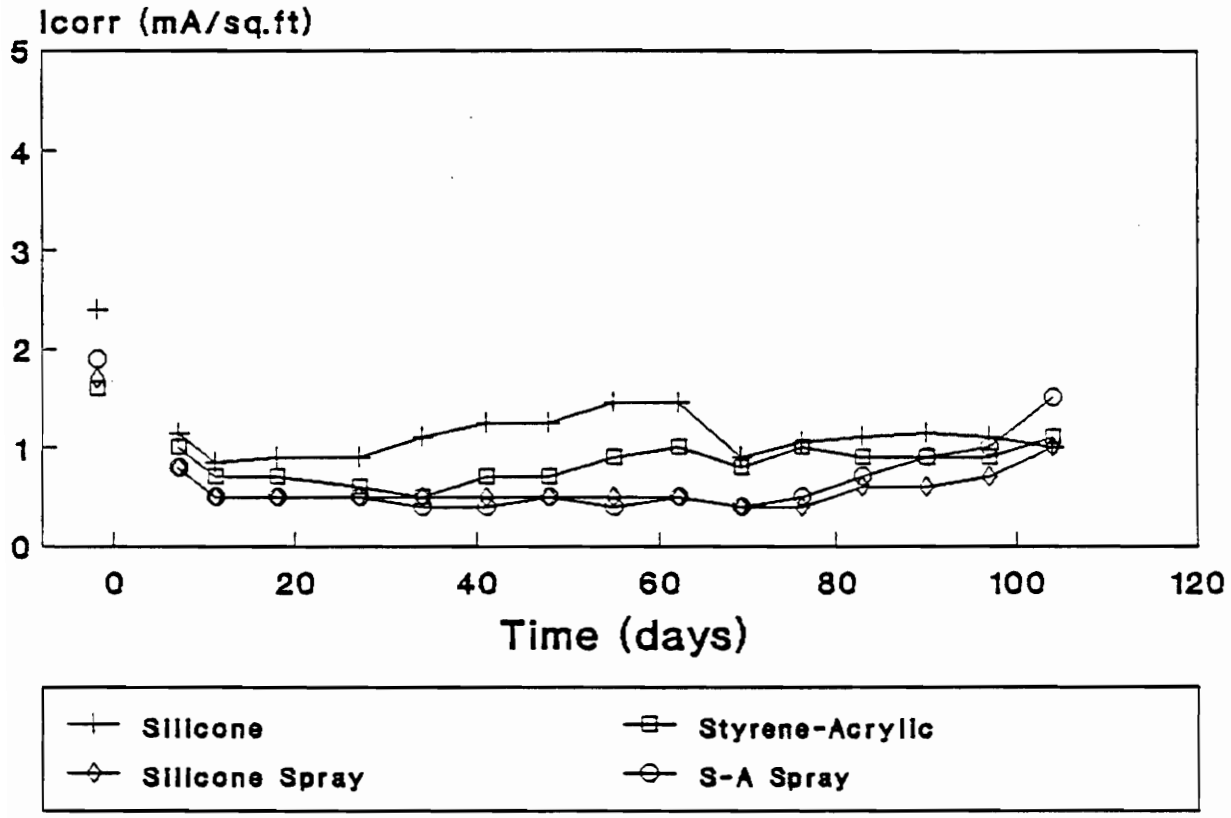

Figure 5G. Mean corrosion rates for DCI ponded specimens with polymer sealers (B-13, B-14, B-15)

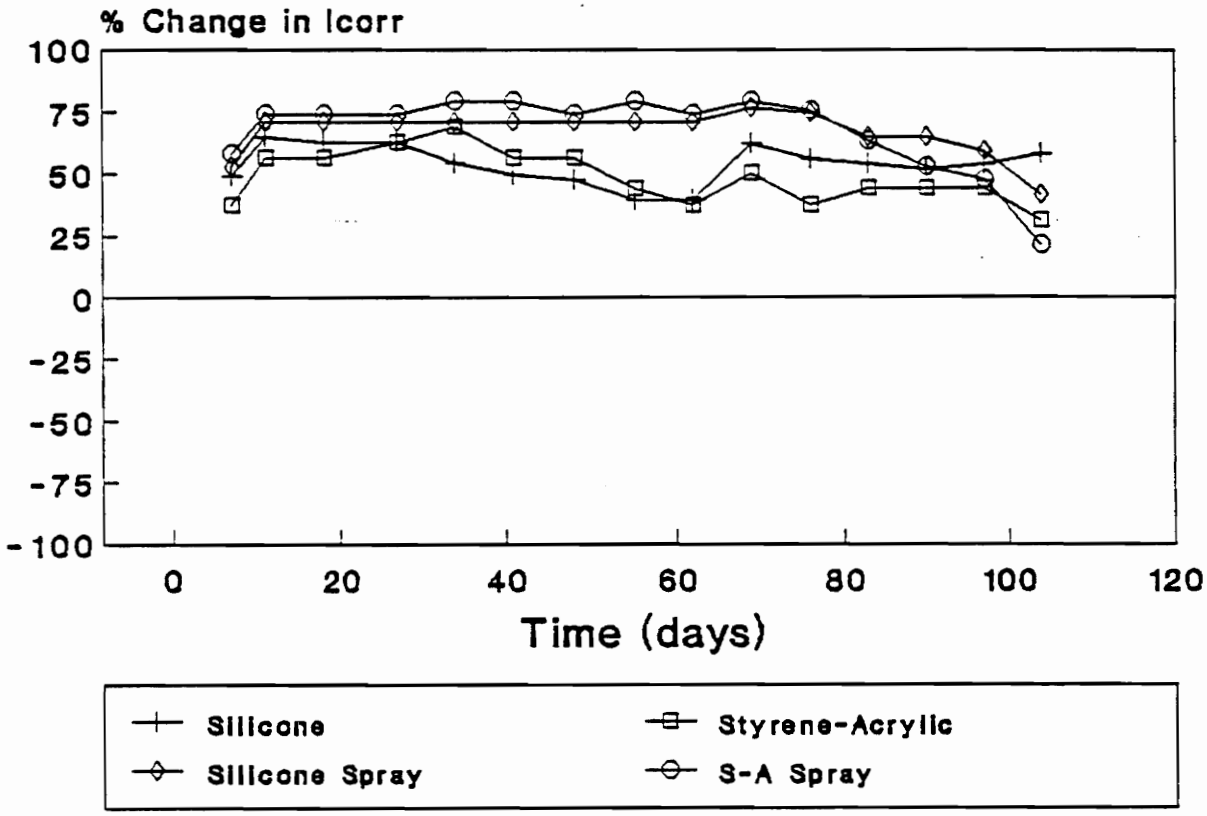

Figure 5H. Post-treatment percent change in corrosion rate for DCI ponded specimens with polymer sealers (B-13, B-14, B-15)

Without distinguishing between the sealers, both the E_{corr} and I_{corr} show an approximate 50% average improvement during the entire 104 days of exposure. However, this is somewhat misleading, because the pre-treatment corrosion rate for each of the specimens was low, falling between 1.5 and 2.5 mA/ft^2. The initial level of corrosion rate can conceivably play a factor in the magnitude of the % change in corrosion potential and rate after treatment. Any treatment method applied to specimens of low corrosion activity would reasonably be expected to cause a greater % change in magnitude than if applied to specimens of higher corrosion activity. Although the absolute change in magnitude would be smaller, the % change in magnitude would most likely be greater. This problem can only be overcome by using specimens of relatively identical corrosion rates or evaluated specimens of varying corrosion rates over a longer duration.

It cannot readily be determined to what degree the polymer sealers play in the corrosion abatement process. Since the DCI pond/mortar specimen showed great reduction in both corrosion potential and rate, it is reasonable to expect that the DCI ponding played a major role in the corrosion abatement of the polymer sealer specimens as well. It is possible that the sealers provided an additional barrier physical barrier to chloride ions, moisture, and

even oxygen diffusion, which would enhance the effectiveness of the DCI.

The sealers alone probably would not have been effective due to the level of chloride present in the specimens. At the rebar level, the specimens contained an average of 8.75 lbs Cl^-/yd^3 (see Table 4) of concrete which is more than seven times the accepted level of 1.2 lbs Cl^-/yd^3 needed to initiate corrosion in concrete. Without the DCI to effectively form a passive layer, the rebars would have still been subjected to this level of chloride underneath the sealant. Since the sealer was only placed in the groove, moisture can still diffuse through the concrete on either side of the groove and around the sealant. The sealers were evaluated in combination with DCI because when used in the field, sealers are applied in conjunction with an inhibitor treatment.

In comparing the different sealants, no great distinction could be made to determine the most effective between silicone and styrene-acrylic, or between ponding the sealers and spraying them. The spraying of the sealants appeared to be just as effective as applying them through ponding. The advantage to spraying, however, is that it uses less material and takes less time for application.

In the overall evaluation of the DCI treated specimens, treatment through a combination of ponding and backfilling

with treated mortar exhibited the greatest effectiveness in reducing corrosion. Such a treatment provides a sufficient NO_2^-/Cl^- ratio to suppress the anodic reaction and increase the stability of the passive film. The application of sealers may aid in the reduction of corrosion in combination with DCI, but to what degree they affect the corrosion process could not be determined.

4.2.3 Borate Treatments

The three specimens solely treated with borate based inhibitors were:

1. B-6, treated with sodium tetraborate placed in the mortar (SB Mortar).
2. B-7, treated with sodium tetraborate ponding and placed in the mortar (SB Pond/Mortar)
3. B-8, treated with zinc borate ponding and placed in the mortar (ZB Pond/Mortar).

The post-treatment corrosion potentials and corrosion rates for each specimen are shown in Figures 6A thru 6D.

All three treatments seemed to have had a similar effect on the evolution of E_{corr} for each specimen. More than a 25% increase in potential was experienced by all three specimens for the majority of the exposure duration. The final values were all greater than the pre-treatment values.

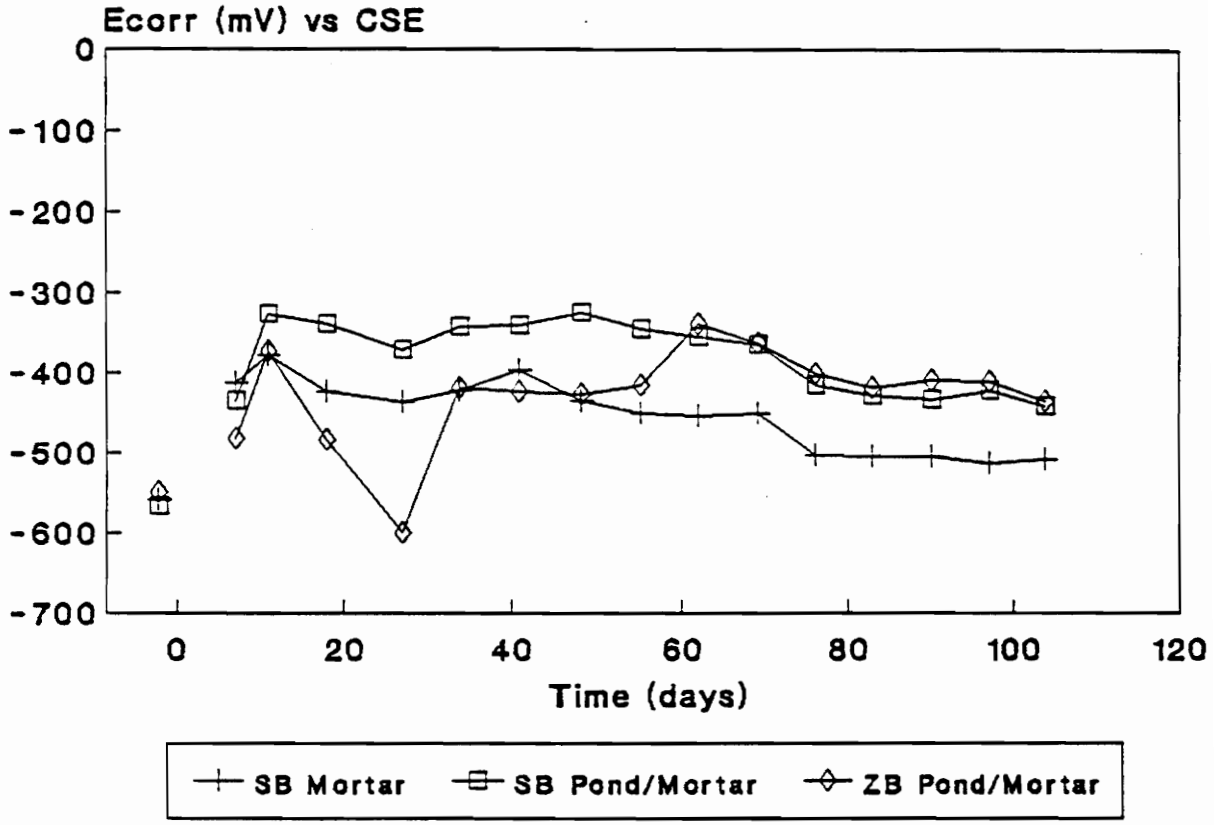

Figure 6A. Mean half-cell potentials for borate treated specimens (B-6, B-7, B-8)

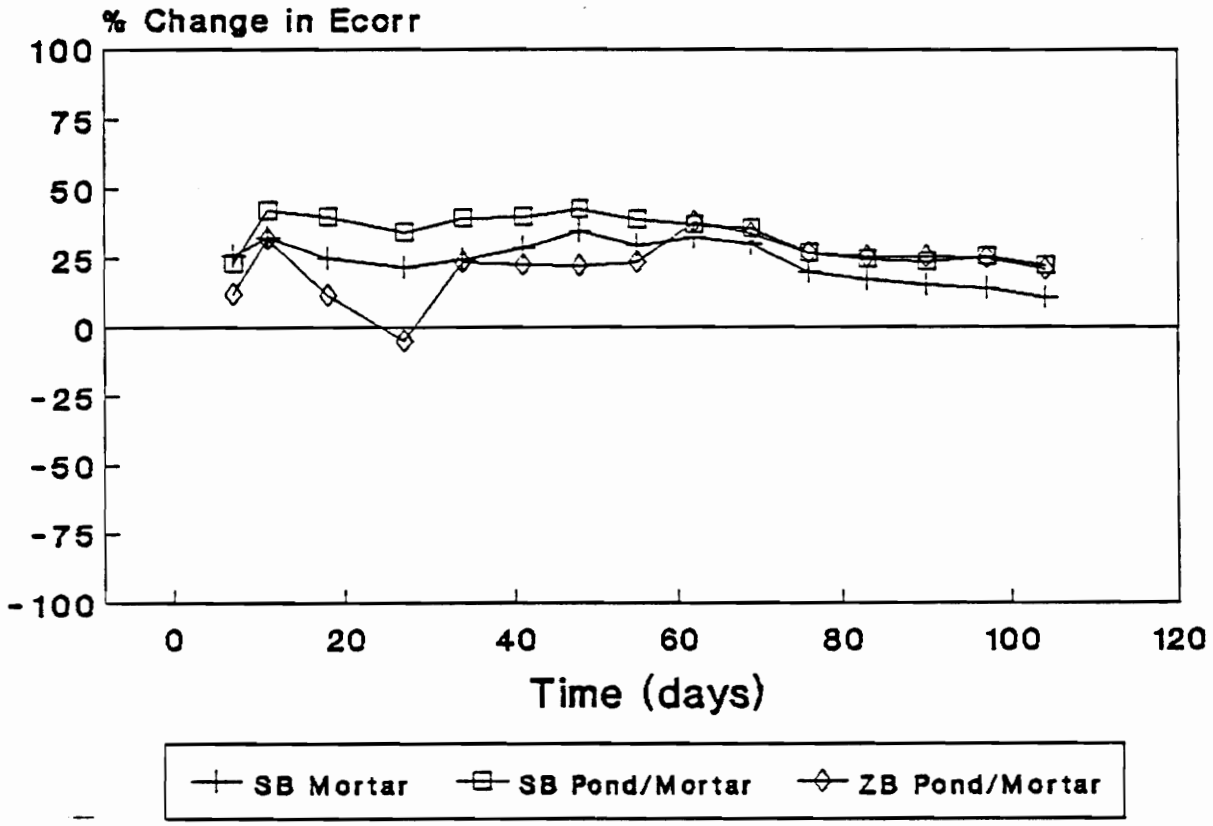

Figure 6B. Post-treatment percent change in half-cell potential for borate treated specimens (B-6, B-7, B-8)

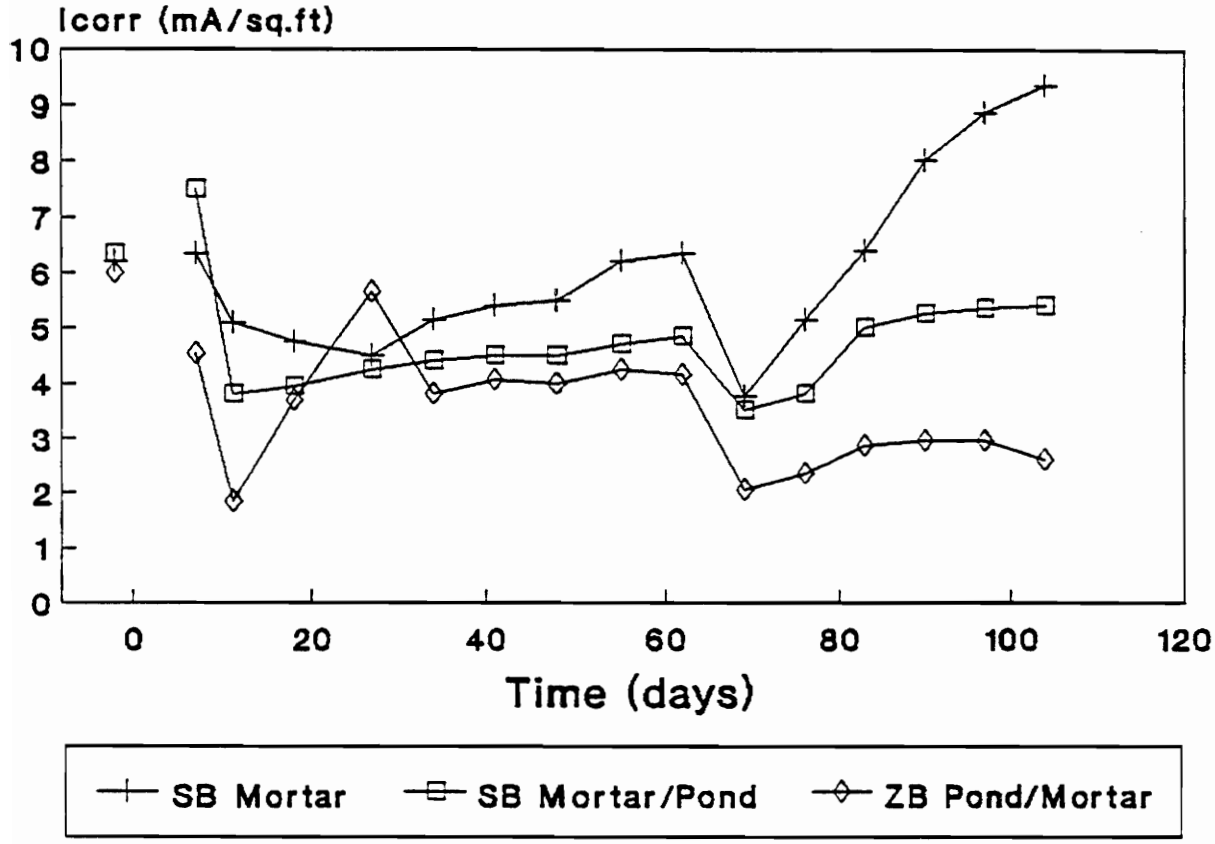

Figure 6C. Mean corrosion rates for borate treated specimens (B-6, B-7, B-8)

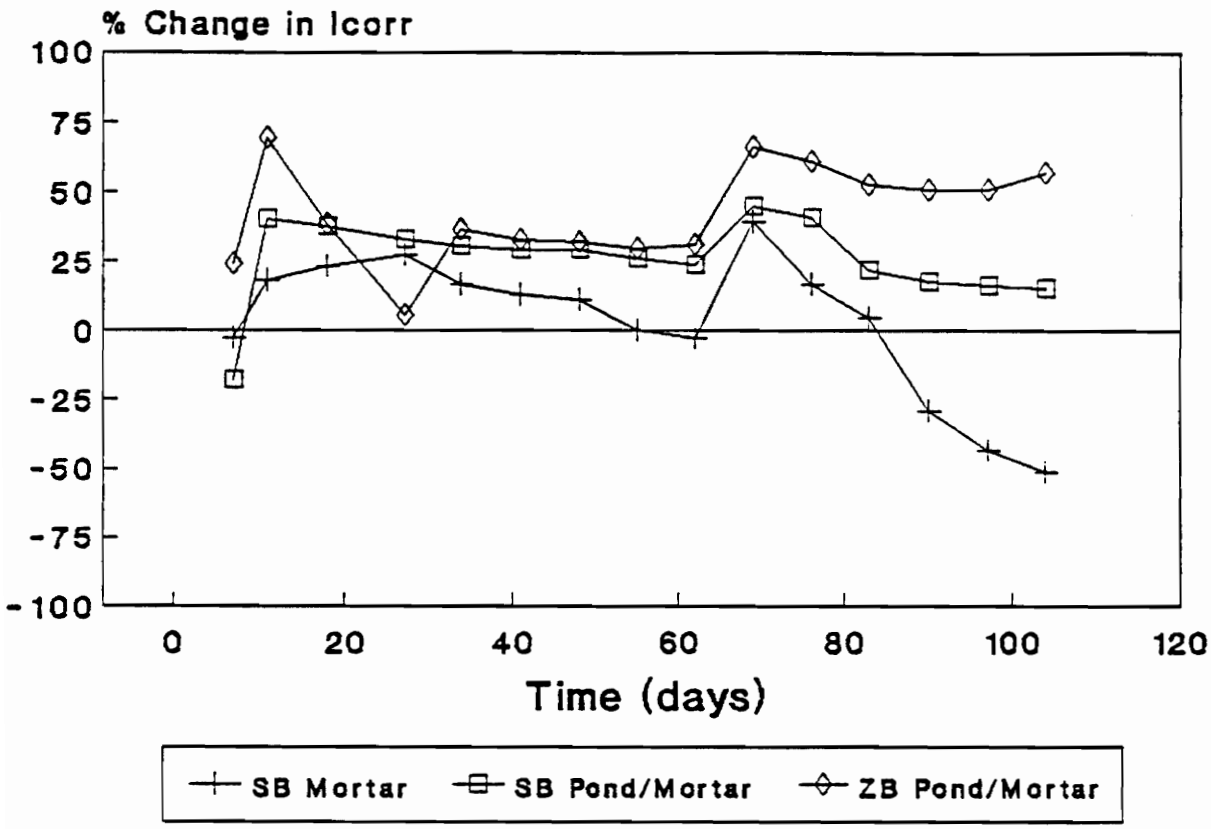

Figure 6D. Post-treatment percent change in corrosion rate for borate treated specimens (B-6, B-7, B-8)

A better comparison between the treatments can be made on the basis of the corrosion rates. The SB mortar specimen displayed the least effect of its treatment with a small decrease in corrosion rate between days 10 and 30, with an eventual 50% increase. Both the SB pond/mortar and ZB pond/mortar specimens showed an average 30% reduction in corrosion rate between days 20 and 60. At longer exposure duration the zinc borate treated specimen experienced an actual further decrease in corrosion rate exceeding 50%.

The borate treatments appeared to be effective for a longer duration when applied both as a ponding and in the mortar than if just added to the mortar. The additional concentration of borate provided via diffusion through the mortar appears to be adequate to extend the time of corrosion abatement. Of the treatments, both the SB and ZB pond/mortar treatments performed equally well initially, but the zinc borate specimen outperformed the SB at the later stages of exposure. This difference in behavior may be related to the rate of diffusion of the inhibitors through mortar. The zinc borate may have a higher rate of diffusion which allows it to better maintain a sufficient concentration at the rebar surface to stem corrosion.

In the borate treated specimens involving both ponding and placement in mortar, the concentration of borate at the rebar level was sufficient to allow the formation of a

corrosion inhibiting coating which served as a barrier to increased metal dissolution.

4.2.4 TCI Treatment

The treatment of specimen B-4 with a TCI (sodium monofluorophosphate) ponding appeared to be effective based on corrosion potentials as shown in Figure 7A. The corrosion potentials remained more noble than the pre-treatment value for the entire exposure period. However, the corrosion rate measurements shown in Figure 7B, show an example of how E_{corr} measurements can be misleading. The specimen experienced only a slight decrease in corrosion rate for 25 days before it began to decrease and exceed the pre-treatment corrosion rate. TCI inhibitor functions as a diffusional inhibitor, however, it does not appear as though it effectively diffused into the concrete surrounding the rebar to provide any substantial inhibition.

The ineffectiveness of TCI may have been a result of a low treatment concentration, but no standard application concentration has been developed except for in conjunction with surface application of de-icing salts (2.5% s/s salt). The concentration used, however, appeared to be high enough to stabilize the corrosion rate between days 35 and 70 at its pre-treatment I_{corr} level before deteriorating. Increased treatment concentrations may yield better results.

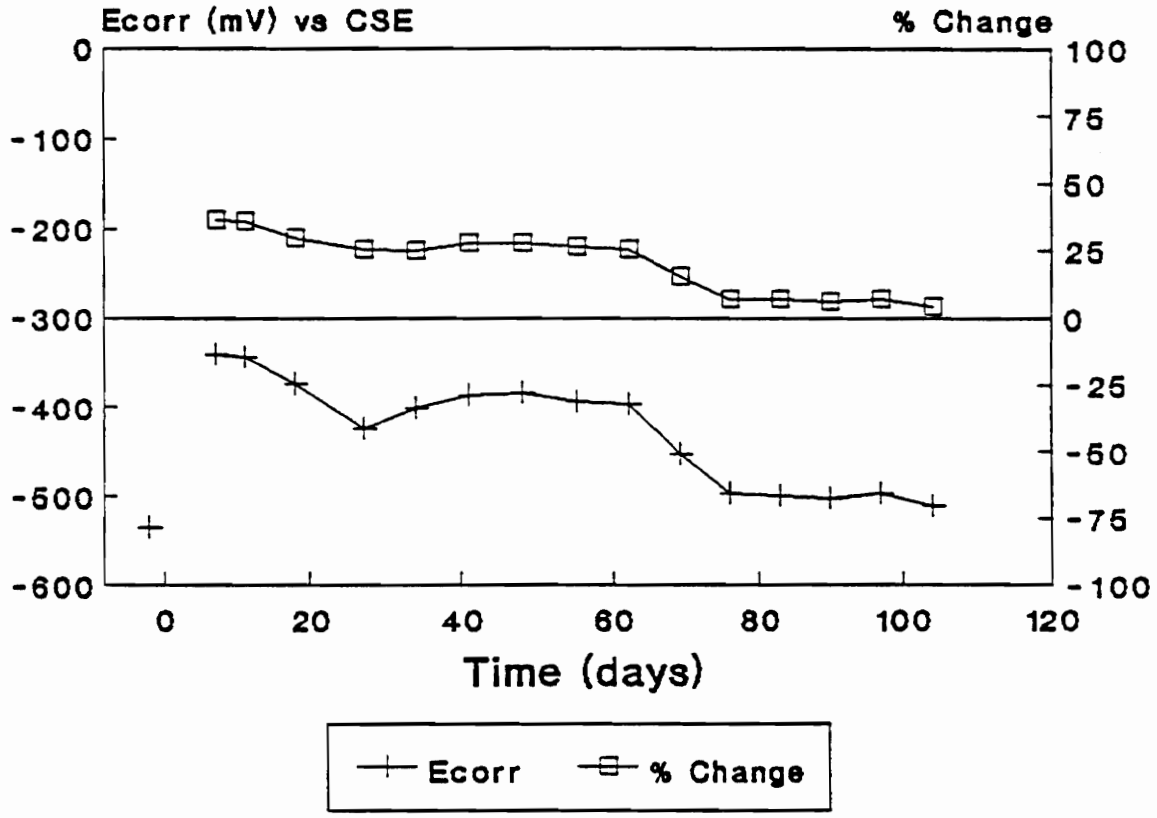

Figure 7A. TCI ponding specimen (B-4) mean half-cell potentials and post-treatment percent change

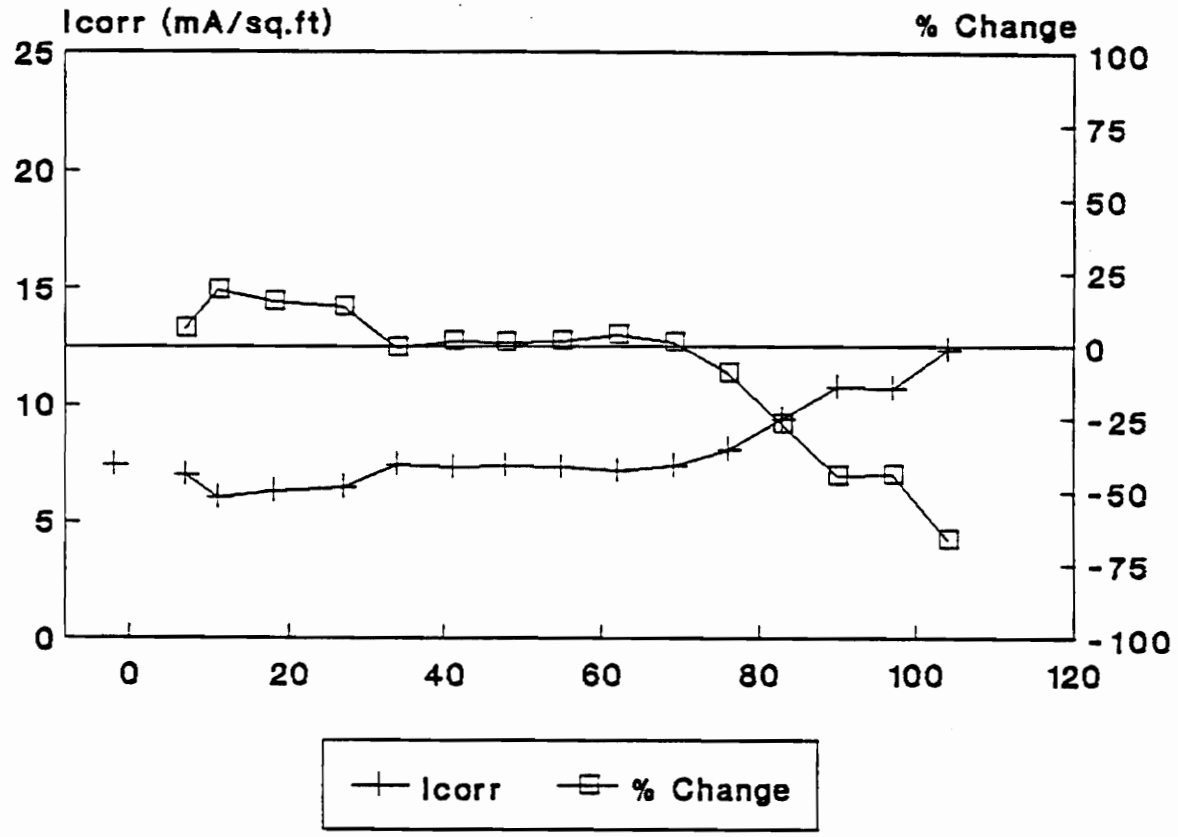

Figure 7B. TCI ponding specimen (B-4) mean corrosion rates and post-treatment percent change

4.2.5 Alox 901 Treatment

The performance of the Alox 901 treatment appeared promising as a possible corrosion inhibitor in concrete. The I_{corr} and E_{corr} measurements shown in Figures 8A and 8B indicate that the treatment was able to keep the corrosion activity from increasing from its initial state for the entire exposure duration. After day 10, the Alox treatment provided an average 40% reduction in corrosion rate for a span of 70 days before decreasing to 9% at day 104.

Although the corrosion rate began to increase over the last 20 days, this is not necessarily a sign of an inhibitor with only a short-term effect. Alox 901 is primarily used as a coating for metallic components exposed to corrosive environments. As a result, it is an extremely viscous liquid which aids in its adhesion to surfaces. In this study, the Alox 901 was dissolved in an ethyl alcohol solvent for ponding because it emulsifies in water. Since there is no known concentration standard for concrete, an equivalent .1M alcohol solution was made for comparison with the other .1M ponding solutions. Therefore, the Alox 901 concentration may not have been the optimum for concrete applications.

The viscous and oily properties of Alox 901 may have caused poor adhesion between the groove and backfilled mortar interface. This could have contributed to the

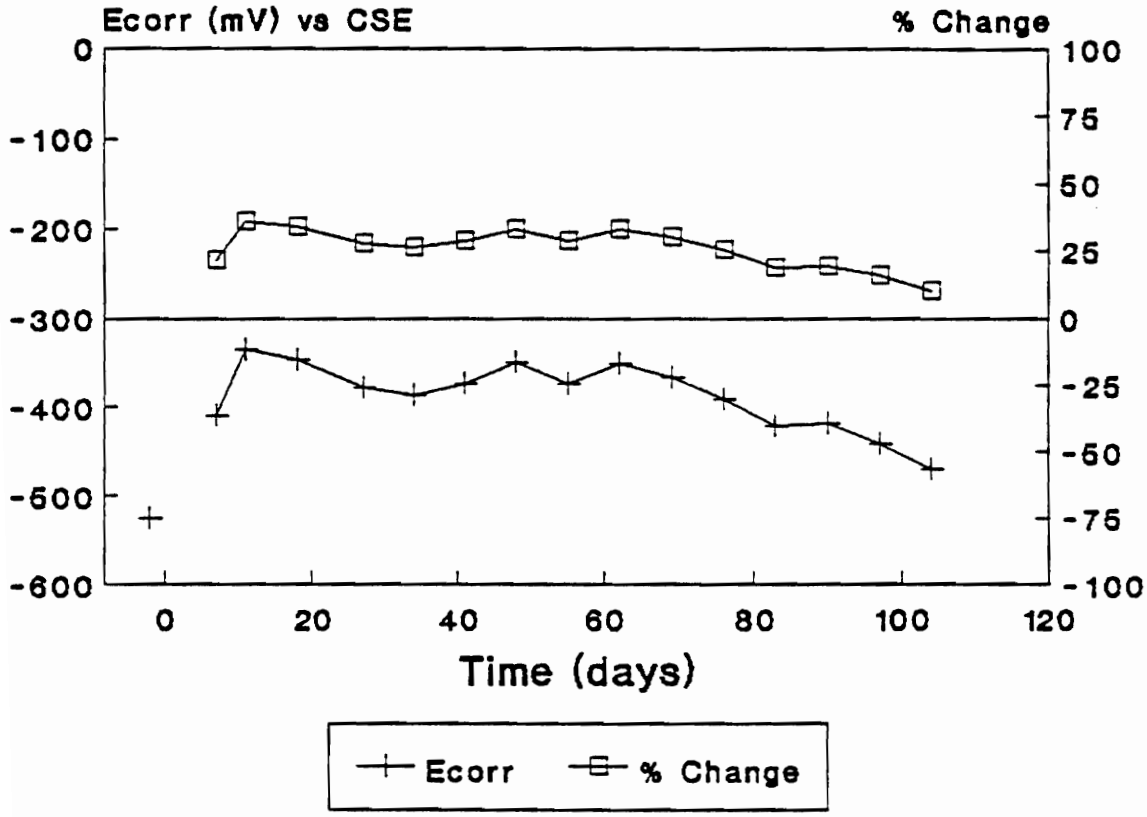

Figure 8A. Alox 901 ponding specimen (B-9) mean half-cell potentials and post-treatment percent change

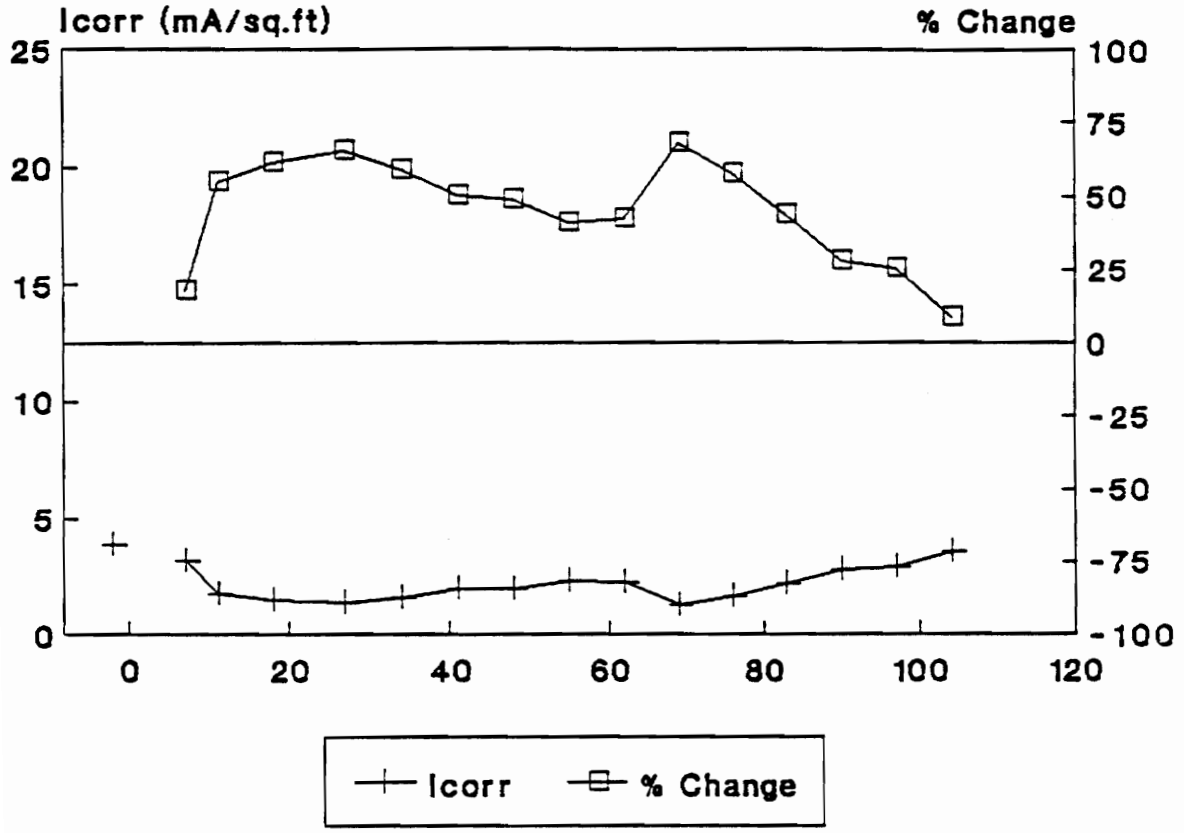

Figure 8B. Alox 901 ponding specimen (B-9) mean corrosion rates and post-treatment percent change

accelerated diffusion of chlorides along this interface, possibly reducing the inhibitor's effectiveness.

4.2.6 Cortec Inhibitor Treatments

The Cortec vapor phase inhibitors were used in several combinations and showed highly effective results both short-term and long term as displayed in Figures 9A thru 9D. Two treatments were applied to specimens of Set A (A-13, A-15) which were highly corroded and exhibiting high corrosion rates, while a third treatment was applied to a specimen of Set B (B-16) with an extremely small corrosion rate.

Cortec 1337 is a surface inhibitor while 1609 is used as an admixture. Cortec 1337 was evaluated applied to the surface of a specimen and applied to grooves, while 1609 was evaluated as a possible ponding treatment as well as being put in the mortar. The surface treatment with 1337 and the combination 1337 pond/1609 mortar treatment could only be evaluated for a short period due to the development of cracks in the specimens.

The application of 1337 to a specimen's surface resulted in nearly a 100% reduction in corrosion rate from 23.5 to 0.75 mA/ft^2. However, cracks developed during drying after the first ponding cycle. The cracks allowed for the ingress of high concentrations of sodium chloride solution during subsequent pondings. As a result, the

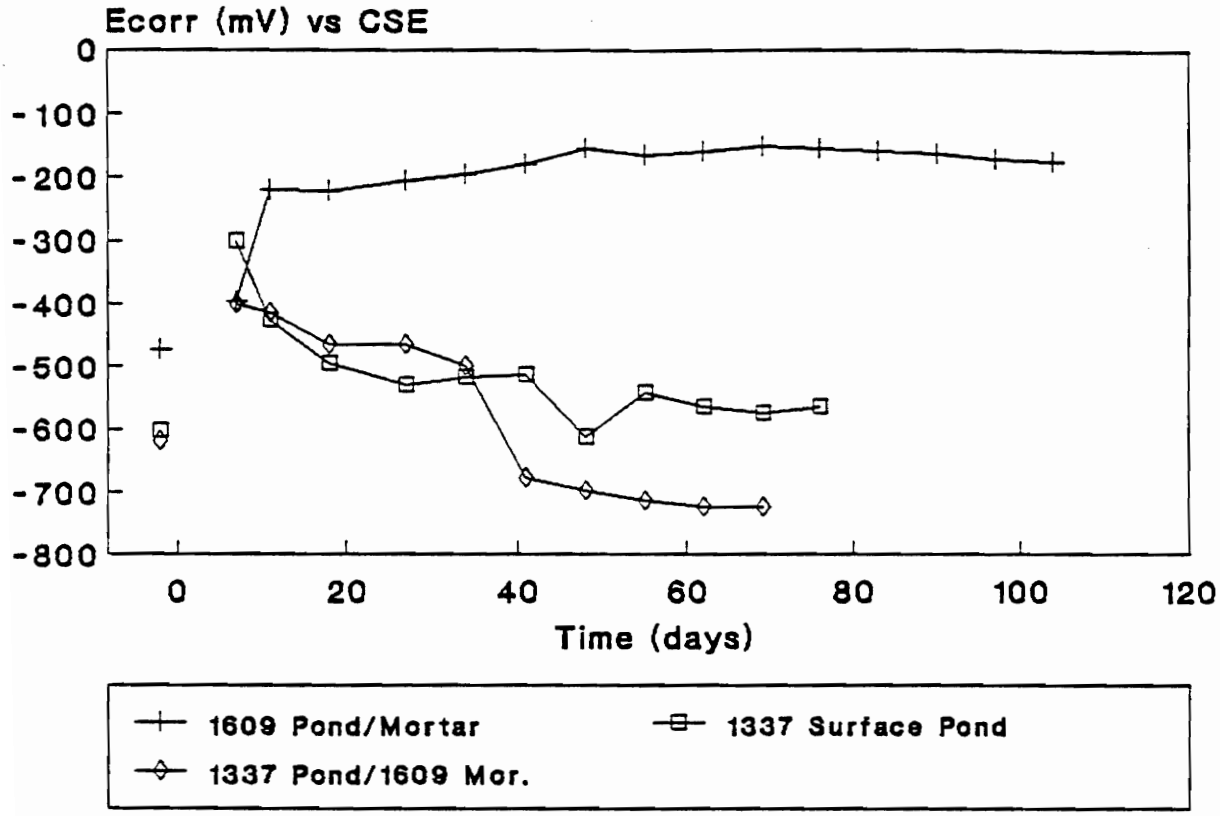

Figure 9A. Mean half-cell potentials for Cortec inhibitor treated specimens (B-16, A-13, A-15)

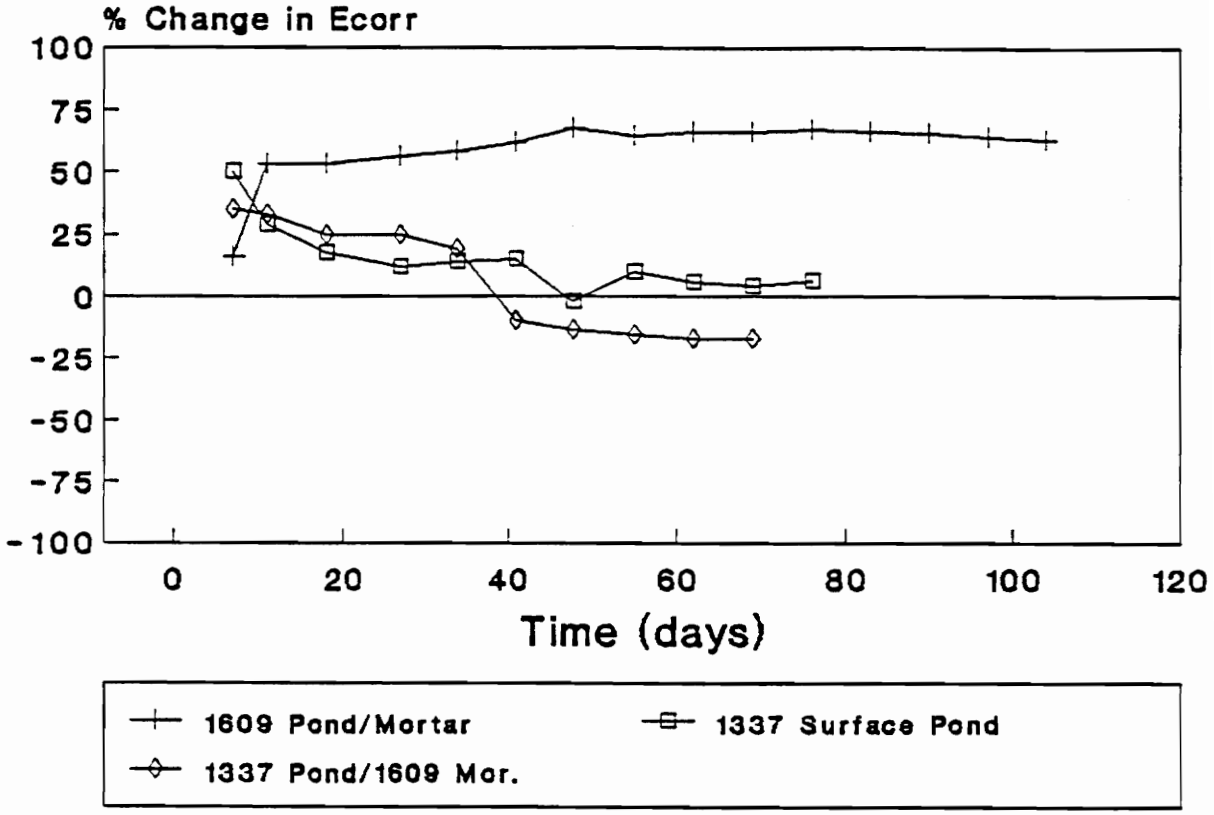

Figure 9B. Post-treatment percent change in half-cell potential for Cortec inhibitor treated specimens (B-16, A-13, A-15)

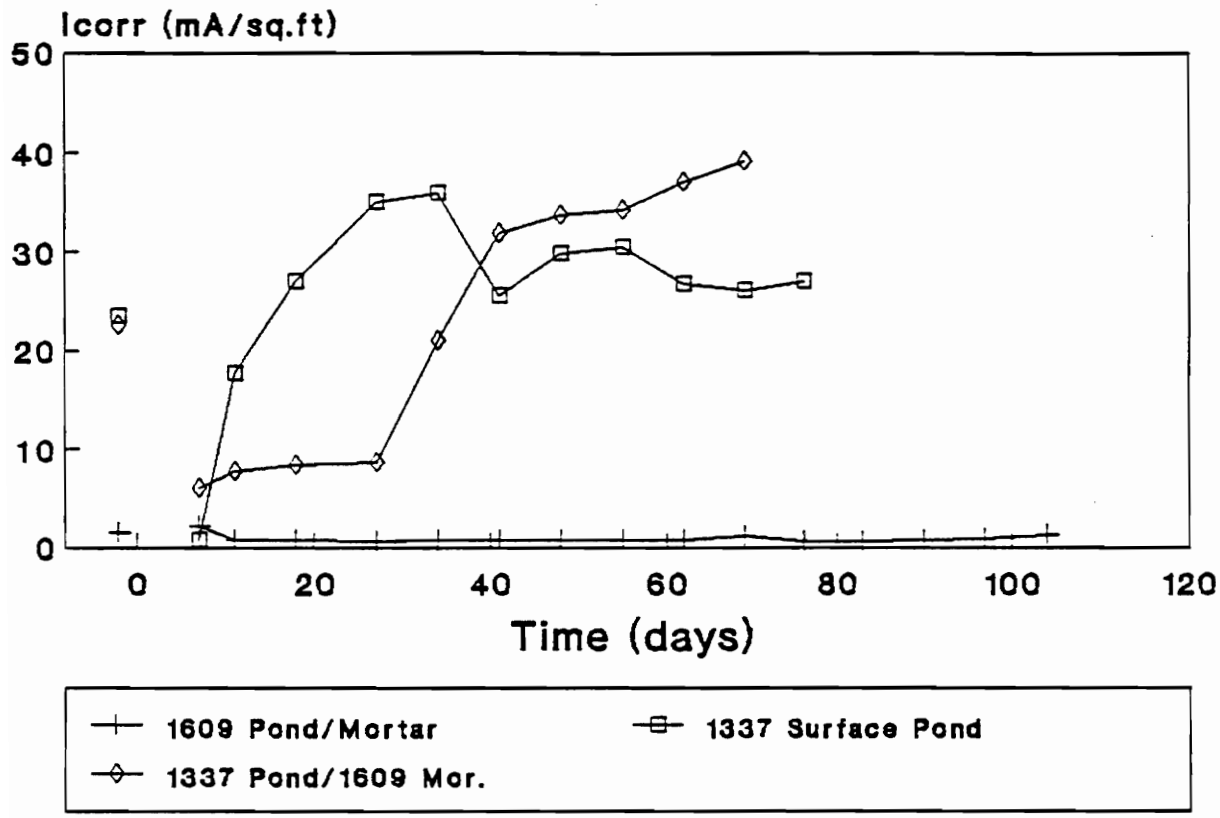

Figure 9C. Mean corrosion rates for Cortec inhibitor treated specimens (B-16, A-13, A-15)

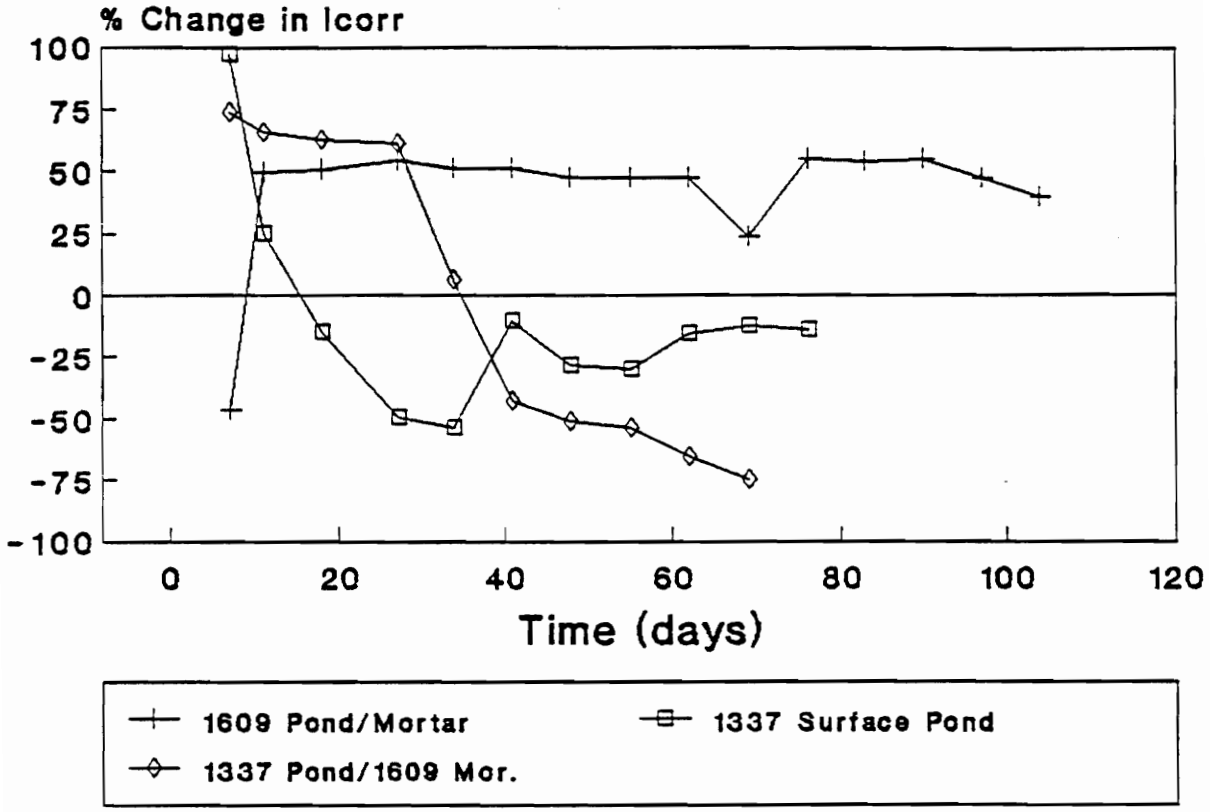

Figure 9D. Post-treatment percent change in corrosion rate for Cortec inhibitor treated specimens (B-16, A-13, A-15)

performance of the inhibitor as a surface treatment could not adequately be evaluated after 10 days.

The combination of a 1337 ponding and 1609 being admixed into the mortar initially proved to be a highly effective inhibitor treatment. During the first 30 days of exposure, the treatment resulted in an average I_{corr} decrease of more than 60%. However, the development of cracks at the groove/mortar interface over each bar allowed the rapid influx of chlorides and resulted in a rapid increase in corrosion rate.

The use of 1609 as a ponding inhibitor was experimental, but resulted in a stable reduction in both E_{corr} and I_{corr}. The specimen in which 1609 was ponded and placed in mortar had an low pre-treatment corrosion rate of 1.45 mA/ft^2, therefore the magnitude of corrosion reduction was small but the percent change in magnitude was great. It is reasonable to expect better performance because of the low corrosion rate, but the stability of the corrosion rate drop in combination with the large drop in E_{corr} magnitude further supports the treatment's effectiveness.

Over a duration of 104 days, the treatment was able to prevent the corrosion rate from increasing from its low initial value, even though the specimen's chloride concentration was increasing. In addition, the corrosion potential increased (became more noble) more than 60% and

remained at this level for the entire exposure duration. No other treatment besides DCI ponding was able to keep the corrosion potentials of a specimen so low for such a duration, regardless of the magnitude of the pre-treatment corrosion rate.

Both Cortec inhibitors appear to be effective corrosion abatement treatments. The ponding of either inhibitor provides adequate reduction in corrosion activity via the vapor phase transport of the inhibitor to the rebar surface and the resulting formation of a protective monolayer. This monolayer reduces both the anodic and cathodic reaction rates. The long-term effectiveness of 1337 ponding treatments was unable to be evaluated and the determination of the more effective ponding agent between 1337 and 1609 could not readily be made. However, since 1337 is recommended as a ponding inhibitor by the manufacturer, it is reasonable to expect 1337 to perform better than 1609 when ponded. The degree to which the 1609 admixed in the mortar plays in corrosion abatement could not readily be determined from the treatment combinations.

4.2.7 Hydroxylapatite Treatments

The treatment effects of using hydroxylapatite alone and in combination with inhibitors can be seen in the E_{corr} and I_{corr} measurements shown in Figures 10A thru 10D. The

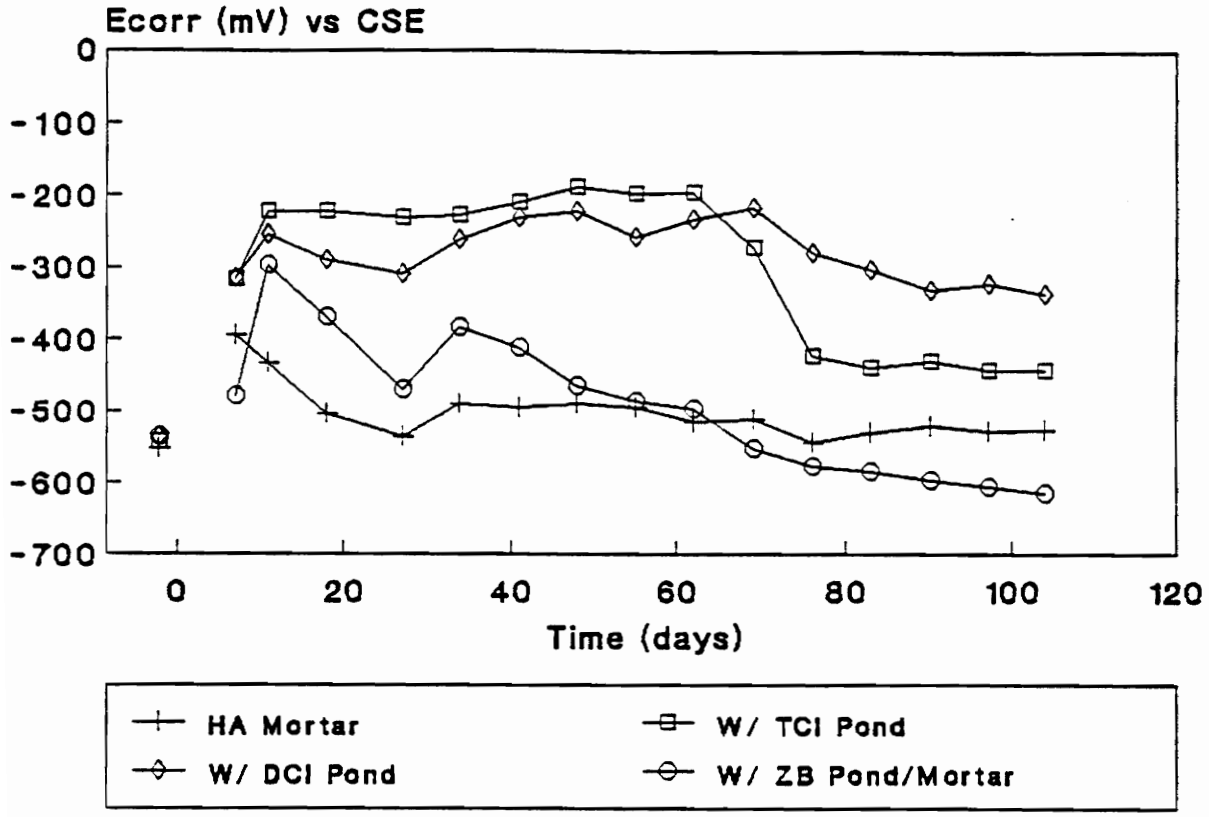

Figure 10A. Mean half-cell potentials for hydroxylapatite treated specimens with added inhibitors (B-5, B-10, B-11, B-12)

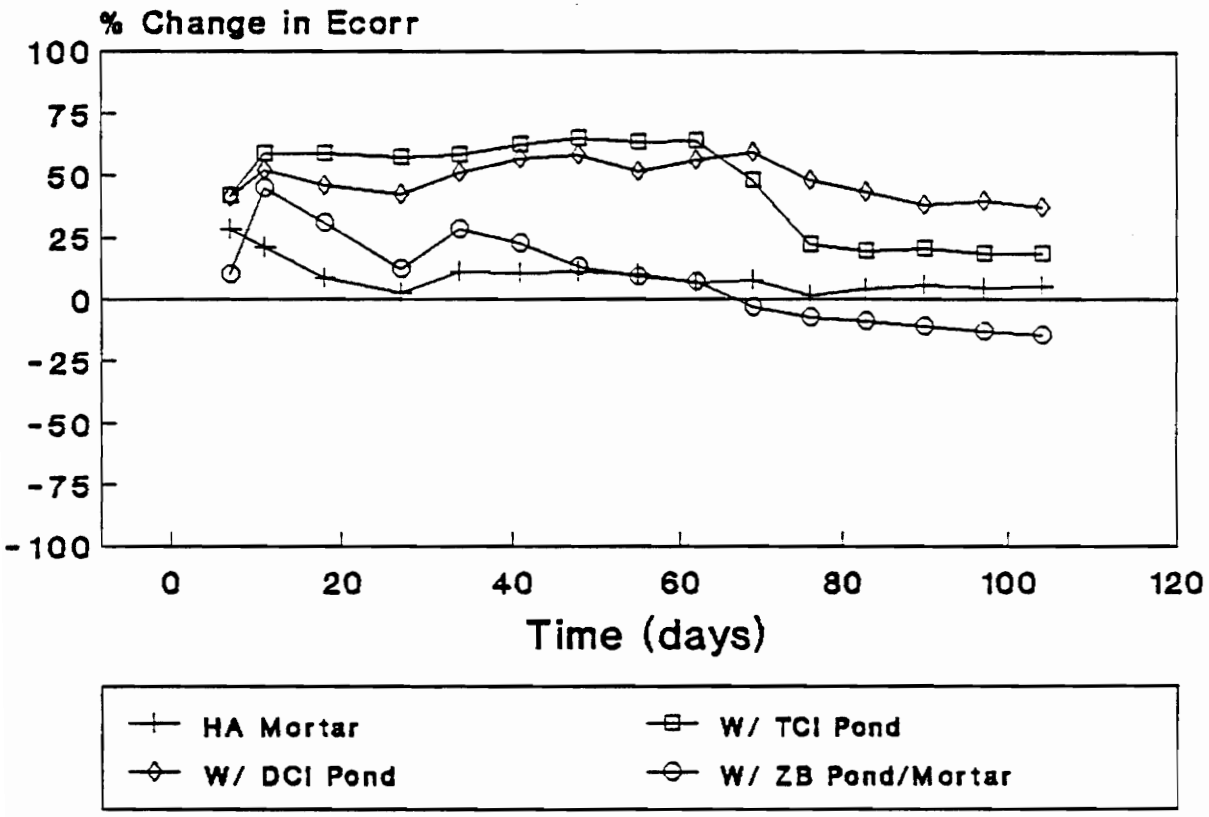

Figure 10B. Post-treatment percent change in half-cell potential for hydroxylapatite treated specimens with inhibitor additions (B-5, B-10, B-11, B-12)

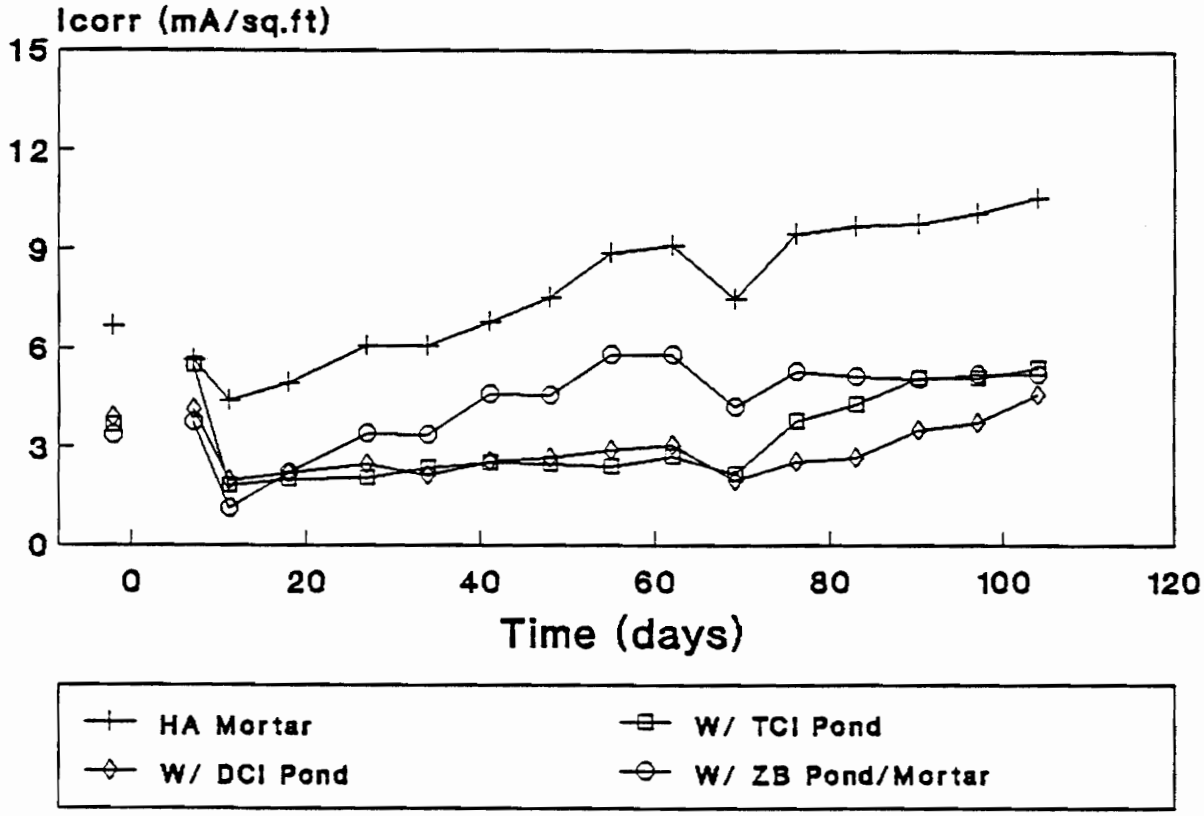

Figure 10C. Mean corrosion rates for hydroxylapatite treated specimens with added inhibitors (B-5, B-10, B-11, B-12)

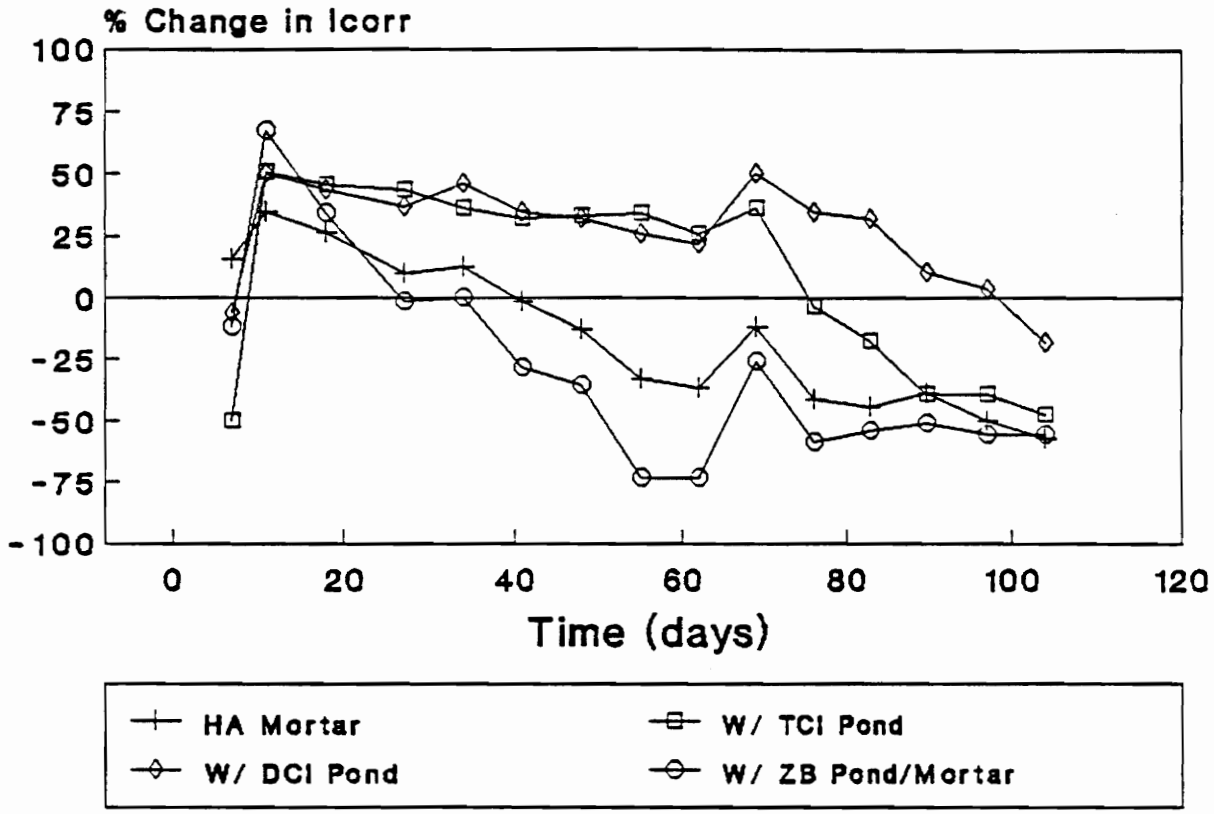

Figure 10D. Post-treatment percent change in corrosion rate for hydroxylapatite treated specimens with inhibitor additions (B-5, B-10, B-11, B-12)

admixing of hydroxylapatite (HA Mortar) to the backfilled mortar showed little effect on the corrosion rate of the treated specimen. However, this is not an accurate measure of the mineral's chloride ion scavenging ability. The chloride threshold level at the rebar surface was equivalent to 12.36 lbs Cl^-/yd^3 (see Table 4). Therefore, even with the removal of the grooved concrete, it could be expected that a chloride level sufficient to still drive the corrosion process would still exist in the concrete surrounding the unexposed portions of the rebars. Since hydroxylapatite is insoluble in high pH environments, it has no ability to diffuse to possibly scavenge chloride ions. The only chloride ions that come in contact with hydroxylapatite are those that diffuse through the backfilled mortar.

The use of hydroxylapatite in combination with an inhibitor treatment showed little benefit when used in combination a zinc borate ponding and mortar admixture. However, when used with TCI ponding or DCI in mortar, there appeared to be some improvement in performance. Both the TCI and DCI specimens with apatite sustained a longer reduction in corrosion rate than the TCI and DCI specimens without apatite. This could possibly be due to chloride scavenging, synergistic effects, or the fact that the apatite specimens with TCI and DCI had pre-treatment

corrosion rates lower than the corresponding specimens without apatite. Despite this improvement, the 30-40% reduction in corrosion rate for both specimens lasted only for a duration of 60 days before increasing to rates higher than pre-treatment.

Hydroxylapatite does not appear to be an effective treatment in itself after removal of chloride contaminated concrete. However, if an inhibitor is used in combination to backfilling with hydroxylapatite treated mortar, some benefit in performance may result.

4.3 Selection of Most Effective Treatments

In determining the most effective corrosion abatement treatments based solely on corrosion measurements, the treatments were evaluated in terms of greatest % improvement in I_{corr}, I_{corr} improvement at selected days during exposure, and length of I_{corr} improvement. The comparison of the best treatment or treatments from each experimental group is detailed in Table 6.

All the following treatments have indicated effectiveness in abating corrosion based on electrochemical measurements and are possible candidates for reinforced concrete treatment after removal of chloride contaminated concrete:

1. DCI ponding and in mortar

Table 6. Treatment Effectiveness Comparison Measures

Treatment	Percent Change in I_{corr}				Final I_{corr} < Pre-Treatment I_{corr} ?
	Greatest	Day 11	Day 55	Day 104	
DCI pond/mortar	71.7	67.8	63.3	65.5	Yes
TCI pond	19.4	19.4	2.0	-66.2	No
Zinc Borate pond/ mortar	69.2	69.2	29.5	57.0	Yes
Sodium Borate pond/mortar	40.6	40.1	25.9	15.3	Yes
Alox 901 pond	65.4	55.2	41.3	9.0	Yes
Hydroxylapatite w/ DCI mortar	50.0	50.0	25.7	-18.0	No
Cortec 1609 pond/ 1609 mortar	55.1	49.8	47.4	39.7	Yes
Cortec 1337 pond/ 1609 mortar	74.0	65.5	-53.7	-75.0	No[1]

[1]Cracks formed in specimen allowing chloride ingress, therfore, values at days 55 and 104 are not representative of treatment corrosion abatement.

2. Alox 901 ponding
3. Cortec 1337 ponding and Cortec 1609 in mortar
4. Cortec 1609 ponding and Cortec 1609 in mortar
5. Zinc borate or sodium tetraborate ponding and in mortar

Of the above treatments, DCI showed the greatest effectiveness based on the level in which a high pre-treatment corrosion rate was reduced and the duration of its effectiveness. The borate based treatments also proved effective for the same duration but at an average corrosion rate reduction of 30-40% compared to DCI's 50-60%. The other three treatments appeared effective, but due to a low pre-treatment corrosion rate or the formation of cracks, their electrochemical data is not as well defined as for the DCI and borate treatments.

Although hydroxylapatite treated specimens did not show great reduction in corrosion or sustained reduction in corrosion, the use of the apatite mineral cannot be rejected as a whole. The hydroxyl form of apatite may not have performed well, but other forms may be more effective in exhibiting any chloride ion scavenging ability.

4.4 Mortar Strength and Resistivity Evaluation

Mortar cube strength and resistivity was evaluated to

determine any deleterious effects that treatments or level of treatments may have on cement mortar properties. The compressive strength measurements would indicated any set retarding or accelerating properties of the treatments used as admixtures. The resistivity would also indicate retardation or acceleration of set based on the fact that resistivity is a function of permeability which increases with higher degrees of hydration. In addition, the resistivity measurements could possibly detect the contribution of ionic species to the mortar which may contribute to increased current flow. An increase in the ability of current to flow through the mortar would increase the rate of corrosion of rebar embedded in the mortar.

4.4.1 Treatment Effects on Mortar Compressive Strength

Compressive strength measurements taken over a span of 20 days indicated little difference in strength between the control group and those cubes treated with Cortec 1609 or hydroxylapatite. To illustrate this, Figure 11 shows a comparison of the control cube strengths with the strengths of the cubes containing the highest concentrations of Cortec 1609 (0.45% l/s cement) and hydroxylapatite (25.00% s/s cement). There was also no observed effect of the concentration level within the Cortec 1609 and hydroxylapatite specimens. The compressive strength data

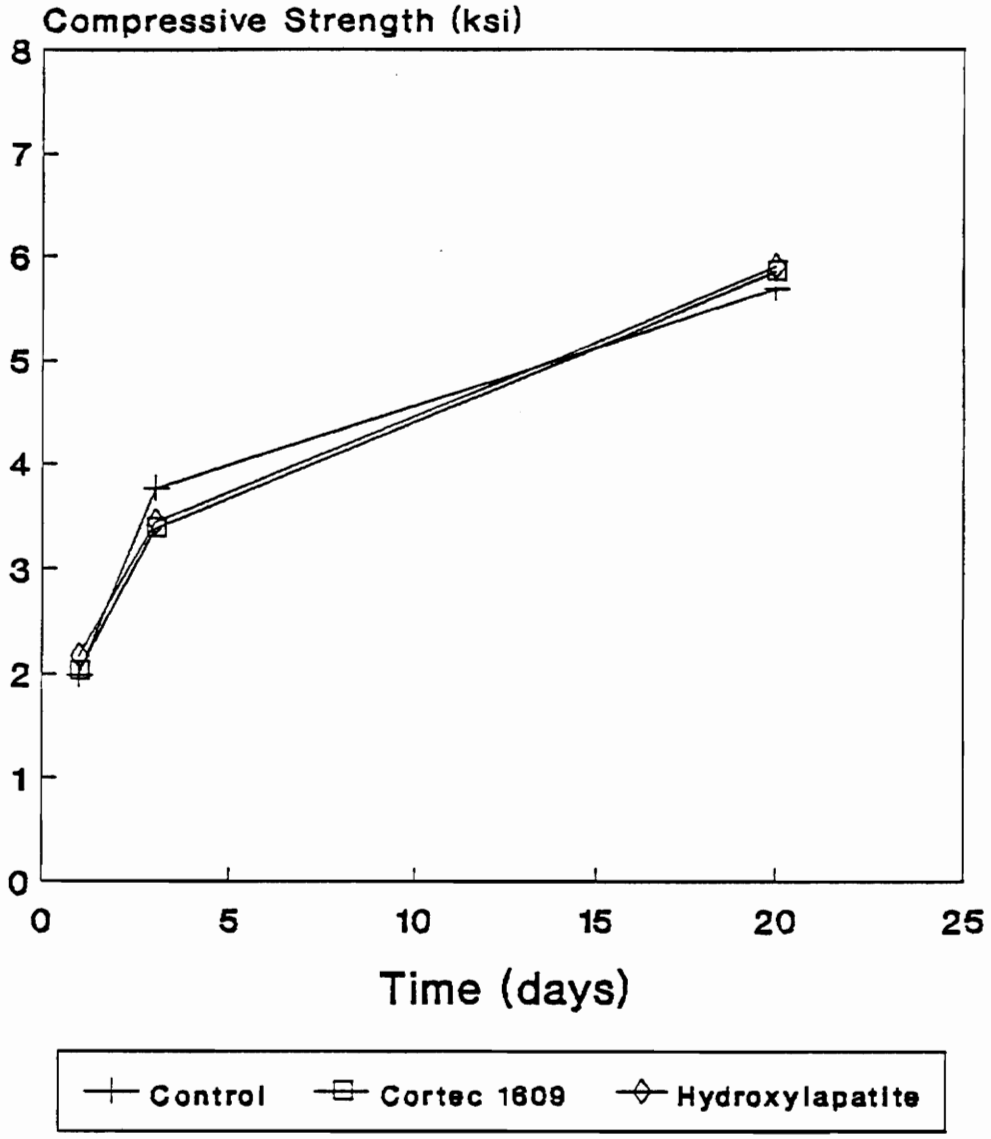

Figure 11. Mortar cube strength vs time for highest concentration Cortec 1609 (0.15%) and hydroxylapatite (25%) cubes

for all the cubes are tabulated in Appendix C, Table C-6.

DCI (calcium nitrite) is a known set accelerator and, at low concentrations, can increase the compressive strength of concrete [30]. This is evident in Figure 12 which compares the control group strength with those of the different DCI concentration groups. For every DCI concentration, the mortar strength was greater than for the untreated control cubes and the difference in magnitude increased with increased curing time. At 20 days, each DCI concentration had increased the mortar strength by more than 20% over untreated mortar. Strength increase was also a function of increasing DCI concentration. It should be noted that a small amount of set retarder was added to the 5% and 10% DCI concentration cubes to combat rapid setting.

The calcium nitrite and small amounts of calcium nitrate in DCI serve as an accelerating admixture. The presence of the strong NO_2^- anion in DCI tends to accelerate the solubility of calcium ions from the cement compounds, resulting in more calcium ions to participate in the aluminate and silicate hydration reactions. An increase in the hydration rate of the cement translates into higher compressive strengths in shorter time. However, long term strengths may be sacrificed because accelerated hydration produces hydration products of smaller particle size which have less strength than larger particles of a slower

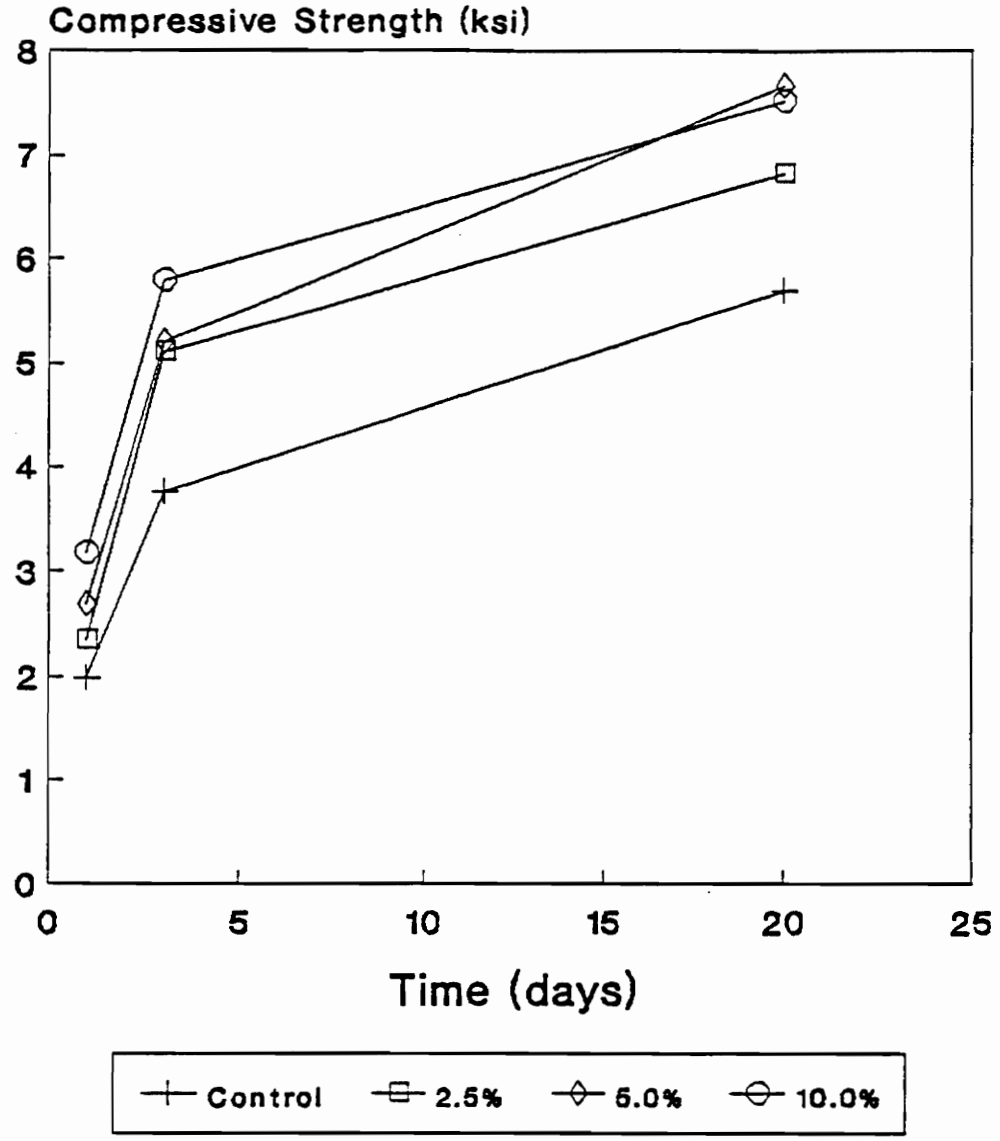

Figure 12. Mortar cube strength as a function of DCI concentration (% s/s cement)

hydration process.

Unlike calcium nitrite, both borate based inhibitors exhibited set retarding properties as seen in Figures 13 and 14. Sodium tetraborate so heavily retarded the set of the cement mortar that cubes of 2.0% s/s cement concentration did not have sufficient set strength at 24 hours to be removed from their molds. Even the 0.5% and 1.0% concentration showed heavy retardation as their compressive strengths were 75% and 96% lower than the control group strength after one day. The 0.5% concentration cubes reduced the strength difference in relation to the controls with time to point of only a 2% difference after 20 days. The two higher concentrations still had extremely low strengths after 3 days, but rapidly increased between days 3 and 20.

Zinc borate exhibited the same type of behavior as the sodium tetraborate but to a higher degree. Original concentrations of 1.7% and 3.4 % s/s cement did not have sufficient set strength at days 1 or 3 to be removed from the mold, therefore, lower concentrations of 0.22%, 0.43%, and 0.85% were used. The 0.22% concentration showed little effect on strength as seen in Figure 14. However, almost doubling the concentration to 0.43% resulted in a 95% reduction in strength after 24 hours and a 66% reduction after 3 days. The 0.85% concentration strength was even

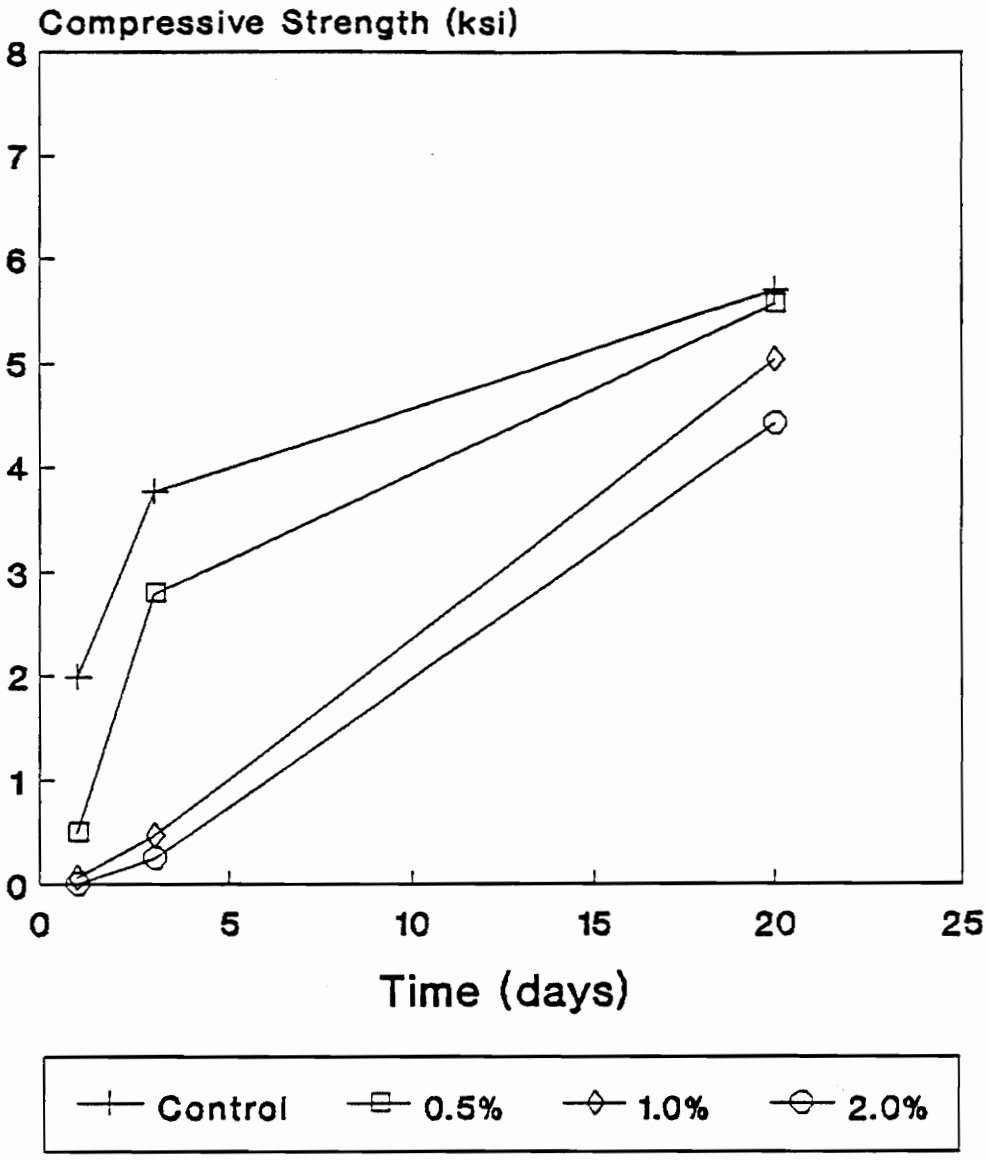

Figure 13. Mortar cube strength as a function of sodium tetraborate concentration (% s/s cement)

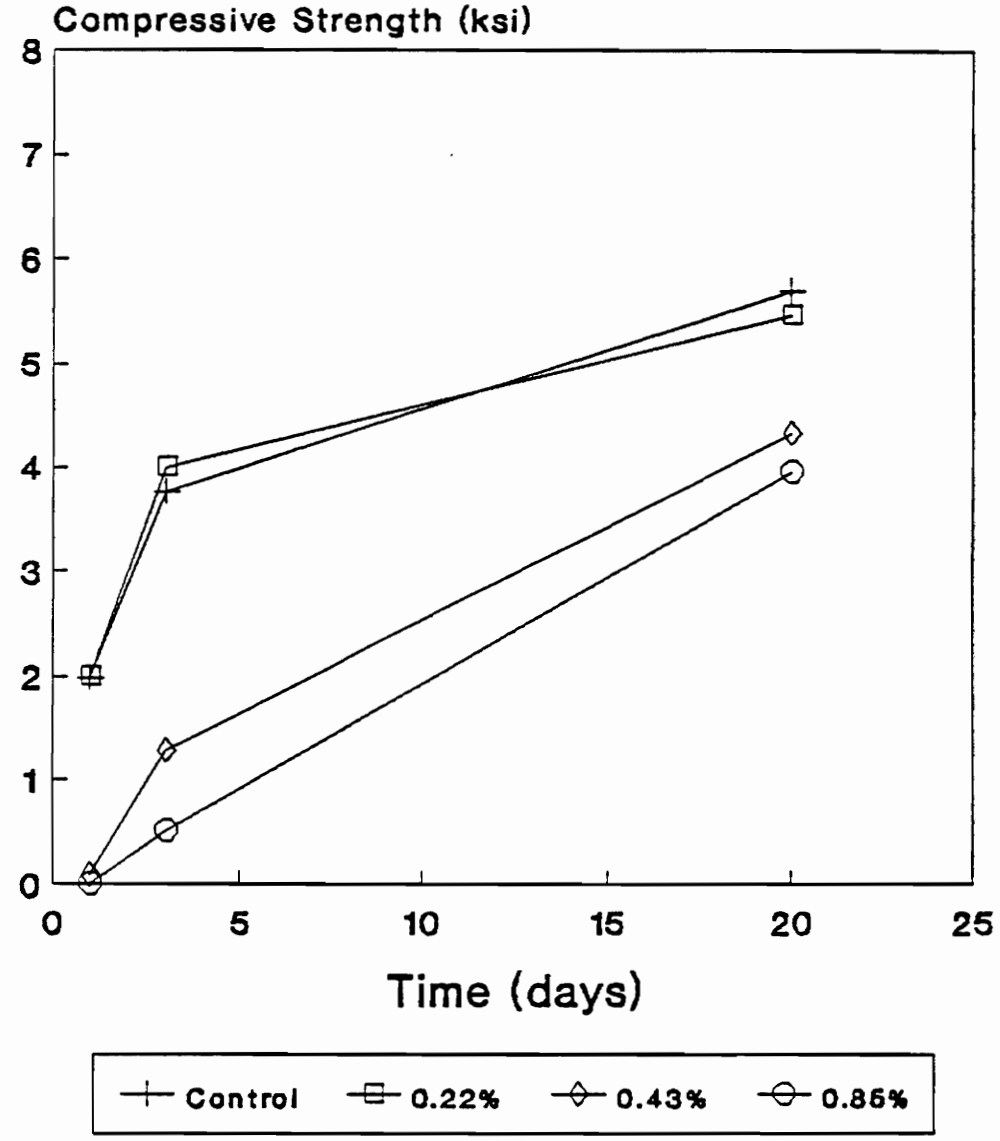

Figure 14. Mortar cube strength as a function of zinc borate concentration (% s/s cement)

lower, with no set strength after 24 hours. However, after 20 days, the 0.22% and 0.43% concentrations had compressive strengths within 30% of the control group. The two highest concentrations eventually set within 20 days with compressive strengths equal to 3.25 and 2.46 ksi respectively.

Both sodium tetraborate and zinc borate showed the same set retarding characteristics. The high concentration mortar cubes began to set in a characteristic manner for both borate treatments. The setting process was most rapid at the open surface of the cube molds and then progressed downward along the outer edges of the cube, with the slowest set being at the bottom surface of the cube in contact with the mold. Also characteristic of the borate treatments was the evolution of the strengths. High concentrations showed drastic reduction in initial strengths, but a rapid increase between days 3 and 20.

Borates are classified under Type B set retarding admixtures and were popular in the 1930's [44] but are rarely seen in use today. The borates form insoluble calcium borate salts which tie up calcium ions needed for the hydration process. The zinc borate may have had a greater set retardation effect because one molecule of zinc borate provides six boride ions while a molecule of sodium tetraborate provides only four boride ions. In addition to

the borate effects, the presence of Na^{+} and Zn^{2+} reduces the solubility of calcium ions, thus reducing the rate of hydration even further.

The long term strengths of set retarded mortars tend to reach and even exceed normally cured mortar strengths [44]. The slower rates of hydration product formation allows greater alignment of the hydration products in the cement paste which produces higher later strengths. This may account for the great increase in strength magnitude between days 3 and 20 for the higher borate concentrations.

Based on the mortar cube strength study, only the borates have a deleterious effect. However, the set retardation effect may be overcome the use of a set accelerating admixture. The admixing of DCI tends to only improve compressive strength which further supports its use a corrosion treatment after removal of chloride contaminated concrete. Both hydroxylapatite and Cortec 1609 showed no positive or negative effects on mortar strength.

4.4.2 Treatment Effects on Mortar Resistivity

Resistivity effects were found only in those treatments that produced compressive strength effects due to a change in setting rate. Since resistivity is a function of permeability which is dictated by the degree of hydration, it is reasonable to expect that set retardation would

decrease resistivity and set acceleration would increase it. This is reflected in Figures 15 thru 17 which display resistivity as a function of inhibitor concentration for sodium tetraborate, zinc borate, and DCI respectively. The average resistivity values for each treatment and concentration group are tabulated in Appendix C, Table C-7.

For sodium tetraborate and zinc borate, the higher concentrations which produced a higher degree of set retardation also exhibited lower resistivity values than the control specimens. Since set retardation means a slower formation of hydration products, the reduction in permeability of the system also proceeds slower. The lower concentration zinc and sodium borate specimens which exhibited strengths more similar to the control cubes, also exhibited like resistivity values. One day resistivity values could not be measured on the two higher zinc and sodium borate concentration specimens because their low set strengths made them too fragile to handle.

The DCI mortar cubes behaved opposite of the borate cubes. Since DCI accelerated the hydration process, the permeability reduction of the cubes was also accelerated due to the rapid formation of hydration products. As a result, increasing DCI concentrations yielded higher resistivity values and all resistivities were greater than the control group resistivities. The difference in resistivities is

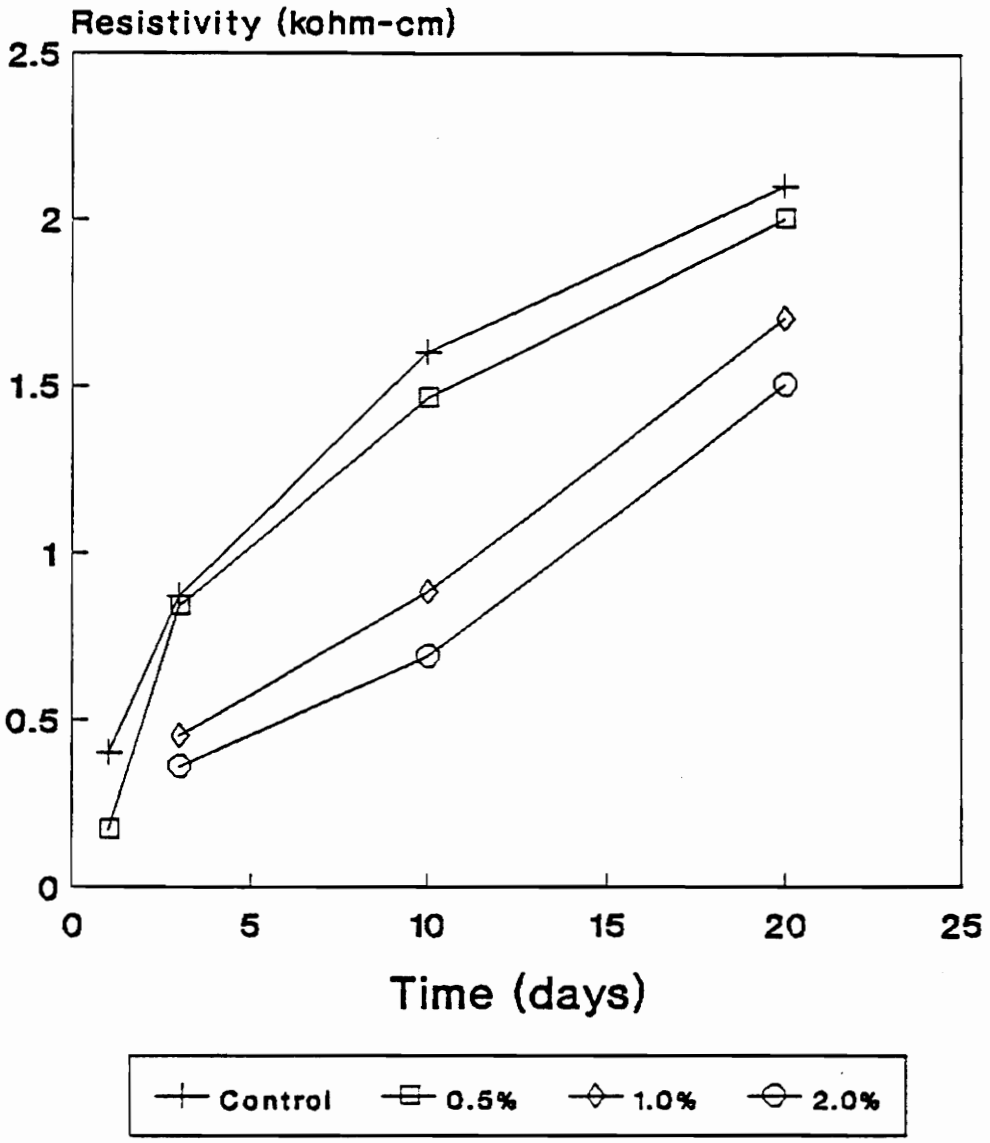

Figure 15. Resistivity as a function of sodium tetraborate concentration

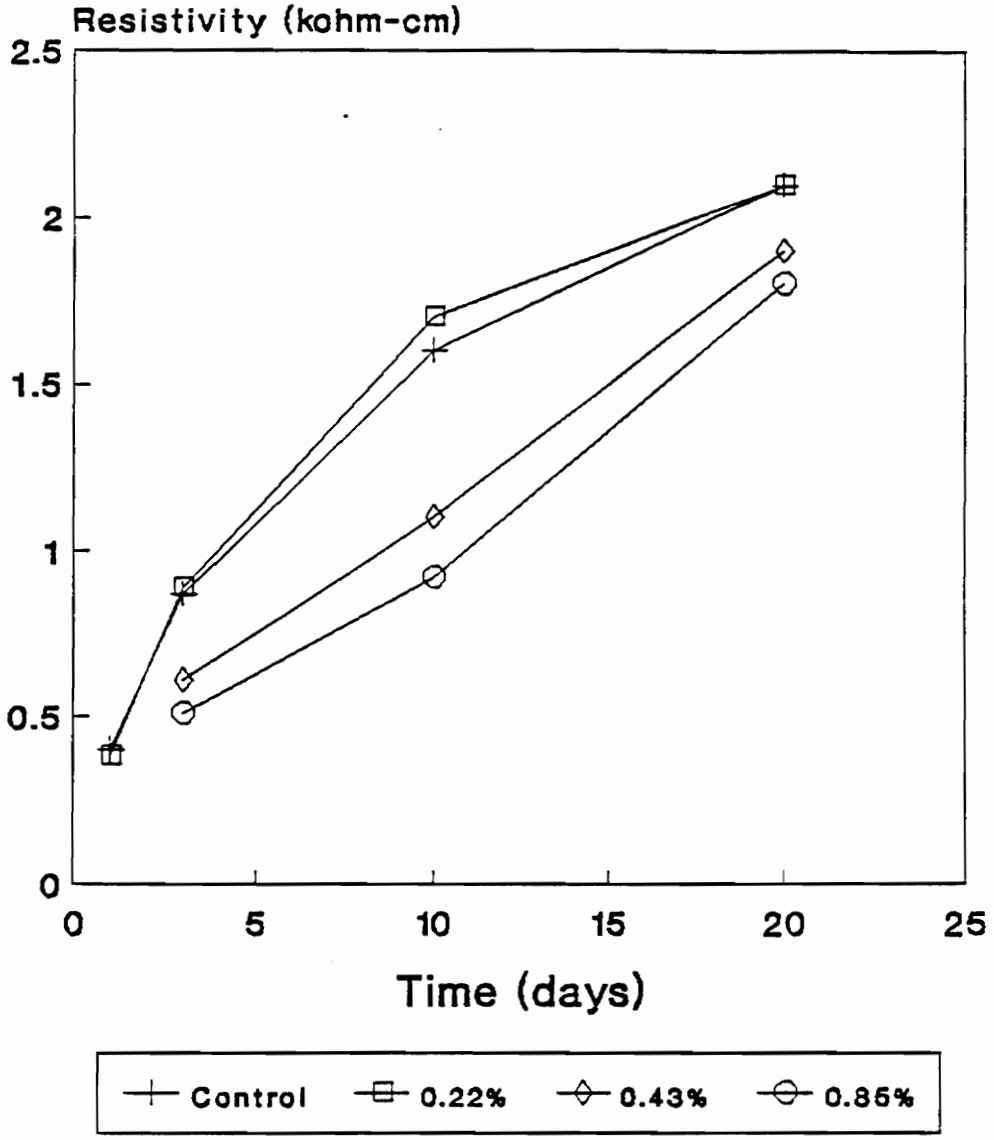

Figure 16. Resistivity as a function of zinc borate concentration

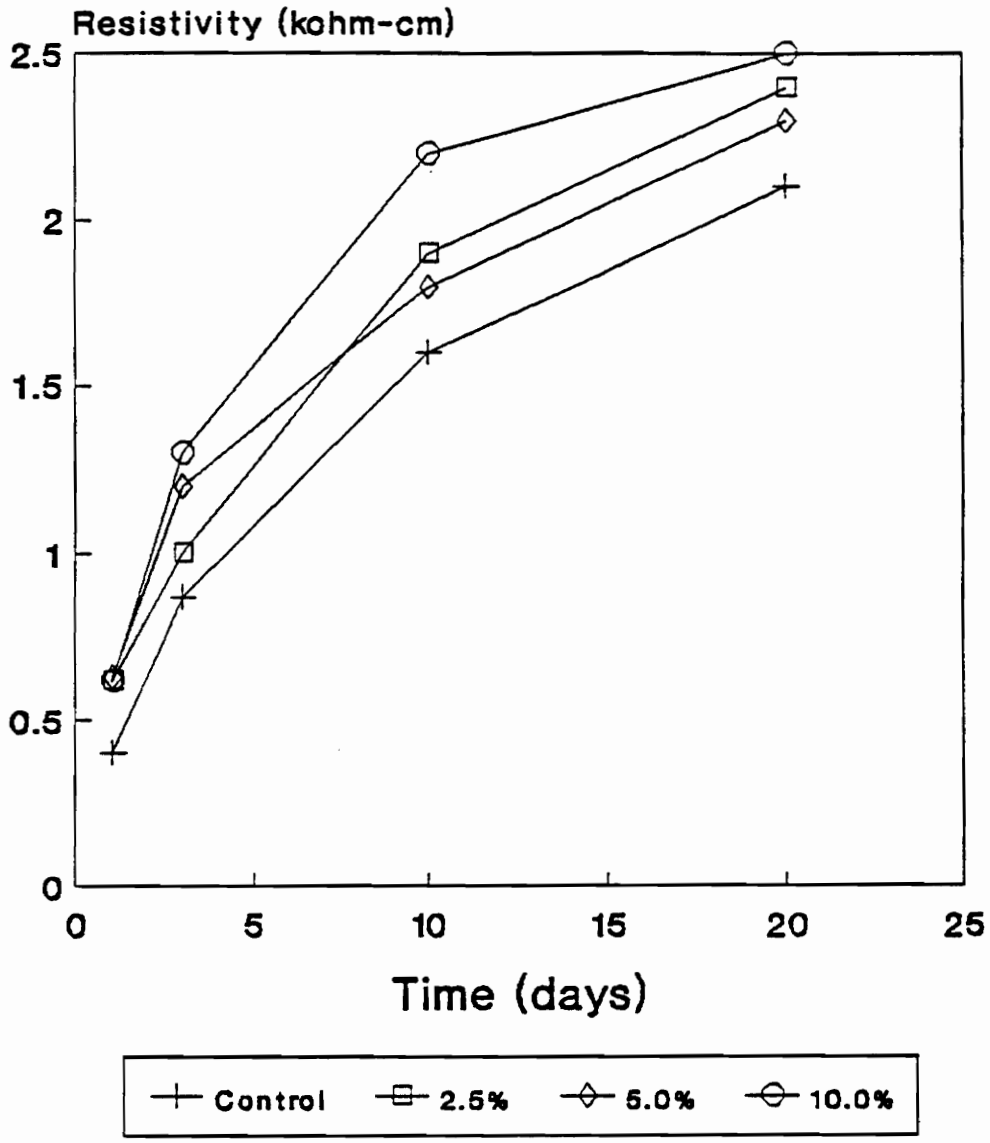

Figure 17. Resistivity as a function of DCI concentration

small after 24 hours but gradually increased with the rapid set of the cubes.

None of the specimens were determined to contribute highly conductive ionic species to the mortar cubes. Hydroxylapatite and Cortec 1609 exhibited resistivities similar to the control, while the rest of the treatments' resistivities were dictated by the change in setting rate.

4.5 Chloride-Ion Scavenging Ability of Hydroxylapatite

The apatite series, all of which has the same type of hexagonal crystal structure, includes hydroxylapatite ($Ca_{10}(PO_4)_6(OH)_2$) and chlorapatite ($Ca_{10}(PO_4)_6Cl_2$). The nature of apatite's structure renders it particularly prone to substitution. Studies have shown that hydroxylapatite readily undergoes an OH^-/F^- substitution in which the product is fluorapatite ($Ca_{10}(PO_4)_6F_2$) [45] and the ion exchange was found to be irreversible. The possible irreversible substitution of Cl^- for OH^- in concrete would provide a means of scavenging the chloride ions and simultaneously releasing hydroxyl ions which would enhance the pH of the concrete. However, three tests were conducted to evaluate the possibility of hydroxylapatite being able to scavenge chloride and the results reflected little if any scavenging ability.

4.5.1 pH Measurements

The results of a pH monitoring test to detect the release of hydroxyl ions as a result of chloride ion substitution are outlined in Table 7. Theoretically, if chloride ions substitute for the hydroxyl ions in the apatite molecule, the release of hydroxyl ions should cause a pH increase. Based on a 25 g sample of apatite, 200 ml of solution, and a water/apatite pH of 7.5, a 100% exchange would result in a pH of 13.40 which is an approximate pH increase of 6 units of magnitude. However, results from pH measurements taken at room temperature and at 150 °F for a 5% by weight NaCl solution with 25 g of apatite showed minimal change in pH over a 24 hour period. The difference in minimum and maximum pH measured was only 0.07 pH at room temperature and 0.12 at 150 °F. In addition, the minimal change was not linear with time.

If a direct substitution of chloride for hydroxyl ion was done for every hydroxyl group, the 25 g of apatite would have theoretically released 0.85 grams of hydroxyl ions which should have been detected with an increase in pH to 13.40. However, no pH change was detected to support this at either room temperature or 150 °F. In addition, the highest pH measurement for both tests never exceeded the pH value of 7.50 measured for hydroxyl apatite in distilled water.

Table 7. Measurement of pH as a function of time for hydroxylapatite treated NaCl solution (5% by weight)

Time	pH Measurement[1]	
	Room Temperature	150 °F
0	7.38	7.30
1 min	7.42	7.35
10 min	7.45	7.35
30 min	7.40	7.32
1 hr	7.42	7.30
2 hr	7.39	7.31
5 hr	7.42	7.39
10 hr	7.45	7.37
24 hr	7.43	7.42

[1]pH measurements of:
distilled water = 6.72
distilled water and apatite (R.T.) = 7.50
distilled water and apatite (150 °F) = 7.44
5% by weight NaCl solution (R.T.) = 7.31
5% by weight NaCl solution (150 °F) = 7.20

4.5.2 Specific Ion Electrode Measurements

An attempt was made to determine the extent of hydroxylapatite's chloride ion scavenging by measuring chloride content via a specific ion probe. In order to determine a baseline value for comparison, the chloride ion concentration of untreated hydroxylapatite was evaluated. However, the specific ion probe system is only calibrated to a lower threshold value of .016% Cl^- for a 3 g sample. All measurements of untreated hydroxylapatite and hydroxylapatite exposed to various % NaCl solutions yielded values below this threshold, therefore, the exact chloride contents could not be determined.

Since the exposed hydroxylapatite samples yielded values less than .016% Cl^-, it is reasonable to assume the maximum chloride concentration an exposed sample could have is .016%. If this is assumed, a 3 g sample of exposed apatite would contain 0.00048 g of Cl^-. However, if enough apatite is desired to scavenge a nominal 10 lbs Cl^-/yd^3 of concrete (4536 g) at a level of 0.00048 g Cl^-/3 g of hydroxylapatite, 12,859 lbs (2.83×10^7 g) of hydroxylapatite/yd^3 of concrete would be needed. This unreasonable and infeasible amount is twenty times the average amount of cement put in a yd^3 of concrete. Based on this analysis, hydroxylapatite is ineffective in scavenging the necessary degree of chloride ions to warrant its

feasibility in concrete.

4.5.3 Differential Thermal Analysis

If the Cl^-/OH^- substitution readily takes place, differential thermal analysis (DTA) could detect the loss of the hydroxyl groups in the apatite molecule. A DTA scan of an untreated hydroxylapatite specimen is shown in Figure 18. The initial valley at 125 °C is due to the release of water from the specimen. The valley at 1000 °C corresponds to a dehydration of the specimen in which the hydroxyl groups are released. Studies have shown that hydroxyapatite does not readily lose OH^- from its crystal lattice, which is stable up to at least 1000 °C [46] which correlates with the DTA scan.

If chloride ions substitute for hydroxyl groups within the hydroxylapatite molecule, the magnitude of the valley at 1000 °C would decrease with increasing loss of OH^-. DTA scans of hydroxylapatite specimens exposed to varying concentrations of NaCl solution showed no indication of ion substitution. All DTA scans of the samples showed minimal to no change from the reference sample scan shown in Figure 18.

The substitution of chloride ion for hydroxyl ion in hydroxylapatite may possibly be inhibited by the size of the chloride ion. The fluoride ion readily substitutes but has

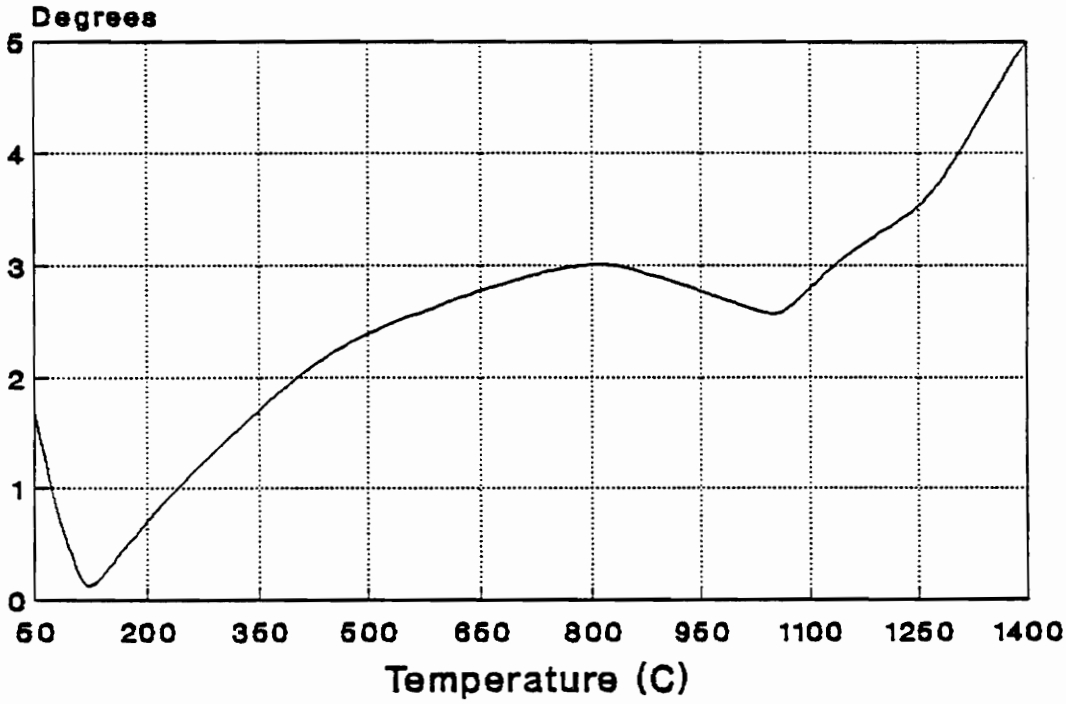

Figure 18. Differential thermal analysis of hydroxylapatite

an ionic radii 25% smaller than the chloride ion. Studies have indicated that structural requirements preclude site-by-site substitution such as Cl^- for F^- [39]. This may be the case in the Cl^-/OH^- substitution as well.

5.0 Conclusions

The removal of chloride contaminated concrete is an effective means through which corrosion abatement treatments can be applied. Several treatments and treatment combinations were found effective and recommended for further evaluation in large-scale and field experimentation.

When chloride contaminated concrete is removed, the combination of DCI (calcium nitrite) inhibitor being ponded and placed in backfilling mortar proved to be the most effective corrosion treatment applied of those treatments under investigation. The treatment exhibited the greatest sustained reduction in corrosion rate. The effectiveness of the DCI is dependent upon an adequate ratio of nitrite to chloride ion ratio. This ratio dictates the degree to which the nitrite ions can compete with the chloride ions for the Fe^{2+} ions in solution. Higher nitrite levels result in the enhanced stability of the passive film due to the reformation of Fe_2O_3. It was also reconfirmed that DCI acts as a set accelerator and increases the compressive strength of the mortar.

The experimental inhibitors sodium tetraborate and zinc borate showed adequate effectiveness in reducing corrosion when applied as both a ponding and mortar admixture. The borate ion's ability to produce a protective layer on steel

resulted in a effective reduction in the corrosion activity by acting as a barrier to increased metal dissolution. However, the borate compounds act as cement set retarders with zinc borate having a greater effect at similar concentrations. As a result, care must be taken if admixed in concrete due to low initial set strengths.

Commercial inhibitors Alox 901, Cortec 1337, and Cortec 1609, are potentially effective treatments for reinforced concrete after removal of chloride contaminated concrete. However, due to their proprietary nature, the exact mechanism of their corrosion inhibition ability is not known.

In general, it was determined that the ponding of treatment solution is more effective in corrosion abatement than solely backfilling with treated mortar. The ponding allows for the diffusion of the inhibitor not only through the concrete but also possibly through the rebar/concrete interface. In addition, the removal of chloride contaminated concrete above a reinforcing bar and subsequent replacement with fresh mortar has little effect on the corrosion activity when the chloride ion concentration at the rebar level is high. Without the presence of a corrosion inhibiting agent, the concrete surrounding a corroding rebar would still have a sufficient chloride concentration to spur the continuation of corrosion.

The evaluation of hydroxylapatite as a chloride ion scavenging mineral showed no indication of chloride ion scavenging ability in aqueous tests or when placed alone in mortar.

6.0 Recommendations for Further Research

Based on the limitations encountered through the course of this study, the following recommendations can be made for further research:

1. In order to determine sustainment of treatment corrosion abatement, long term evaluation of treated specimens should be addressed. This would aid in estimating treatment life-cycles in bridge deck systems.
2. Tests should be conducted to determine the optimum treatment concentration based on the volume of chloride contaminated concrete removed.
3. In order to aid in the diffusion of treatment chemicals, the concrete should be dried prior to ponding treatment.
4. The removal of all concrete to the rebar level as opposed to solely grooving above the rebar could possibly enhance treatment effectiveness.
5. Economic feasibility studies should be performed on effective treatments.
6. The use of a linear polarization device that prevents the applied current from straying from the specified counter electrode area could effectively be used to more accurately determine corrosion rate.
7. Surface analysis on the rebar should be conducted after the termination of the exposure period to detect the

presence of passive films or adsorbed species.

8. Evaluation of the chloride ion scavenging ability of other apatite forms should be performed. Other minerals, such as sodalite, should also be evaluated.

REFERENCES

1. Locke, C.E. and Simon, A., "Electrochemistry of Reinforcing Steel in Salt-Contaminated Concrete," Corrosion of Reinforcing Steel in Concrete, ASTM STP 713, ASTM, Philadelphia, PA, 1980, pp. 3-4.

2. Wood, F.O., "Survey of Salt Usage for Deicing Purposes," Automotive Corrosion by Deicing Salts, NACE, Houston, TX, 1981, pp. 25-35.

3. P.D. Cady, "Corrosion of Reinforcing Steel in Concrete - A General Overview of the Problem," Chloride Corrosion of Steel in Concrete, ASTM 629, ASTM, Philadelphia, PA, 1977, pp. 7-8.

4. Strategic Highway Research Program - Research Plans, Final Report, Technical Research Area 43, May 1986, pp. TRA 4-1 thru TRA 4-60.

5. Slater, J.E., Corrosion of Metals in Association with Concrete, ASTM STP 818, ASTM, Philadelphia, PA, 1983, pp. 48-67.

6. Schiessel, P. and Bakker, R., "Measure of Protection," Corrosion of Steel in Concrete, Chapman and Hall, New York, 1988, pp. 75-77.

7. Slater, J.E. et al, "Electrochemical Removal of Chlorides from Concrete Bridge Decks," Materials Performance, Nov 1976, pp. 23

8. "Corrosion of Metals in Concrete," Report by ACI Committee 222, Report No. ACI 222B-89, American Concrete Institute, Detroit, MI, 1990, pp. 18-19.

9. Lehmann, J., "Cathodic Protection (Corrosion Control) of Reinforced Concrete Structures Using Conductive Coatings," Corrosion, Concrete, and Chlorides - Steel Corrosion in Concrete: Causes and Restraints, American Concrete Institute, Detroit, MI, 1987, pp. 130-131.

10. Bakker, R.F.M., "Initiation Period," Corrosion of Steel in Concrete, Chapman and Hill, New York, 1988, pp. 22-25.

11. Wheat, H.G. and Eliezer, Z., Corrosion, Vol. 41, No. 7, 1988, pp. 489-499.

12. T. Yonezawa et al, Corrosion Engineering, Vol 44, No. 7, 1988, pp. 489-499.

13. Fontana, M.G., Corrosion Engineering, McGraw-Hill, New York, 1986, pp. 20.

14. Rosenberg, A. et al, "Mechanisms of Corrosion of Steel in Concrete," Materials Science of Concrete, pp. 285-309.

15. Mehta, P.K., Concrete: Structure, Properties, and Materials, Prentice-Hall, Englewood Cliffs, NJ, 1986, pp. 152-158

16. Cook, H.K. and McCoy, W.J., "Influence of Chloride in Reinforced Concrete," Chloride Corrosion of Steel in Concrete, ASTM STP 629, ASTM, Philadelphia, PA, 1977, pp. 20-29.

17. Shiessel, P. and Bakker, R., "Measures of Protection," Corrosion of Steel in Concrete, Chapman and Hill, New York, 1988, pp. 71-78.

18. Cady, P.D. and Weyers, R.E., "Chloride Penetration and Deterioration of Concrete Bridge Decks," Cement, Concrete, and Aggregates, CCAGDP, Vol. 5, No. 2, Winter 1983, pp. 81-82.

19. Verbeck, G.J., "Mechanisms of Corrosion of Steel in Concrete," Corrosion of Metals in Concrete, SP 49-3, ACI, 1975, pp. 21-38.

20. Locke, C.E., "Corrosion of Steel in Portland Cement Concrete: Fundamental Studies," Corrosion Effects of Stray Currents and the Techniques for Evaluating Corrosion of Rebars in Concrete, ASTM STP 906, ASTM, Philadelphia, PA, 1985, pp. 5-13.

21. Shalon, R. and Raphael, M., "Influence of Seawater on Corrosion of Reinforcement," ACI Journal, Proceedings Vol. 55, No. 8, Feb 1959, pp. 1251-1268.

22. "Standard Test Method for Half-Cell Potentials of Uncoated Reinforcing Steel in Concrete," C-876-87, Annual Book of ASTM Standards, ASTM, Philadelphia, PA, 1987, pp. 563-570.

23. Page, C.L., "Basic Principles of Corrosion," Corrosion of Steel in Concrete, Chapman and Hall, New York, 1988, pp. 3-21.

24. Dawson, J.L., "Corrosion Monitoring of Steel in Concrete," Corrosion of Reinforcement in Concrete Construction, Ellis Horwood Limited, West Sussex, England, 1983, pp. 176-191.

25. Andrade, C. et al, "The Determination of the Corrosion Rate of Steel Embedded in Concrete by Polarization Resistance and AC Impedance Methods," Corrosion Effect of Stray Current and the Techniques for Evaluating Corrosion of Rebar in Concrete, ASTM STP 906, ASTM, Philadelphia, PA, 1985, pp. 43-63.

26. MacDonald, D.D. and McKubre, M.C.H., "Electrochemical Impedance Techniques in Corrosion Science," Electrochemical Corrosion Testing, ASTM STP 727, ASTM, Philadelphia, PA, 1981, pp. 110-166.

27. Epelboin, I. et al, "AC Impedance Measurements Applied to Corrosion Studies and Corrosion-Rate Determination," Electrochemical Corrosion Testing, ASTM STP 727, ASTM, Philadelphia, PA, 1981, pp. 150-166.

28. Griffin, D.F., "Corrosion Inhibitors for Reinforced Concrete," Corrosion of Metals in Concrete, SP 49-8, ACI, Detroit, MI, pp. 95-101.

29. Boyd, W.K. and Tripler, A.B., "Corrosion of Reinforcing Steel Bars in Concrete," Materials Protection, Vol. 7, No. 10, 1968, pp. 40-47.

30. Rosenberg, A.M. et al, "A Corrosion Inhibitor Formulated with Calcium Nitrite for Use in Reinforced Concrete," Chloride Corrosion of Steel in Concrete, ASTM STP 629, ASTM, Philadelphia, PA, 1977, pp. 89-99.

31. Craig, R.J. and Wood, L.E., "Effectiveness of Corrosion Inhibitors and the Influence on the Physical Properties of Portland Cement Mortars," Highway Research Record, No. 328, Highway Research Board, 1970, pp. 77-88.

32. Bishara, A.G., "Latex Modified Concrete Bridge Deck Overlays," Field Performance Analysis," FHWA/Oh/79/004, Federal Highway Administration, Washington, D.C., 1979.

33. Kukacka, L.E., "The Use of Concrete Polymer Materials

for Bridge Deck Applications," Chloride Corrosion of Steel in Concrete, ASTM STP 629, ASTM, Philadelphia, PA, 1977, pp. 100-109.

34. Frascoia, R.I., "Vermont's Experience with Bridge Deck Protective Systems," Chloride Corrosion of Steel in Concrete, ASTM STP 629, ASTM, Philadelphia, PA, 1977, pp. 69-81.

35. Mathey, R.G. and Clifton, J.R., "Bond of Coated Reinforcing Bars in Concrete," Proceedings, ASCE, Vol. 102, ST1, Jan 1976, pp. 215-229.

36. Clifton, J.R. et al, "Creep of Coated Reinforcing Bars in Concrete," Proceedings, ASCE, V. 105, ST10, Oct 1979, pp. 1935-1947.

37. Quarterly Report, Strategic Highway Research Program, Contract C-103, Subtask 2A, Sept 1990, pp. 1-66.

38. Berke, N.S. and Rosenberg, A., "Technical Review of Calcium Nitrite Corrosion Inhibitor in Concrete," unpublished paper, W.R. Grace and Company

39. Berry, L.G. et al, Mineralogy, 2nd ed., W.H. Freeman and Company, San Francisco, CA, 1983, pp. 372-376.

40. KCC Inc. 3LP Package: Test Procedures, Data Analysis, and General Information, July 1990, Appendix, p. 9.

41. Henry, M, personal communication, graduate student, Civil Engineering Department, Virginia Polytechnic Institute and State University, Blacksburg, VA, May 1991, thesis work in progress.

42. Berke, N., "Calcium Nitrite Impregnation of US 460 over VA 723," Strategic Highway Research Program, Project C-103, Subtask 5, pp. 1-30.

43. Ott, L., An Introduction to Statistical Methods and Data Analysis, 3rd ed., PWS-Kent Publishing, Boston, MA, 1988, pp. 149-151.

44. Dodson, V.H., Concrete Admixtures, Van Nostrand Reinhold, New York, 1990, pp. 103-127.

45. Chander, S. and Fuerstenau, D.W., "Solubility and Interfacial Properties of Hydroxyapatite: A Review," Adsorption on and Surface Chemistry of Hydroxyapatite,

Plenum Press, New York, 1984, pp. 29-50.

APPENDIX A

Concrete and Mortar

Table A-1. Gradations of coarse (CA) and fine (FA) aggregates

Sieve Size	CA % Passing	FA % Passing
1/2"	100	100
3/8"	93	98
No. 4	17	91
No. 8	9	73
No. 16	1	52
No. 30	---	32
No. 50	---	8
No. 100	---	2
No. 200	---	0.2

Table A-2. Characteristic properties of coarse (CA) and fine (FA) aggregates

Property	CA (3/8" limestone)	FA (natural sand)
Dry Unit Weight	89.3 lbs/ft^3	----
Specific Gravity	2.73 g/cc	2.66 g/cc
Absorption	1.36%	0.36%
Fineness Modulus	----	3.39

Table A-3. Concrete mix design for specimen set A

Component	Quantity (SSD) in lb
Cement	39.04
Water	19.72
Coarse Aggregate	68.50
Fine Aggregate	107.91
AEA (Microair)	2.89 ml
WR-R	92.45 ml
Total	235.17 lbs

Table A-4. Concrete properties for specimen set A

Property	Batch 1	Batch 2	Batch 3	Batch 4
Slump	2.25"	2.50"	2.50"	2.25"
Air	6%	5.7%	5.3%	6.2%
Unit Wt. (pcf)	141.4	141.8	141.9	141.6
Temperature	59 °F	61 °F	62 °F	61 °F
Strength (ksi)				
7-day	4.97	5.37	5.09	4.93
28-day	6.57	5.97	6.45	6.41

Table A-5. Concrete mix design for specimen set B

Component	Quantity (SSD) in lb
Cement	39.04
Water	19.73
Coarse Aggregate	68.47
Fine Aggregate	107.93
AEA (Microair)	2.43 ml
WR-R	80.89 ml
Total	235.17 lbs

Table A-6. Concrete properties for specimen set B

Property	Batch 1	Batch 2	Batch 3	Batch 4
Slump	3.5"	4.0"	3.75"	3.75"
Air	6.9%	6.6%	7.0%	6.8%
Unit Wt. (pcf)	141.4	141.8	141.9	141.6
Temperature	63 °F	60 °F	60 °F	62 °F
Strength (ksi)				
7-day	5.01	4.87	5.12	5.05
28-day	6.72	6.34	6.43	6.27

Table A-7. Backfill mortar mix design with treatment variations

Basic mix used to fill two grooves:

Cement	1.75 lbs
Fine Aggregate (dry)	5.28 lbs
Water	0.61 lbs

List of treatments placed in mortar, amount of additional water needed to obtain adequate workability, and resulting w/c ratio based on 0.36% FA absorption:

Treatment	Additional Water	w/c Ratio
Blank (B-1,B-4,B-9 B-13, B-14, B-15)	20.5%	.42
DCI (B-2,B-3)	18.0%	.41
Sodium Tetraborate (B-6,B-7)	25.8%	.44*
Zinc Borate (B-8)	29.3%	.45*
Apatite (B-5, B-10)	30.9%	.45*
Zinc Borate/Apatite (B-12)	32.5%	.46*
DCI/Apatite (B-11)	29.3%	.45*
CORTEC 1609 (B-16,A-15)	21.0%	.42

*These water/cement ratios may be high due to the fact that that apatite and both the borates are applied as powders into the mixing water, therefore, they may have absorbed or adsorbed some of the water, taking it away from the hydration process.

Table A-8. Mortar cube mix design with treatment variations

Basic mortar cube mix (9 cubes):

Cement	740 g
Fine Aggregate (dry)	2035 g
Water	369 ml*

*10 ml of additional water were needed above the ASTM C 109 standard (359 ml) due to the use of the dry sand.

The following treatments required additional water or the addition a set retarder:

Treatment	Addition
DCI 5% s/s cement	Set retarder 0.3% s/s cement
DCI 10% s/s cement	Set retarder 0.6% s/s cement
Apatite 25% s/s cement	10 ml of water for workability
Cortec 1337	No additions
Sodium tetraborate	No additions
Zinc borate	No additions

APPENDIX B

Measurement Procedures

Part B-1. Half-Cell Potential Measurement Technique

According to ASTM standard C-876-87, the measurement of half-cell potentials is performed with a copper-copper sulfate (CSE) half-cell. However, at the initiation of this study, a saturated calomel electrode (SCE) was used instead because of its readable availability. The potential reading from an SCE can be converted into an equivalent CSE potential value by simply subtracting 70 mV. The advantage of using a SCE was that it was small in size and would leave a small electrode footprint. Therefore, several measurements could be taken across the top surface of a specimen, without the electrode footprints interfering with each other.

The measurement apparatus consisted of a multimeter with the half-cell connected to the positive terminal and the negative terminal connected to the working electrode or anode (rebar) by means of an alligator clip. The multimeter was auto-adjusting and readily displayed the half-cell potentials in millivolts.

The SCE was placed into a small square sponge in which a slit had been cut. A rubber band was used to secure the sponge around the shaft of the SCE. In order to provide a conductive electrolyte, the sponge was soaked with soap solution.

Three potential measurements were taken across the surface of the concrete above each rebar at equidistant positions correlating to the front, middle, and back of each rebar. The voltage reading on the multimeter was allowed to stabilize within a few millivolts of fluctuation before recording the value. Potential measurements were always taken one day after a ponding cycle, so as to assure enough moisture for adequate conductivity, but allowing sufficient time for the concrete surface to dry.

Part B-2. Three Electrode Linear Polarization (3LP) Measurements

The 3LP device used to measure corrosion rates in the specimens is manufactured by Kenneth C. Clear, Inc. The device operates on the principal that the DC current required to alter the natural electrical half-cell potential of steel rebar a few millivolts, is proportional to the natural corrosion rate of the steel rebar. The three electrode configuration consists of the working electrode (rebar), a counter electrode mesh, and a pen-sized copper-copper sulfate half-cell. 3LP testing involves defining the applied current (I_{appl}) required to cathodically polarize a steel rebar by 4, 8 and 12 mV from the natural electrical half-cell potential of the steel.

The testing procedure is simple in nature. An area equivalent to the sponge area on the 3LP portable probe is marked on each specimen. Prior to testing, the area, in addition to the probe sponge, is wetted with a conductive soap solution. The probe is placed on the concrete surface and a connection is also made to the reinforcing bar. The rebar is polarized with a current supplied and controlled by the 3LP device and the resulting data is monitored. The measurement time per bar is approximately 10 minutes.

A software package is utilized for the analysis of the applied current values corresponding to the counter potentials. Based on the Stern-Geary equation (see section 2.5.3), the software is able to calculate the corrosion current values. K. C. Clear has simplified the Stern-Geary equation based on experimentally determined Tafel slopes for steel in concrete [40]. The simplified equation used in the software package is:

$$I_{corr} = 14953.95 \times S/(K \times B_{BAR}) \qquad (8)$$

where,

I_{corr} = corrosion current in mA/ft^2

K = equivalent bar length beneath counter electrode (in.)

B_{BAR} = equivalent bar size beneath counter electrode

$S = \Delta I_{appl}/\Delta\rho$ = applied current/polarization potential

During the tests of this study, K was 7.25" and B_{BAR} was 4.

The corrosion current values measured by the 3LP cannot be viewed as totally accurate. Since the 3LP device has no means to guard against nonuniform current distribution, a length of rebar greater than 7.25" may have been polarized underneath the counter electrode. Since the length of exposed rebar in the concrete specimens was 12.5", nonuniform polarization would have resulted in lower calculated I_{corr} values.

Part B-3. Resistivity Measurements Using a Soil Resistance Meter

The resistivity of the 2" mortar cubes was found through the use of a modified Nilsson soil resistance meter. Two metal filled copper rings secured to an insulative backing were soldered onto the two contact cables of the resistance meter. These circular metallic surfaces, 1 in^2, served as the two contact surfaces between which current was passed.

Based on Ohm's Law,

$$R = V/I \tag{9}$$

where,

R = resistance in Ω

V = potential in Volts

I = current in Amperes

resistance can be expressed as:

$$R = \rho L/A \tag{10}$$

where,

ρ = resistivity in Ω-in.

L = length in in.

A = cross sectional area in in^2

From this, resistivity can be expressed in terms of centimeters:

$$\rho = A \times R/L \tag{11}$$
$$= 0.997 \times R$$

where A and L have been converted to centimeters and the units of resistivity are ohms-cm. Based on equation eleven, the resistance readings from the meter can be directly converted to resistivity.

The resistance measurements were taken between all three opposite faces of each cube. Electroconductive gel was used to assure a conductive contact with the mortar cube surfaces. The metal contacts were clamped down over the opposite surfaces and a current was applied. A resistance dial was turned until the current was nulled and the dial reading was taken as the resistance across the mortar cube. The rough surface of each mortar cube that corresponded to the open surface of the mortar molds appeared to affect the

resistivity measurements. The resistivity across this surface always appeared higher than the other surfaces. This is probably due to the rough surface affecting the contact area. As a result, only the two resistivity measurements taken across the smooth surfaces was recorded for each cube.

Part B-4. Differential Thermal Analysis Procedure

The differential thermal analysis conducted on hydroxylapatite was performed using a Perkin Elmer high temperature differential thermal analysis system in combination with a thermal analysis controller and data station.

Samples were weighed and placed in a small platinum crucible which was positioned in the DTA heating chamber next to the standard reference sample. The following parameters were used in controlling the thermal analysis:

Final temperature = 1400 °C

Minimum temperature = 30 °C

Temperature increment = 140 °C

Y-range = 20

Heating rate = 20 °C/min

Cooling rate = 30 °C/min

After completion of the thermal analysis, the DTA scan was

plotted and evaluated for any noticeable peaks or valleys indicating a thermally induced reaction.

APPENDIX C

Experimental Data

Table C-1. Pre-Treatment Half-Cell Potentials of Set A and B in Reference to Copper-Copper Sulfate Electrode

		Half-Cell Potential (-mV)								
Specimen	Bar	Day 1	Day 8	Day 15	Day 22	Day 29	Day 36	Day 43	Day 50	Day 57
A-1	A	480	480	441	377	401	444	446	433	445
	B	482	492	436	384	399	437	452	440	444
A-2	A	494	498	452	400	412	462	468	438	441
	B	475	487	447	440	443	476	498	489	500
A-3	A	492	488	462	465	471	522	533	520	499
	B	486	489	452	433	466	497	512	510	497
A-4	A	490	488	435	404	415	444	480	442	436
	B	488	480	458	399	410	456	478	452	447
A-5	A	488	498	450	412	415	437	446	412	420
	B	488	494	465	460	462	476	476	480	492
A-6	A	491	490	462	432	438	461	475	455	462
	B	487	484	453	421	419	444	452	432	435
A-7	A	491	491	447	450	451	499	504	510	515
	B	486	496	450	439	423	487	503	487	492
A-8	A	518	428	406	333	350	392	420	395	400
	B	499	507	469	365	390	442	445	438	449
A-9	A	473	479	435	378	398	454	461	435	440
	B	469	477	428	388	401	481	492	467	469
A-10	A	498	506	465	440	440	493	501	500	498
	B	510	510	472	381	414	451	466	462	468
A-11	A	484	497	472	398	422	472	480	453	452
	B	509	521	489	412	431	488	495	482	481
A-12	A	496	520	480	409	416	456	463	412	420
	B	490	502	475	354	360	410	430	414	423
A-13	A	480	503	462	405	436	466	470	448	450
	B	491	510	500	493	511	544	544	523	522
A-14	A	506	514	491	478	487	533	552	500	495
	B	511	531	501	501	526	550	543	523	523
A-15	A	490	522	503	501	517	537	504	475	482
	B	488	504	474	472	485	513	536	535	520
A-16	A	495	516	494	494	522	545	563	543	548
	B	500	512	478	470	487	533	565	551	560

Table C-1. Pre-Treatment Half-Cell Potentials of Set A and B in Reference to Copper-Copper Sulfate Electrode (continued)

Specimen	Bar	Day 64	Day 71	Day 78	Day 85	Day 92	Day 99	Day 106	Day 113
A-1	A	448	443	469	488	490	520	520	545
	B	450	452	498	509	512	543	567	572
A-2	A	446	445	467	498	499	516	522	542
	B	498	488	515	512	503	507	515	564
A-3	A	515	492	522	533	545	526	543	552
	B	512	489	513	507	508	517	546	558
A-4	A	442	441	463	476	479	482	512	584
	B	452	438	449	480	483	503	545	601
A-5	A	433	428	435	488	490	523	568	610
	B	490	462	488	507	511	523	555	584
A-6	A	455	452	475	483	490	513	547	579
	B	444	438	451	513	541	558	606	639
A-7	A	521	503	542	506	538	589	623	641
	B	493	476	482	507	522	580	604	623
A-8	A	400	410	428	417	451	498	532	572
	B	450	444	453	480	498	513	541	584
A-9	A	452	452	457	507	505	525	569	590
	B	466	448	466	496	505	537	536	575
A-10	A	509	462	512	560	564	592	600	622
	B	477	452	476	489	503	545	564	584
A-11	A	460	468	465	488	501	548	571	599
	B	491	468	493	507	521	537	568	602
A-12	A	433	432	472	508	512	516	554	588
	B	433	441	446	468	488	524	578	613
A-13	A	452	461	464	462	488	512	566	592
	B	533	520	545	560	572	612	642	611
A-14	A	502	511	545	552	566	574	611	625
	B	541	501	523	548	542	555	584	622
A-15	A	497	481	497	545	550	559	599	607
	B	533	498	568	572	575	589	623	631
A-16	A	559	539	562	558	562	581	605	624
	B	575	562	588	598	603	601	635	647

Table C-1. Pre-Treatment Half-Cell Potentials of Set A and B in Reference to Copper-Copper Sulfate Electrode (continued)

Half-Cell Potential (-mV)

Specimen	Bar	Day 1	Day 8	Day 15	Day 22	Day 29	Day 36	Day 43	Day 50	Day 57	Day 64	Day 71	Day 78
B-1	A	266	284	329	354	404	458	470	461	460	491	566	588
	B	249	266	312	348	395	439	429	448	433	441	512	534
B-2	A	266	289	351	388	423	445	462	447	445	462	518	542
	B	255	288	334	369	413	448	444	444	441	447	469	498
B-3	A	254	289	326	337	391	445	475	438	442	448	465	470
	B	258	266	317	341	399	436	436	446	438	455	504	523
B-4	A	249	278	322	347	392	442	451	448	435	466	547	571
	B	251	285	328	355	407	450	469	458	448	472	556	587
B-5	A	261	298	354	360	404	443	451	433	437	447	490	505
	B	246	269	309	375	422	458	460	448	451	482	553	567
B-6	A	278	311	336	366	423	461	448	452	439	461	503	524
	B	267	310	347	363	418	444	451	425	433	458	519	524
B-7	A	256	287	307	338	387	434	438	439	438	442	493	516
	B	245	270	313	346	393	426	440	435	430	449	511	530
B-8	A	240	261	312	333	385	429	452	440	442	468	514	542
	B	234	255	316	324	384	421	426	426	427	443	524	533
B-9	A	237	254	307	333	378	453	469	452	451	477	534	567
	B	253	286	321	348	391	440	425	433	430	457	509	543
B-10	A	279	309	334	367	422	466	462	451	461	491	544	566
	B	274	300	333	381	433	452	468	452	426	454	490	517
B-11	A	244	281	307	338	377	407	409	408	410	435	489	499
	B	249	278	316	356	420	464	455	438	433	452	517	524
B-12	A	255	281	329	360	396	445	458	443	411	438	488	503
	B	266	272	322	354	390	390	406	414	421	434	481	497
B-13	A	251	290	331	374	411	451	466	448	441	469	511	534
	B	259	279	330	362	412	458	481	453	436	448	491	520
B-14	A	245	276	326	353	404	434	457	451	437	436	472	487
	B	248	288	326	349	395	447	454	458	448	477	533	523
B-15	A	215	248	295	332	384	433	488	448	444	482	546	540
	B	224	252	303	337	386	439	444	439	438	452	496	511
B-16	A	236	253	310	341	397	442	452	450	440	449	481	496
	B	237	250	308	337	384	450	449	431	433	441	478	487

Table C-2. Post Treatment Half-Cell Potential as a Function of Time in Reference to Copper-Copper Sulfate Electrode

Half-Cell Potential, Ecorr (-mV)

Specimen	Bar	Pre-Treat	Day 7	Day 11	Day 18	Day 27	Day 34	Day 41	Day 48
B-1	A	546	399	431	497	519	492	499	496
	B	521	399	432	504	525	490	495	491
B-2	A	542	368	378	446	488	431	492	513
	B	550	380	375	460	506	455	521	547
B-3	A	540	301	240	243	239	234	225	192
	B	533	325	263	259	252	240	231	197
B-4	A	548	326	345	363	408	393	370	371
	B	521	354	340	385	440	408	401	397
B-5	A	561	402	431	498	529	486	489	479
	B	545	388	437	511	546	495	498	501
B-6	A	558	419	370	411	434	424	392	369
	B	559	407	386	426	440	421	406	359
B-7	A	562	447	314	322	346	328	330	295
	B	571	422	342	359	398	359	353	357
B-8	A	547	482	373	490	626	418	413	400
	B	552	484	374	478	575	421	436	454
B-9	A	530	398	315	324	355	370	355	325
	B	519	422	355	368	401	403	392	373
B-10	A	542	299	224	225	233	233	191	196
	B	545	334	219	219	228	221	218	181
B-11	A	534	314	255	292	318	269	226	218
	B	537	313	254	287	299	252	236	227
B-12	A	545	480	301	373	489	393	429	491
	B	528	480	290	364	450	373	397	438
B-13	A	494	191	192	203	230	220	208	187
	B	503	220	183	190	210	189	181	158
B-14	A	488	199	169	198	204	191	185	183
	B	484	269	224	242	274	265	296	371
B-15	A	475	291	227	254	287	251	245	217
	B	480	208	174	222	238	210	200	188
B-16	A	477	408	222	229	210	202	179	146
	B	470	381	218	214	201	189	180	161
A-13	A	592	305	432	507	536	515	518	649
	B	611	294	419	485	522	518	507	577
A-15	A	607	409	430	478	479	507	679	702
	B	631	391	400	451	448	492	677	694

Table C-2. Post-Treatment Half-Cell Potential as a Function of Time in Reference to Copper-Copper Sulfate Electrode (continued)

Half-Cell Potential, Ecorr (-mV)

Specimen	Bar	Day 55	Day 62	Day 69	Day 76	Day 83	Day 90	Day 97	Day 104
B-1	A	500	497	502	542	572	645	650	662
	B	501	485	502	544	592	623	666	711
B-2	A	515	502	550	640	543	520	548	535
	B	562	549	549	712	537	531	537	529
B-3	A	211	188	239	262	249	241	250	230
	B	209	225	271	237	242	220	230	223
B-4	A	381	358	419	485	472	465	440	480
	B	406	436	484	527	526	540	551	542
B-5	A	484	502	498	529	520	501	517	523
	B	507	528	523	558	540	540	537	527
B-6	A	396	382	379	450	472	470	490	490
	B	386	372	402	442	451	477	469	507
B-7	A	317	308	312	350	367	388	379	408
	B	377	404	418	482	490	480	465	474
B-8	A	390	315	333	362	367	370	366	380
	B	448	364	396	439	453	449	455	492
B-9	A	346	325	331	364	384	401	412	446
	B	399	374	400	415	466	444	469	492
B-10	A	196	208	278	482	475	456	462	441
	B	198	182	285	361	400	404	423	444
B-11	A	256	254	220	333	382	440	422	459
	B	260	211	214	224	221	222	219	210
B-12	A	520	500	512	592	601	633	651	653
	B	454	494	591	561	567	558	559	574
B-13	A	223	224	202	282	283	280	280	273
	B	217	165	148	170	172	179	200	193
B-14	A	205	211	247	272	272	280	289	283
	B	407	409	407	446	451	466	472	472
B-15	A	247	241	263	274	280	272	270	283
	B	207	194	217	240	276	308	322	353
B-16	A	160	156	146	150	152	150	158	165
	B	170	162	153	160	167	173	183	184
A-13	A	532	593	601	567				
	B	551	537	549	561				
A-15	A	750	735	749					
	B	680	712	700					

Table C-3. Percent Change in Half-Cell Potential After Treatment, CSE Reference

Positive (+) % = increase to more noble potential
Negative (-) % = decrease to more active potential

Percent Change in Potential Magnitude

Specimen	Bar	Day 7	Day 11	Day 18	Day 27	Day 34	Day 41	Day 48	Day 55
B-1	A	26.9	21.1	9	5	9.9	8.6	9.2	8.4
	B	23.4	17.1	3.3	-0.8	6	5	5.8	3.8
B-2	A	32.1	30.3	17.7	10	20.5	9.2	5.4	5
	B	30.9	31.8	16.4	8	17.3	5.3	0.6	-2.2
B-3	A	44.3	55.6	55	55.7	56.7	58.3	64.4	60.9
	B	39	50.7	51.4	52.7	55	56.7	63	60.8
B-4	A	40.5	37	33.8	25.6	28.3	32.5	32.3	30.5
	B	32.1	34.7	26.1	15.6	21.7	23	23.8	22.1
B-5	A	28.3	23.2	11.2	5.7	13.4	12.8	14.6	13.7
	B	28.8	19.8	6.2	-0.2	9.2	8.6	8.1	7
B-6	A	24.9	33.7	26.3	22.2	24	29.8	33.9	29
	B	27.2	31	23.8	21.3	24.7	27.4	35.8	31
B-7	A	20.5	44.1	42.7	38.4	41.6	41.3	47.5	43.6
	B	26.1	40.1	37.1	30.3	37.1	38.2	37.5	34
B-8	A	11.9	31.8	10.4	-14.4	23.6	24.5	26.9	28.7
	B	12.3	32.3	13.4	-4.2	23.7	21	17.8	18.8
B-9	A	24.9	40.6	38.9	33	30.2	33	38.7	34.7
	B	18.7	31.6	29.1	22.4	22.4	24.5	28.1	23.1
B-10	A	44.8	58.7	58.5	57	57	64.8	63.8	63.8
	B	38.7	59.8	59.8	58.2	59.5	60	66.8	63.7
B-11	A	41.2	52.3	45.3	40.5	49.6	57.7	59.2	52.1
	B	41.7	52.7	46.6	44.3	53.1	56.1	57.7	51.6
B-12	A	11.9	44.8	31.6	10.3	27.9	21.3	9.9	4.6
	B	9.09	45.1	31.1	14.8	29.4	24.8	17.1	14
B-13	A	61.3	61.1	58.9	53.4	55.5	57.9	62.2	54.9
	B	56.3	63.6	62.2	58.3	62.4	61	68.6	56.9
B-14	A	59.2	65.4	59.3	58.2	60.9	62.1	62.5	58
	B	44.4	53.7	50	43.4	45.3	38.8	23.4	15.9
B-15	A	38.7	52.2	46.5	39.6	47.2	48.4	54.3	48
	B	56.7	63.8	53.8	50.4	56.3	58.3	60.1	56.9
B-16	A	14.5	53.5	52	56	57.7	62.5	69.4	66.5
	B	18.9	53.6	54.5	57.2	59.8	61.7	65.7	66.8
A-13	A	48.5	27	14.4	9.5	13	12.5	-9.6	10.1
	B	51.9	31.4	20.6	14.6	15.2	17	5.6	9.8
A-15	A	32.6	29.2	21.3	21.1	16.5	-11.9	-15.7	-23.6
	B	38	36.6	28.5	29	22	-7.3	-10	-7.8

Table C-3. Percent Change in Half-Cell Potential After Treatment, CSE Reference (continued)

Positive (+) % = increase to more noble potential
Negative (-) % = decrease to more active potential

Percent Change in Potential Magnitude

Specimen	Bar	Day 62	Day 69	Day 76	Day 83	Day 90	Day 97	Day 104
B-1	A	9	8.1	0.7	-4.8	-18.1	-19.1	-21.3
	B	6.9	3.7	-4.4	-13.6	-19.6	-27.8	-36.5
B-2	A	7.4	-1.5	-18.1	-0.2	4.1	-1.1	1.3
	B	0.2	0.2	-29.5	2.4	3.5	2.4	3.8
B-3	A	65.2	55.7	51.5	53.9	55.4	53.7	57.4
	B	57.8	49.2	55.5	54.6	58.7	56.9	58.2
B-4	A	34.7	23.5	15.2	13.9	15.2	19.7	12.4
	B	16.3	7.1	-1.2	-1	-3.7	-5.8	-4
B-5	A	10.5	11.2	5.7	7.3	10.7	7.8	6.8
	B	3.1	4	-2.4	0.9	0.9	1.5	3.3
B-6	A	31.5	32.1	19.4	15.4	15.8	12.2	12.2
	B	33.5	28.1	20.9	19.32	14.7	16.1	9.3
B-7	A	45.2	44.5	37.7	34.7	30.1	32.6	27.4
	B	29.3	26.8	15.6	14.2	15.9	18.6	17
B-8	A	42.4	39.1	33.8	32.9	32.7	33.1	30.5
	B	34.1	28.3	20.5	17.9	18.7	17.6	10.9
B-9	A	38.7	37.6	31.3	27.6	24.3	22.3	15.9
	B	27.9	22.9	20	10.2	14.5	9.6	5.2
B-10	A	61.6	48.7	11.1	12.4	15.6	14.8	18.6
	B	66.6	47.7	33.8	26.6	25.9	22.4	18.5
B-11	A	52.4	58.8	37.6	28.5	17.6	21	14
	B	60.7	60.2	58.3	58.9	58.7	59.2	60.9
B-12	A	8.3	6.1	-8.6	-10.3	-16.2	-19.5	-19.8
	B	6.4	-11.9	-6.3	-7.4	-5.7	-5.9	-8.7
B-13	A	54.7	59.1	42.9	42.7	43.3	43.3	44.7
	B	67.2	70.6	66.2	65.8	64.4	60.2	61.6
B-14	A	56.8	49.4	44.3	44.3	42.6	40.8	42
	B	15.5	15.9	7.9	6.8	3.7	2.5	2.5
B-15	A	49.3	44.6	42.3	41.1	42.7	43.2	40.4
	B	59.6	54.8	50	42.5	35.8	32.9	26.5
B-16	A	67.3	69.4	68.6	68.1	68.6	66.9	65.4
	B	65.5	67.5	66	64.5	63.2	61.1	60.9
A-13	A	-0.2	-1.5	4.2				
	B	12.1	10.2	8.18				
A-15	A	-21.1	-23.4					
	B	-12.8	-10.9					

Table C-4. Post-Treatment Corrosion Current as a Function of Time

		Corrosion Current, Icorr (mA/sq.ft)							
Specimen	Bar	Pre-Treat	Day 7	Day 11	Day 18	Day 27	Day 34	Day 41	Day 48
B-1	A	8.7	8.2	8.5	9.2	10.3	10.5	9.9	10.1
	B	8.2	8.6	7	7.4	7.4	8	9.7	10.2
B-2	A	9.1	9.4	5.8	6.3	7.3	6.23	7.6	9.1
	B	9.3	10.5	5.1	5.9	7.5	5.9	7.8	12
B-3	A	12	8.1	4.1	4.1	3.9	4.3	4	4
	B	11	7.2	3.2	3.3	3.5	4	4.2	4.1
B-4	A	7.5	6.1	4.9	5.8	6.3	6.9	6.8	6.8
	B	7.4	7.9	7.1	6.8	6.6	8	7.8	7.9
B-5	A	6.5	5.6	3.9	4.4	5.3	6.4	7	7.2
	B	6.9	5.7	4.9	5.5	6.8	5.3	6.6	7.9
B-6	A	6.1	6.9	4.4	4.5	4.5	5.2	5.5	5.6
	B	6.3	5.8	5.8	5	4.5	5.1	5.3	5.4
B-7	A	6.2	7.1	3.9	4.1	4.4	4.2	4.5	4.4
	B	6.5	7.9	3.7	3.8	4.1	4.6	4.5	4.6
B-8	A	5.9	4.3	1.9	3.3	5.7	3.8	3.5	3.6
	B	6.1	4.8	1.8	4.1	5.6	3.8	4.6	4.6
B-9	A	4	3.4	1.8	1.6	1.3	1.9	2.2	2.4
	B	3.8	3	1.7	1.4	1.4	1.3	1.7	1.6
B-10	A	3.5	4.6	1.5	1.9	2.1	1.8	2.1	2.1
	B	3.8	6.4	2.1	2.1	2	2.9	2.9	2.8
B-11	A	3.9	4.2	1.8	2.2	2.4	2.3	2.8	2.6
	B	3.9	4.1	2.1	2.2	2.5	1.9	2.3	2.7
B-12	A	3.4	3.5	1.3	2.1	3.4	3	4	4.8
	B	3.3	4	0.9	2.3	3.4	3.7	4.6	4.3
B-13	A	2.3	1.1	0.8	0.9	0.9	1.1	1.4	1.3
	B	2.5	1.3	0.9	0.9	0.9	1.1	1	1.2
B-14	A	1.6	1	0.7	0.7	0.6	0.5	0.7	0.7
	B	1.4	1.1	0.6	0.6	0.7	0.8	1	0.9
B-15	A	1.7	0.8	0.5	0.5	0.5	0.5	0.5	0.5
	B	1.9	0.8	0.5	0.5	0.5	0.4	0.4	0.5
B-16	A	1.3	2.1	0.9	0.8	0.7	0.7	0.7	0.8
	B	1.6	2.1	0.5	0.6	0.6	0.7	0.7	0.7
A-13	A	25	1.3	19.4	28.7	36.7	37.3	22	29
	B	22	0.2	15.9	25	33.2	34.5	29	30.7
A-15	A	23	6.2	7.1	7.4	7.6	22	27.6	29.4
	B	22	5.9	8.3	9.2	9.7	20	36	37.9

Table C-4. Post-Treatment Corrosion Current as a Function of Time (continued)

Corrosion Current, Icorr (mA/sq.ft)

Specimen	Bar	Day 55	Day 62	Day 69	Day 76	Day 83	Day 90	Day 97	Day 104
B-1	A	9.7	10.1	10.5	13.2	12.6	12.9	12.9	13.3
	B	10.1	10.3	12.2	12.6	13	13.3	13.8	15
B-2	A	12.9	13.6	13	12	12	12.2	12.1	11.7
	B	16	16	13.8	21.4	19.5	18.6	19	20.4
B-3	A	4.2	4.2	3.6	3.3	3.5	3.8	3.9	3.9
	B	4.1	4.4	3.2	3.1	3.9	3.8	3.8	3.9
B-4	A	7	6.8	6.6	6.2	6.6	7.8	7.9	8.6
	B	7.6	7.5	8.1	10	12.2	13.7	13.5	16.1
B-5	A	8.5	8.8	7.2	8.2	8.2	8.6	8.8	9.6
	B	9.3	9.5	7.8	10.8	11.2	10	11.4	11.5
B-6	A	6.4	6.4	4.4	5.6	6.6	8.2	10	10.2
	B	6	6.3	3.1	4.7	6.2	7.8	7.7	8.5
B-7	A	4.8	4.8	3.1	2.5	4	4.4	4.3	4.4
	B	4.6	4.9	3.9	5.1	6	6.1	6.4	6.4
B-8	A	3.3	3.3	1.5	1.3	2	1.9	2	1.4
	B	5.2	5	2.6	3.4	3.7	4	3.9	3.8
B-9	A	2.7	2.6	1.3	1.7	2.5	2.6	2.9	3.7
	B	1.9	1.9	1.2	1.6	1.9	3	2.9	3.4
B-10	A	2.2	2.6	1.8	3.3	3.9	4.4	4.6	4.9
	B	2.6	2.8	2.5	4.3	4.7	5.8	5.6	5.9
B-11	A	3	3.3	2.2	2.9	3	4.2	4.8	6
	B	2.8	2.8	1.7	2.2	2.3	2.8	2.7	3.2
B-12	A	5.9	5.7	3.4	4	4.4	4.3	4.3	4.5
	B	5.7	5.9	5	6.6	5.9	5.8	6.1	5.9
B-13	A	1.5	1.6	1	1.3	1.3	1.3	1.2	1.2
	B	1.4	1.3	0.8	0.8	0.9	1	1	0.8
B-14	A	0.9	1	0.8	1	0.9	0.9	0.9	1.1
	B	1.2	1.2	1	1.7	1.6	1.4	1.6	1.9
B-15	A	0.5	0.5	0.4	0.4	0.6	0.6	0.7	1
	B	0.4	0.5	0.4	0.5	0.7	0.9	1	1.5
B-16	A	0.8	0.8	0.6	0.6	0.7	0.6	0.8	1
	B	0.7	0.7	1.7	0.7	0.6	0.7	0.7	0.7
A-13	A	32.1	24.5	25.2	26				
	B	28.7	29	27	28				
A-15	A	28.3	31.1	30.1					
	B	40.2	42.8	48.2					

Table C-5. Percent Change in Corrosion Current After Treatment

Positive (+) % = decrease in corrosion rate
Negative (-) % = increase in corrosion rate

Percent Change in Corrosion Current Magnitude

Specimen	Bar	Day 7	Day 11	Day 18	Day 27	Day 34	Day 41	Day 48	Day 55
B-1	A	5.7	2.3	-5.7	-18.4	-20.7	-13.8	-16.1	-11.5
	B	-4.9	14.6	9.8	9.8	2.4	-18.3	-24.2	-23.2
B-2	A	-3.3	36.3	30.8	19.8	31.9	16.5	0	-41.8
	B	-12.9	45.2	36.6	19.4	36.6	16.1	-29	-72
B-3	A	30.8	65	65	66.7	63.2	65.8	65.8	64.1
	B	33.9	70.6	69.7	67.9	63.3	61.5	62.4	62.4
B-4	A	18.7	34.7	22.7	16	8	9.3	9.3	6.7
	B	-6.8	4.1	8.1	10.8	-8.1	-5.4	-6.8	-2.7
B-5	A	13.8	40	32.3	18.5	1.5	-7.7	-10.8	-30.8
	B	17.4	29	20.3	1.4	23.2	4.3	-14.5	-34.8
B-6	A	-13.1	27.9	26.2	26.2	14.8	9.8	8.2	-4.9
	B	7.9	7.9	20.6	28.6	19	15.9	14.3	4.8
B-7	A	-14.5	37.1	33.9	29	32.3	27.4	29	22.6
	B	-21.5	43.1	41.5	36.9	29.2	30.8	29.2	29.2
B-8	A	27.1	67.8	44.1	3.4	35.6	40.7	39	44.1
	B	21.3	70.5	32.8	8.2	37.7	24.6	24.6	14.8
B-9	A	15	55	60	67.5	52.5	45	40	32.5
	B	21.1	55.3	63.2	63.2	65.8	40	57.9	50
B-10	A	-31.4	57.1	45.7	40	48.6	23.7	40	37.1
	B	-68.4	44.7	44.7	47.4	23.7	28.2	26.3	31.6
B-11	A	-7.7	53.8	43.6	38.5	41	41	33.3	23.1
	B	-5.1	46.2	43.6	35.9	51.3	-17.6	30.8	28.2
B-12	A	-2.9	61.8	38.2	0	11.8	-39.4	-41.2	-73.5
	B	-21.2	72.7	30.3	-3	-12.1	39.1	-30.3	-72.7
B-13	A	52.2	65.2	60.9	60.9	52.2	60	43.5	34.8
	B	48	64	64	64	56	56.3	52	44
B-14	A	37.5	56.3	56.3	62.5	68.8	28.6	56.3	43.8
	B	21.4	57.1	57	50	42.9	70.6	35.7	14.3
B-15	A	52.9	70.6	70.6	70.6	70.6	78.9	70.6	70.6
	B	57.9	73.7	73.7	73.7	78.9	46.2	73.7	78.9
B-16	A	-61.5	30.8	38.5	46.2	46.2	56.3	38.5	38.5
	B	-31.1	68.8	62.5	62.5	56.3	11.6	56.3	56.3
A-13	A	94.8	22.1	-15.3	-47.4	-49.8	-32.4	-16.5	-28.9
	B	99.1	27.4	-14.2	-51.6	-57.5	-20	-40.2	-31.1
A-15	A	73	69.1	67.8	67	4.3	-65.1	-27.8	-23
	B	72.9	61.9	57.8	55.5	8.3	-7.3	-73.9	-84.4

Table C-5. Percent Change in Corrosion Current After Treatment (continued)

Positive (+) % = decrease in corrosion rate
Negative (-) % = increase in corrosion rate

Percent Change in Corrosion Current Magnitude

Specimen	Bar	Day 62	Day 69	Day 76	Day 83	Day 90	Day 97	Day 104
B-1	A	-16.1	-20.7	-51.7	-44.8	-48.3	-48.3	-52.9
	B	-25.6	-48.8	-53.7	-58.5	-62.2	-68.3	-82.9
B-2	A	-49.5	-42.9	-31.9	-31.9	-34.1	-33	-28.6
	B	-72	-48.4	-130.1	-109.7	-100	-104.3	-119.4
B-3	A	64.1	69.2	71.8	70.1	67.5	66.7	66.7
	B	59.6	70.6	71.6	64.2	65.1	65.1	64.2
B-4	A	9.3	12	17.3	12	-4	-5.3	-14.7
	B	-1.4	-9.5	-35.1	-64.9	-85.1	-82.4	-117.6
B-5	A	-35.4	-10.8	-26.2	-26.2	-32.3	-35.4	-47.7
	B	-37.7	-13	-56.5	-62.3	-44.9	-65.2	-66.7
B-6	A	-4.9	27.9	8.2	-8.2	-34.4	-63.9	-67.2
	B	0	50.8	25.4	1.6	-23.8	-22.2	-34.9
B-7	A	22.6	50	59.7	35.5	29	30.6	29
	B	24.6	40	21.5	7.7	6.2	1.5	1.5
B-8	A	44.1	74.6	78	66.1	67.8	66.1	76.3
	B	18	57.4	44.3	39.3	34.4	36.1	37.7
B-9	A	35	67.5	57.5	37.5	35	27.5	7.5
	B	50	68.4	57.9	50	21.1	23.7	10.5
B-10	A	25.7	48.6	5.7	-11.4	-25.7	-31.4	-40
	B	26.3	34.2	-13.2	-23.7	-52.6	-47.4	-55.3
B-11	A	15.4	43.6	25.6	23.1	-7.7	-23.1	-53.8
	B	28.2	56.4	43.6	41	28.2	30.8	17.9
B-12	A	-67.6	0	-17.6	-29.4	-26.5	-26.5	-32.4
	B	-78.8	-51.5	-100	-78.8	-75.8	-84.8	-78.8
B-13	A	30.4	56.5	43.5	43.5	43.5	47.8	47.8
	B	48	68	68	64	60	60	68
B-14	A	37.5	50	37.5	43.8	43.8	43.8	31.3
	B	14.3	28.6	-21.4	-14.3	0	-14.3	-35.7
B-15	A	70.6	76.5	74.7	64.7	64.7	58.8	41.2
	B	73.7	78.9	75.3	63.2	52.6	47.4	21.1
B-16	A	38.5	53.8	53.8	46.2	53.8	38.5	23.1
	B	56.3	-6.2	56.3	62.5	56.3	56.3	56.3
A-13	A	1.6	-1.2	-0.04				
	B	-32.4	-23.3	-27.3				
A-15	A	-35.2	-30.9					
	B	-96.3	-119.1					

Table C-6. Average mortar cube strength for treated specimens

Treatment	Concentration (% s/s cement)	Compressive Strength (ksi)		
		Day 1	Day 3	Day 20
Control	-----	1.98	3.76	5.69
Cortec 1609	0.15 %	2.03	3.43	5.59
	0.30 %	1.89	3.14	5.11
	0.45 %	2.02	3.38	5.86
Hydroxyl-apatite	6.25 %	2.36	3.59	5.69
	12.50 %	2.02	3.27	5.33
	25.00 %	2.17	3.45	5.90
DCI	2.50 %	2.34	5.10	6.83
	5.00 %	2.69	5.20	7.67
	10.00 %	3.17	5.79	7.53
Sodium Borate	0.50 %	0.50	2.80	5.56
	1.00 %	0.07	0.47	5.03
	2.00 %	0.00	0.24	4.42
Zinc Borate	0.22 %	2.00	4.00	5.46
	0.43 %	0.09	1.28	4.32
	0.85 %	0.00	0.51	3.95
	1.70 %	0.00	0.00	3.25
	3.40 %	0.00	0.00	2.46

Table C-7. Average mortar cube resistivity for treated specimens

Treatment	Concentration (% s/s cement)	Resistivity (kohm-cm)			
		Day 1	Day 3	Day 10	Day 20
Control	-----	.40	.87	1.6	2.1
Cortec 1609	0.15 %	.37	.90	1.5	2.2
	0.30 %	.37	.85	1.6	2.0
	0.45 %	.47	.85	1.5	2.0
Hydroxyl-apatite	6.25 %	.49	.87	1.6	2.2
	12.50 %	.47	.84	1.4	2.3
	25.00 %	.52	.86	1.6	2.3
DCI	2.50 %	.62	1.0	1.9	2.4
	5.00 %	.63	1.2	1.8	2.3
	10.00 %	.62	1.3	2.2	2.5
Sodium Borate	0.50 %	.17	.84	1.4	2.0
	1.00 %	*	.45	.88	1.7
	2.00 %	*	.36	.69	1.5
Zinc Borate	0.22 %	.38	.89	1.7	2.1
	0.43 %	*	.61	1.1	1.9
	0.85 %	*	.51	.92	1.8
	1.70 %	*	*	*	.76
	3.40 %	*	*	*	.68

* = insufficient set strength to test resistivity

VITA

The author was born on October 10, 1967, in Monterey, California. He received his high school diploma in June, 1985, from Menchville High School in Newport News, Virginia. September of that same year, he enrolled in the College of Engineering at Virginia Polytechnic Institute and State University. After four years, he received his Bachelor of Science degree in Materials Engineering in August, 1989. After his undergraduate studies, the author began his graduate study at VPI & SU in the Fall of 1989 in the Materials Engineering Department.